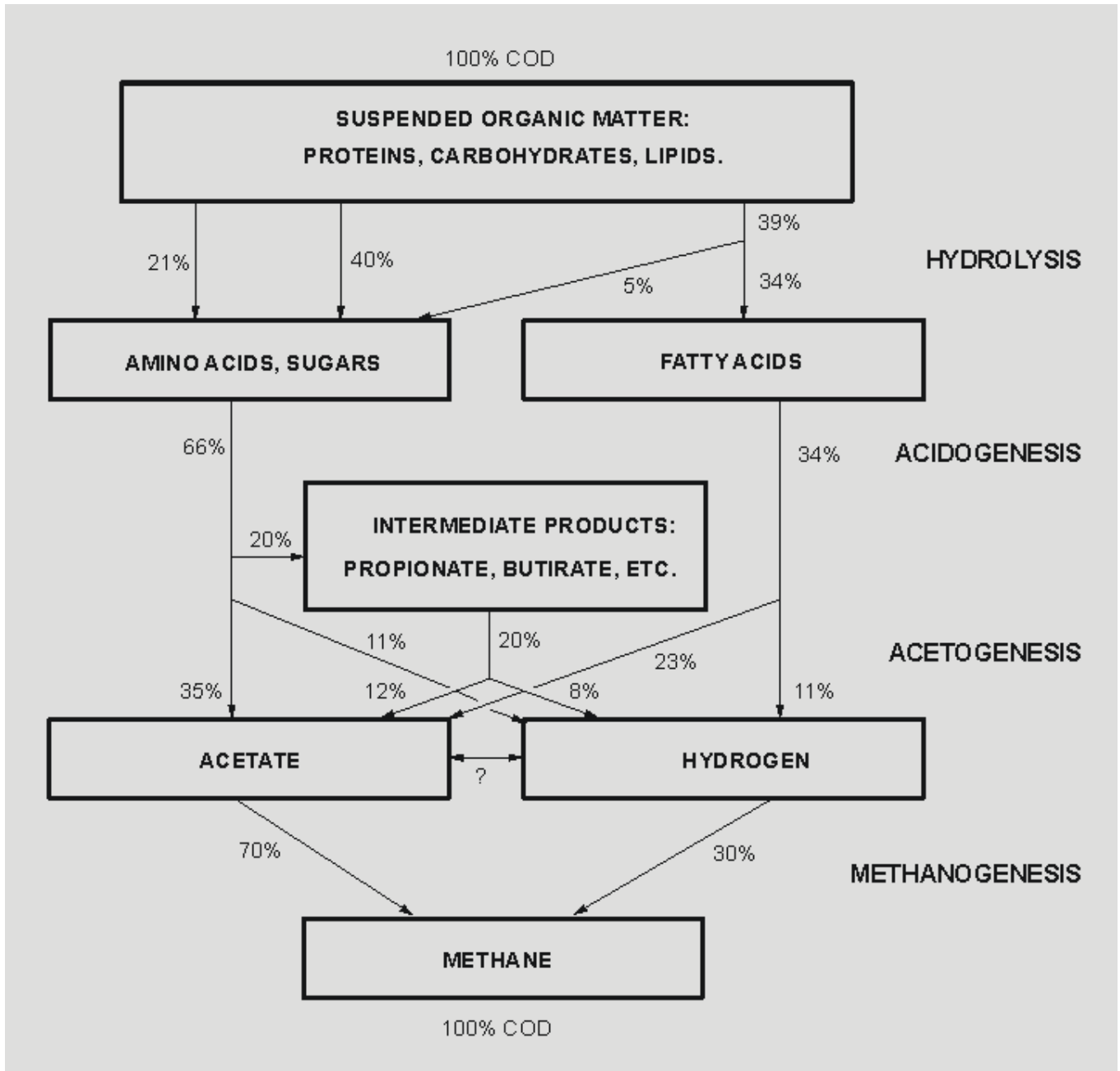


Validation and improvement of the OPTI-VFA sensor for online VFA monitoring



Zhe Deng

September, 2015

Validation and improvement of the OPTI-VFA sensor for online VFA monitoring

Zhe Deng

Sanitary Engineering Section, Department of Water Management
Faculty of Civil Engineering and Geosciences
Delft University of Technology, Delft

for the degree of:

Master of Science in Civil Engineering

Date of submission: 14 September 2015

Date of defense: 24 September 2015

Committee:

Prof. dr.ir. J. B. van Lier

Dr.ir. H. Spanjers

Dr.ir. R. Kleerebezem

Dr.ir X. Zhang

Delft University of Technology
Sanitary Engineering Section
Delft University of Technology
Sanitary Engineering Section
Delft University of Technology
Environmental Biotechnology Section
Delft University of Technology
Sanitary Engineering Section

Summary

In order to deal with the increasing amount of solid organic waste, an environmentally friendly waste management method is preferred. The AD (anaerobic digestion) process utilizes a complex consortium of microorganisms to convert organic matter into methane and carbon dioxide, in the absence of oxygen and nitrate. It is able to reduce the waste while also recovering energy from it. Although it is a powerful technology for waste/wastewater treatment, there are several reasons why many industrial companies do not want to apply AD. One important reason is that the process is easily disturbed and it takes a lot of time to recover from a process failure. Separating the process into two phases is reported as a method to improve the process performance. Monitoring and controlling the process is also considered as a good solution for a sustainable performance. The short chain volatile fatty acids (VFA) have proven to be a proper indicator for the process state. Offline VFA measurements are not sufficient for effective control, thus there is a large demand of a reliable online VFA monitoring method.

The OPTI-VFA project, started in 2013, is aiming to develop a novel monitoring and control tool, in order to improve the reliability, efficiency and profitability of the AD process. This tool is named as the OPTI-VFA sensor, which is designed to online monitor VFA concentrations in AD processes. Calibration models of total VFA and 3 individual VFAs (acetate, propionate and butyrate) were built by our Finnish partner, the Technical Research Centre of Finland (VTT). Before it can be applied commercially, the performance of the sensor needs to be validated, which is the main focus of this study.

The OPTI-VFA sensor was validated through experiments in laboratory and full-scale biogas plant, with Gas chromatography (GC) measurements as a reference. In the lab-scale validation, batch tests and online monitoring were carried out. First, a lab-scale two-phase system was established, with a leaching bed reactor as the first-phase and an upflow anaerobic sludge blanket (UASB) reactor as the second-phase. The sensor was used to monitor the VFA concentrations in the leaching process (high VFA concentrations) and the methanogenesis process (low VFA concentrations). In addition to the online monitoring, sample matrices were prepared with the presence of impact factors, that is: pH, temperature, HCO_3^- and NH_4^+ . Second, in the full-scale validation, the OPTI-VFA sensor was brought to the biogas plant of Attero, which is also a two-phase AD system, with 12 hydrolysis tunnels and a UASB reactor. The sensor was installed in a bypass to monitor the dynamic VFA profile in the process waters.

By analysing the results, it was found that in case with high VFA concentrations, the sensor was able to give good predictions of total VFA and acetate in both the lab-scale and full-scale AD systems. The sensor could also follow the dynamic VFA concentrations indicated by the GC reference. For VFA concentrations lower than 1000 mg/L, the sensor was not able to present a reliable prediction. The concentration of propionic acid and butyric acid was low in both phases (0-1000 mg/L), the current calibration model was not suitable to predict these concentration levels.

The sensor gave a better performance in the pH range of 6-8, the concentration of bicarbonate and ammonia could cause a 1000-1500 mg/L offset in total VFA and acetic acid predictions. The sample temperature in the range of 33-44 °C did not show a significant impact on the sensor performance.

The re-measurement of the calibration samples revealed that the offset in reference values did not have a significant contribution to the offset in prediction values. However, the ambient humidity was found to introduce periodic noise to the measured spectra, which can only be partly removed by processing the data before applying it in the calibration model.

The calibration was done by using the partial least regression (PLS) and spectral matched filter (SMF) method. SMF showed a better performance for predicting total VFA concentrations that were less than 4000 mg/L, and it needed less data than PLS for high VFA concentration predictions.

To further improve the OPTI-VFA sensor, it is recommended to build a separate calibration model to measure the buffer capacity (HCO_3^- and NH_4^+ concentrations). The fouling potential of the sensor still needs to be studied under long-term operation and in easily fouling samples (i.e. high lipid-containing streams). Additionally, shortening the optical fibre (connecting the light source and the measuring probe) can also improve the sensitivity of the system, while reducing the costs. Moreover, since VFA has a higher priority in the waste hierarchy than biogas, this sensor with improved models would be interesting for VFA recovery from organic residues.

Acknowledgement

It would have been impossible to finish my thesis, required for finishing the Master Track Water Management, in the Sanitary Engineering department, without the guidance of my committee members, support of my family and the encouragement of my friends. It has been a long journey from which I have learned a lot and I would like to express my gratitude to the people that helped me through it.

First of all I would like to thank my committee members for their guidance. Foremost I would like to express my deepest gratitude to my supervisor, Dr. Xuedong Zhang for his assistance, patience and supervision. Your supervision helped throughout the entire research. From you I have gained so much experience, knowledge and motivation that will be greatly valued in the future.

Henri Spanjers, thank you for your supervision and for being available for discussions. Your insightful questions and constructive comments at different times during my research helped focus my ideas.

I would also like to thank all the OPTI-VFA partners. Thank you for accepting me on board of your team and for sharing your ideas and concepts.

The staff members from the laboratory of TU Delft, Armand Middeldorp and Tony Schuit, without your help and assistance it would have been impossible to finish my experiments.

Finally, I would like to thank all my friends and family for always being there, for their support and encouragements. Thank you for being there and cheering me!

Contents

List of Figures.....	viii
List of tables.....	x
CHAPTER 1 INTRODUCTION	1
1.1 Background & problem statement	1
1.2 Two-phase AD system.....	4
1.3 Methods for online VFA monitoring.....	7
1.4 Mathematical calibration methods & relevant factors for IR technique.....	10
CHAPTER 2 RESEARCH QUESTIONS & OBJECTIVES.....	11
CHAPTER 3 MATERIALS & METHODOLOGY	13
3.1 Characteristics of the substrates, inoculum and effluents	13
3.2 Experimental setup of the two-phase system.....	14
3.3 In-process & off-process VFA measurements.....	20
3.4 Batch tests	22
3.5 Methods for OPTI-VFA sensor improvements.....	25
CHAPTER 4 RESULTS & DISCUSSION	28
4.1 System performance.....	28
4.2 Validation.....	34
4.3 Dataset analysis.....	51
4.4 Calibration model improvement	53
CHAPTER 5 CONCLUSION & RECOMMENDATION	57
Reference.....	60
Appendix.....	64
A. System performance	64
B. pH & Temperature tests	70
C. Re-measure of Oulu calibration samples.....	72
D. Titration.....	73
E. Additional experimental details.....	74

List of Figures

Figure 1 A scheme of AD process	2
Figure 2 Deterioration cycle of AD system	3
Figure 3 Spectrum of acetate under different pH	10
Figure 4 Research scheme	13
Figure 5 Process of the Attero full-scale treatment plant	13
Figure 6 Biowase (left), Leachate (middle), inoculum (right)	14
Figure 7 Two-phase anaerobic system	15
Figure 8 Metrohm AG 787 KF auto-Titrator.....	18
Figure 9 Agilent 7890A GC.....	18
Figure 10 pH and temperature sensor.....	19
Figure 11 Gas meter	19
Figure 12 Bruker Matrix MF FT-IR system , and ATR fibre probe.....	20
Figure 13 VFA profile monitoring with OPTI-VFA system	21
Figure 14 Installation point of OPTI-VFA sensor in the full-scale biogas plant	22
Figure 15 In-process measurement in Venlo	22
Figure 16 COD results of cycle 3 and cycle 6	29
Figure 17 VFA results of cycle 3 and cycle 6	30
Figure 18 Ammonia results of cycle 3 and cycle 6.....	30
Figure 19 Alkalinity and VFA results of cycle 5 and cycle 6.....	31
Figure 20 UASB performance during the whole experimental period	33
Figure 21 Results of partial and total alkalinity	34
Figure 22 Results of online monitoring in the lab leachate (Cycle 3)	35
Figure 23 Results of online monitoring in the lab leachate (Cycle 6)	37
Figure 24 Results of online monitoring in Venlo leachate.....	38
Figure 25 Results of online monitoring in Venlo UASB effluent	39

Figure 26 Comparison of baseline spectra measured in laboratory and full-scale	39
Figure 27 Results of pH test (demi water matrix).....	41
Figure 28 VFA results of pH test (leachate matrix)	42
Figure 29 VFA dissociation level under different pH	43
Figure 30 VFA results of temperature test.....	44
Figure 31 Sensor performance under different HCO_3^- concentrations.....	45
Figure 32 Sensor performance under different NH_4^+ concentrations	47
Figure 33 Absorption peaks of HCO_3^- and NH_4^+	48
Figure 34 Comparison of two reference concentrations in UASB matrix.....	50
Figure 35 Comparison of two reference concentrations in leachate matrix.....	51
Figure 36 Measured spectrum with ambient humidity noise	52
Figure 37 Spectrum of individual VFAs.....	53
Figure 38 Improvement of C2 prediction after removal of ambient humidity.....	54
Figure 39 Comparison of three different calibration models	55
Figure 40 Total VFA profile predicted by PLS and SMF models	56

List of tables

Table 1 A comparison of different two-phase anaerobic systems digesting solid waste	6
Table 2 Reference upper-limits of inhibitors in AD system.....	7
Table 3 Characteristics of biowaste, leachate and inoculum for system start-up	14
Table 4 Feeding strategy for leaching bed reactor	16
Table 5 Feeding strategy for UASB reactor	16
Table 6 Cell kits used for variables measurement	17
Table 7 Measure frequency for manual measurements	18
Table 8 Chemicals used for pH tests	23
Table 9 pH changes for sensor validation	23
Table 10 pKa values of individual VFA	23
Table 11 Temperature variation for sensor validation.....	24
Table 12 Compositions of HCO_3^- and NH_4^+ Matrix	24
Table 13 $\text{HCO}_3^- / \text{NH}_4^+$ concentrations in each sample.....	25
Table 14 List of Spiked calibration samples with reference VFA concentrations.....	27
Table 15 Conductivity and salinity of the two sample matrices.....	42
Table 16 Correlation coefficient between the interference and $\text{HCO}_3^-/\text{NH}_4^+$ concentration.....	47

CHAPTER 1 INTRODUCTION

1.1 Background & problem statement

The accumulation of solid organic waste (i.e. biowaste, sludge, cattle manure, food waste) is leading to many issues including public health concerns, environmental burdens and ecosystem imbalance (Angelidaki et al., 2009; Khalid et al., 2011). As the global population and economy grow rapidly, the amount of solid waste is increasing. This leads to an impending need of an appropriate management approach to the waste (Khalid et al., 2011; Melikoglu et al., 2013).

Incineration, landfilling, composting, and animal feeding are common means to deal with food waste. However, these approaches are not as environmental friendly as anaerobic digestion (AD). For example in landfills, odor and greenhouse gases emissions can cause pollution to the atmosphere, leachate might cause pollution of groundwater, and large scale land use is required for this method (Zhu et al., 2009). While using AD, it is possible to reduce the waste and recover bioenergy (Angelidaki et al., 2009; Lee et al., 2014; Schober et al., 1999; Zhu et al., 2009). AD has been proven to be a competitive tool for handling slowly degradable high solid content material such as grass silage (Nizami & Murphy, 2011). Advantages of applying this method for waste management are less energy input, low yield of sludge, and the recovery of biochemical energy from the organic waste in the form of methane (Demirel & Yenigun, 2002; Steyer et al., 2002).

AD is a complex process (see Figure 1) that utilizes various microbial groups to convert organic matter into intermediates, and further to biogas in the absence of O_2 and NO_3^- (Gujer & Zehnder, 1983). Many academic and industrial studies have been carried out in the past decades, however, the intricate biological AD processes are not yet fully understood (Madsen et al., 2011). The overall conversion process of complex organic matter into biogas (CH_4 and CO_2) is concluded as four main steps: hydrolysis, acidogenesis, acetogenesis, and methanogenesis (Gujer & Zehnder, 1983; Kondusamy & Kalamdhad, 2014). These steps involve a complicated consortium of microorganisms. They have diverse growth kinetics, which are often affected by the environmental conditions. The optimum conditions, such as temperature, pH, hydraulic retention time (HRT), and organic loading rate (OLR) for each step vary vastly. For instance, pH 4 does not influence the acidogenic bacteria, while it inhibits the methanogens; a short HRT of 2-3 days can be enough for hydrolytic bacteria, but the methanogens will be flushed out of the system (Kondusamy & Kalamdhad, 2014). The AD process is slow and easily disturbed, and it might take weeks to recover from a failure. To ensure a safe and continuous operation, the AD plants are often conventionally designed (i.e. unnecessary large reactors) and operated (i.e. neutral pH, low OLR). These facts cause a high investment cost and a low profitability (Spanjers et al., 2006).

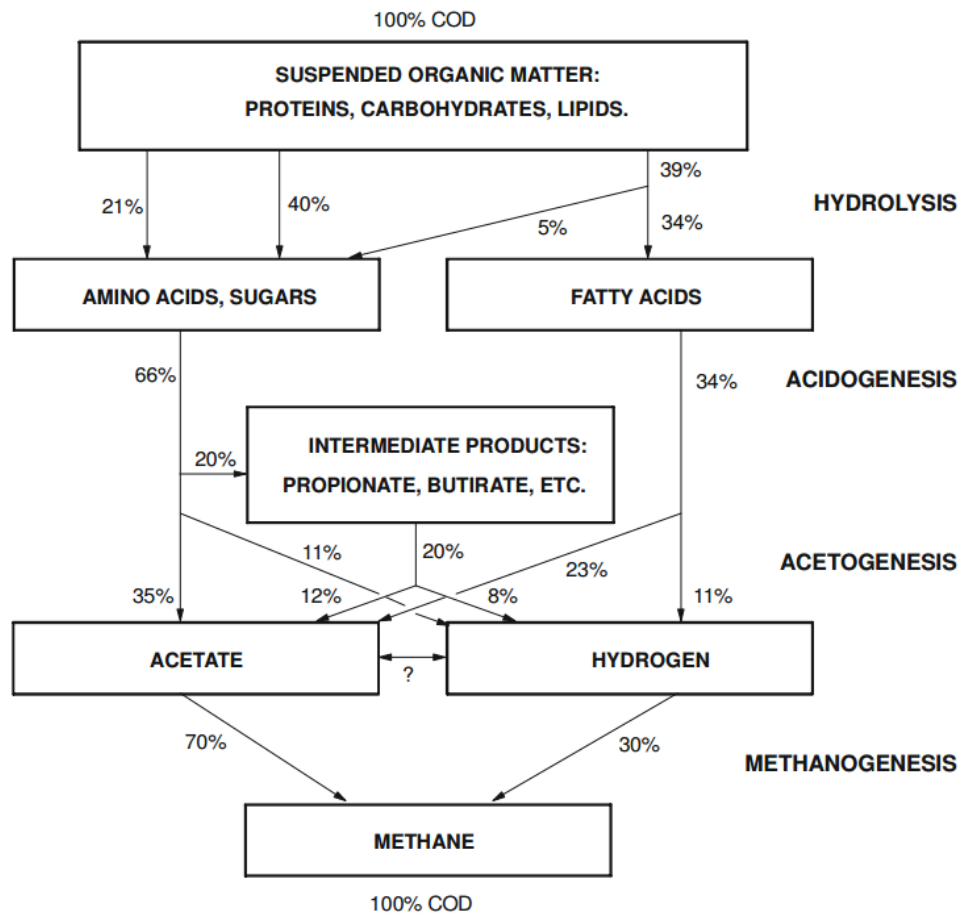


Figure 1 A scheme of AD process

(Gujer & Zehnder, 1983)

In general, a single-phase AD system is used for biogas production because of its simplicity. In a single-phase anaerobic reactor, all steps are carried out simultaneously in one reactor. Due to a lack of process information data, the system is often operated under suboptimal conditions. For example, food waste is found to have a high biogas production potential, and can be used as a substrate for sustainable anaerobic systems operations (Grimberg et al., 2015; Li, 2014). However, the high solid content and chemical composition of food waste can easily cause problems for the AD process (Grimberg et al., 2015). Especially for single-phase AD systems, the rapid acidification of food waste will result in a sudden pH drop when it is overloaded, and the pH drop may inhibit the consumption of short chain volatile fatty acids (VFA). A further accumulation of the VFA can lead to a system failure. This deterioration cycle is shown in Figure 2 (Van Lier et al., 2008). Therefore, a low maximal loading rate (3.6 kg VS/m^3) for these systems was reported by many researchers (Bouallagui et al., 2003; Lin et al., 2011; Mata-Alvares et al., 1992; Penaud et al., 1997). The conservative low OLR promises a stable performance of the system but also limits its potential.

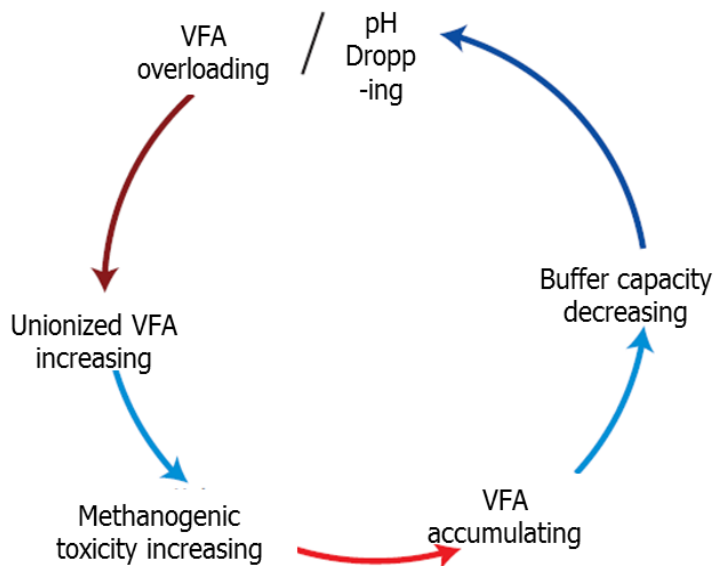


Figure 2 Deterioration cycle of AD system
(Van Lier et al., 2008)

Controlling the digestion process, by applying a monitoring system, is considered to be the most important solution for improving the profitability and sustainability (Dias et al., 2008; Spanjers et al., 2006). Online monitoring can be used not only to improve the accuracy of the manually controlled process, but also to achieve an automatic process control (Jacobi et al., 2009). Online monitoring systems are supposed to be able to give a real-time and continuous indication of process performance, while requiring less labour. As stated by Spanjers et al. (2006) online monitoring systems with effective indicators might allow 1) a shorter overall start-up time, higher stability and robustness by more automatically controlled operations; 2) a lower investment cost with less conservative system; 3) a lower operation cost with acceptable effluent quality.

However, most of the present monitoring of key parameters in the AD process is carried out by taking and analysing samples manually, which requires time, high-level skills and a lot of attention (Dias et al., 2008; Spanjers et al., 2006). Measurements such as simple online pH and temperature monitoring, biogas flow registration combined with offline analysis (using high performance liquid chromatography, gas chromatography and flow injection analysis) are commonly used in biogas plants (Holm-Nielsen et al., 2008). However, the above process indicators are not able to predict the imbalance in the process at an early stage, and the offline measurements are not efficient enough.

Many studies have been carried out to find proper process state indicators and to build up dependable online monitoring systems. Proper indicators were sought among the intermediate and final products, and VFA concentrations combined with other parameters (i.e. biogas production, total alkalinity or partial alkalinity) were found to be effective (Boe et al., 2010; Hasson et al., 2002; Kleybocker et al., 2012; Li et al., 2014; Molina et al., 2009).

The VFAs, which were the focus of this study, are the short chain volatile fatty acids that consist of less than six carbon atoms. They can be applied widely for bioplastic production, bioenergy production, and biological removal of nutrients (Lee et al., 2014). Compared to the final product methane, VFA is a higher resource value since it is placed higher in the waste hierarchy (Directive, 2008). And a higher production rate can be achieved with a higher biomass yield (about 0.15 g VSS/g

COD for acidogenesis and 0.03 g VSS/g COD for methanogenesis) (Van Lier et al., 2008). Being an important and versatile intermediate product, VFA is gaining intensive research interests. It is not only a critical substrate for microorganisms, but also a crucial state indicator for the AD process (Ahring et al., 1995; Cobb & Hill, 1991; Jacobi et al., 2009; Molina et al., 2009). Its accumulation indicates the imbalance in a biogas anaerobic reactor. In addition, individual VFA (i.e. butyrate and isobutyrate) can give specific information for process diagnosis, and contribute to the understanding of the process (Ahring et al., 1995; Nielsen et al., 2007).

Although VFA has been reported to be an effective process indicator, accurate measurements have always required time-consuming preparations, expensive equipment, and skilled laboratory technicians (Holm-Nielsen et al., 2008). With a high accuracy, GC is a commonly used method to measure VFA concentration. However, its online implementation has significant drawbacks: complex pre-treatment, low measuring frequency, high capital and maintenance costs, and substantial delays. The evaluation of individual VFA is still limited by the lack of online sensors (Boe et al., 2010). More efficient VFA online monitoring and control are required to optimize the AD process.

1.2 Two-phase AD system

Different from the single-phase system, the two-phase system separates the AD process into two steps. The production of VFA takes place in the first phase, and methane production takes place in the second phase, which uses the VFA from the first phase. To achieve the separation of the two microbial groups, the difficulty and complexity of the system design and operation are increased, which certainly leads to a higher investment cost (Ganesh et al., 2014). But it has been found that the two-phase AD is more efficient for digesting high-organic-content (solid) waste (Battimelli et al., 2009; Ghosh et al., 1985; Kuba et al., 1990; Lissens et al., 2001; Mata-Alvares, 1987; Mouneimne et al., 2003; Palmowski et al., 2006; Sonakya et al., 2001; Yu et al., 2002). A higher loading rate can be applied with the buffering effect in the first phase; a stable pH of 6 in the first phase and 7 in the second phase can be self-maintained in the system; and it can be more advantageous under fluctuating OLR (Costello et al., 1991a; Costello et al., 1991b; Grimberg et al., 2015). Generally it has a shorter HRT, a higher VS reduction rate and a higher biogas production rate (Grimberg et al., 2015; Held et al., 2002; Ince et al., 1995; Kim et al., 2002; Kondusamy & Kalamdhad, 2014). The two-phase system also allows a higher VFA production while avoiding the inhibition of methane production (Kim et al., 2002).

1.2.1 Basic operation parameters

Critical operational parameters, such as HRT, pH, temperature, and OLR, are compared among four two-phase anaerobic systems digesting solid waste (see Table 1).

Pavan et al. (2003) used two continuous stirred-tank reactors (CSTR) as a two-phase anaerobic system to digest the organic fraction of municipal solid waste (OFMSW). They found an overall HRT of 12 days (2-3 days in the hydrolytic reactor and 8-9 days in the methanogenic reactor) was a safe range, when the first reactor was operated under mesophilic condition and the second under thermophilic condition. The first reactor was able to handle an extremely high OLR (68.5 kg TVS/(m³·d)). However, the second phase might be overloaded by a total VFA above 3.5 g/L. When OLR applied for hydrolytic reactor was 31.2 kg TVS/(m³·d) and methanogenic reactor was 6.9 kg TVS/(m³·d), a gas production of

5.1 m³/(m³·d) and an overall removal of 77.3 % TVS was obtained. In their study, the pH in both phases was not controlled.

Shin et al. (2001) carried out a study on the performance of an upflow anaerobic sludge blanket (UASB) treating leachate from FW fermenters in Korea. FW was pre-acidified and stabilized in the acidogenic fermenters, and then fed to the UASB, which has a working volume of 41 L. A consistent high COD removal of 96 % was maintained while the HRT decreased from 3.9 d to 0.44 d, corresponding to an OLR raised from 1.8 kg COD/(m³·d) to 15.8 kg COD/(m³·d). The maximum production rate of biogas was 279 L/d at an OLR of 15.8 kg COD/(m³·d). The UASB performance started to deteriorate when the HRT was less than 0.44 d. At a HRT of 0.33 d, only 55 % COD was removed, while the pH was still at a constant level of 7.5 – 7.6.

A hybrid two-phase system was applied by Wang et al. (2002) to digest FW, which consisted of a semi-liquid recycle reactor and a UASB. The whole system was operated batch-wise. Food waste collected from a university canteen was pre-acidified in the acidification reactor. Leachate produced by the first reactor was 5 times diluted with the UASB effluent before being fed to the UASB. Two batch cycles (Run A and Run B) were performed, with 2 kg food waste fed into the acidification reactor and less than 10 kg COD/(m³·d) OLR for methanogenic reactor during each cycle. They reported that pre-acidification could be sufficient within 4 days, and 80 % of the total COD was removed in 10 days, with a methane production of 0.25 L/g VS_{added}. Without any control, pH in the first reactor dropped from 7.1 to 4.5 on day 1, and remained around 5.5 as the acidification continued. Because the leachate was diluted, and the granular sludge in UASB reactor was acclimated to the substrate with a pH of 5.5-6, the uncontrolled pH did not impose impacts on the UASB performance.

A recent study carried out by Grimberg et al. (2015) showed significantly higher methane production in two-phase mesophilic digestion than the single-phase operation (359 L CH₄/kg COD_{removed} and 481 L CH₄/kg COD_{removed} respectively). They employed one digester as an acid fermentation reactor, and two digesters working in parallel as methanogenesis reactors. Both phases were operated under mesophilic conditions (37.3 °C). Although the influent concentrations were highly fluctuating, the two-phase system was still able to sustain good performance over a long period of 400 days, and it was successfully maintained through low-loading summer periods.

- **Discussion**

By comparing the results listed in Table 1, it is clear that with an UASB reactor as a second-phase to treat pre-acidified food waste, a significantly higher OLR loading rate can be applied. All the systems compared were without any pH control, which proves that a two-phase system is pH self-maintained. Although two-phase systems gave a higher biogas production, the overall COD removal did not show a big difference. A suitable HRT or batch running time for hydrolysis depends on the specific type of substrate used, while a possible range of OLR for UASB can be 10-15 kg COD/(m³·d).

Table 1 A comparison of different two-phase anaerobic systems digesting solid waste

Reference	Phase	Reactor	HRT/running time*	OLR	pH	Temperature	Removal	
			(day)			°C	(%)	
(Pavan et al., 2003)	1	CSTR (1 m ³)	2-3	31.2 TVS/(m ³ ·d)	kg	4-5	Meso	83.5 (TVS)
	2	CSTR (0.8 m ³)	8-9	6.9 TVS/(m ³ ·d)	kg		Thermo	
(Shin et al., 2001)	1	Acidogenic fermenter						96 (COD)
	2	UASB	0.44	15.8 COD/(m ³ ·d)	kg	7.5-7.6	Meso	
(Wang et al., 2002)	1	Leaching bed (5.4 L)	4*	2 kg shredded food		4.5-7.5	Meso	80 (COD)
	2	UASB (3.0 L)	10*	10-2 COD/(m ³ ·d)	kg		Meso	
(Grimberg et al., 2015)	1	Digester (1 m ³)			kg	5.2	Meso	91 (COD)
	2	Digester (4.5 m ³)		0.79 COD/(m ³ ·d)		8.4	Meso	

*: Running time of the batch-wise system.

1.2.2 Toxicity and inhibition

VFAs and ammonia can cause a process failure or biogas reduction when their concentrations exceed a certain level. An upper limit of the concentration of these substances was summarized from several studies (Table 2).

VFAs concentrations up to 5000 mg COD/L do not show any inhibition to the AD system at a neutral pH, while a propionate concentration of 6000 mg/L can lead to a system imbalance (Khanal, 2008). Free ammonia is more toxic than ammonium, and ammonia toxicity is pH independent when exceeding 3000 mg N/L; methanogens are more sensitive to free ammonia compared to acidifiers (Khanal, 2008).

Heavy metals such as copper, zinc, and lead can also be toxic for AD process, but they are not covered in this study.

- **Discussion**

In most of the cases, the negative effects of these parameters are related to the pH value, the specific type of system, and the specific sludge. When several substances are present at the same time, they might lead to process deterioration at a low concentration. Hence, it is difficult to give exact limits of these toxicants/inhibitors. However, it is good to have estimation before starting a system.

Table 2 Reference upper-limits of inhibitors in AD system

Substance	Upper-limit		Reference
	Acidogenesis mg/L	Methanogenesis mg/L	
Ammonia	3000 (N)	700 (N)	(Khanal, 2008)
Acetate		5000 (COD)	(Khanal, 2008; Labib et al., 1992)
Propionate		6000	(Khanal, 2008)
Butyrate		>10000	(Khanal, 2008)

1.3 Methods for online VFA monitoring

Since VFA is proven to be an efficient indicator for AD process, many techniques have been investigated to develop an online VFA monitoring method, such as the Fourier-transformed infrared spectroscopy (FT-IR), titrimetry and electronic sensors (electronic noses). A short introduction and a comparison of these methods are presented in this section.

1.3.1 Fourier transform infrared spectroscopy (FT-IR)

The basic theory for infrared spectroscopy is that each compound has a unique absorbance pattern, in terms of shapes and band positions in the infrared absorption spectrum (Steyer et al., 2002). According to the Beer-Lambert law, the composition of the sample can be identified by comparing the sample spectrum with the reference spectra for targeted compounds, and the concentrations are related to the height of the absorbance bands (Steyer et al., 2002). An infrared spectrometer (or spectrophotometer) is used to produce sample spectrum.

FT-IR is developed based on an interferometer, in which the infrared light is split, and recombined after going through different paths. The interference patterns (between the initially identical light) created by the path differences can be Fourier transformed to get the actual spectrum. The Fourier transform has been applied in generating near-, mid- and far-infrared spectrum.

● Mid-infrared spectroscopy (MIR)

According to Steyer et al., (2002) MIR (wavelength 2-10 μm) was used only in the gas phase monitoring until 1990s, after which, the technology started to be applied in the liquid phase for online measurements in AD processes. The MIR is able to study the fundamental vibrations and associated rotational-vibrational structure of the targeted compounds.

FT-MIR was used to measure VFA continuously/semi-continuously in many studies. For example, works carried out by Steyer et al. (2002) and Spanjers et al. (2006) showed that FT-MIR was simple to use and to maintain. It was able to give accurate and reliable results over time and varied liquid characteristics, while no additional chemical is needed (Steyer et al., 2002).

In-line MIR monitoring was used for VFA, soluble Chemical Oxygen Demand (sCOD), acetate, bicarbonate, phosphate, sulphate, nitrate, nitrite, ammonium and Total Kjeldahl nitrogen (TKN) measurements simultaneously, and satisfactory agreement between in-line and manual analysis could be obtained for most measured variables (Spanjers et al., 2006). However, samples were required to be taken to the instrument, and an ultrafiltration loop as a pre-treatment system was needed to ensure a clear sample, otherwise the high solids content effluent would disturb the in-line

measurements. Using optical fibres for mid-IR spectroscopy (in the range of 2-10 μm) was not yet easy, and additionally, the pre-treatment system was still under development (Steyer et al., 2002).

Another study was done using ATR (attenuated total reflection)-MIR-FTIR to measure VFAs, in which a good prediction for acetic acid, propionic acid, isobutyric acid and isovaleric acid was achieved, while butyric acid could not be detected (Falk et al., 2015). In Falk's study, samples from a digester were also required to be filtered and transferred to a measurement cell for IR spectra recording.

- **Near-infrared spectroscopy (NIR)**

NIR is a technique using infrared spectroscopy in the wavelength range of 0.75-2.00 μm . Slightly different from MIR, it is based on molecular overtone and combination vibrations. According to Osborne et al. (1993), the chemical or physical composition of a sample can be reflected by the absorption of energy (caused by overtones and combination bands from fundamental infrared vibrations) in the -CH, -NH and -OH molecular groups.

With a high photon energy, near-infrared has low reflectivity and absorptivity, thus NIR is able to analyse samples that are strongly light scattering (i.e. opaque liquids, slurries) (Nordberg et al., 2000). It is rapid and non-invasive, and requires no chemical addition. Once calibrated with the help of multivariate data analysis, the sensor needed little maintenance (Holm-Nielsen et al., 2008).

In Holm-Nielsen's study, he used a Transflexive Embedded Near Infrared Sensor (TENIRS) to monitor glycerol and VFA contents in the biomass (Holm-Nielsen et al., 2008). The sensor was able to give excellent predictions; all pertinent levels of VFA could be quantified, with chemo-metric regression models being used. Jacobi et al. (2009) integrated a NIR-sensor into a full-scale biogas plant for 500 days, calibration models were built with the NIR-spectra collected in the fermenter. They reported a capability of the NIR-sensor to predict total VFA ($R^2=0.94$), acetic acid ($R^2=0.69$) and propionic acid ($R^2=0.89$). However, they also reported that bulb aging and temperature could have an impact on the spectra, which should be avoided during practical implementations (Jacobi et al., 2009).

1.3.2 Titrimetry

Titrimetric methods are generally accepted as superior for routine monitoring and control in terms of simplicity, speed and cost effectiveness (Feitkenhauer et al., 2002; Lahav et al., 2002). In titrimetric method, a titration curve is built to determine the VFA concentration, with the assumption that VFA is mainly acetic acid (Bouvier et al., 2002). In many studies, different pH points and various methods (i.e. two-point method, five-point method and n-point method) were applied based on different study purposes (Anderson & Yang, 1992; Bisogni et al., 1998; Feitkenhauer et al., 2002; Moosbrugger et al., 1993a; Moosbrugger et al., 1993b). For example, a point at pH 5.75 was chosen to minimise the influence of VFA, and a point at pH 4.30 was chosen to include the buffering capacity of both bicarbonate and VFA (Bouvier et al., 2002; Ripley et al., 1986). An n-point method with a least square linear regression model was applied to differentiate the VFAs (Bisogni et al., 1998).

Over the last decades, numerous quantitative and semi-quantitative titrimetric methods have been proposed for measuring VFA/alkalinity, but were found to be too complicated or not accurate enough (Lahav et al., 2002). A new method developed by Lahav et al. (2002) was reported to be able to process data for control purpose. This method used a mathematical model that requires 8 pH observations to determine VFA and alkalinity, which was evaluated to be accurate and repeatable.

Bouvier et al. (2002) also designed a titrimetric sensor, which was managed by home-built software. After five years of testing, they concluded that their titrimetric system was able to provide reliable

information for process monitoring and control; the sample taking, the titration and the calculation were fully autonomous, which only takes less than 3 minutes (Bouvier et al., 2002).

In Feitkenhauer's study, an online measurement cell applying a simple two-point method was developed (Feitkenhauer et al., 2002). The cost of this system was relatively low, and it was able to handle unfiltered samples from various points of an anaerobic treatment plant, with very low or very high VFA concentrations. Feitkenhauer's method could give high throughputs, a high reproducibility, and a stable performance under different salt concentrations (Feitkenhauer et al., 2002). In a VFA concentration range of 10-60 mmol/L, the corresponding factor was 0.998 between the titration and GC results.

The procedure proposed by Lahav et al. (2002) was relatively simple and can be easily implemented in field labs, while proper execution is still needed to achieve a high accuracy. A low VFA concentration sample should be adjusted (i.e. by adding a known amount of acetic acid) to increase the measurement accuracy for the Lahav's method (Lahav et al., 2002). The measurements were done every 30 minutes and manual maintenance was required (compatible with industrial applications) for the method of Bouvier et al. (2002).

1.3.3 Electronic sensors

The electronic sensors based on potentiometric sensors are used in arrays, which are also known as "electronic noses/tongues" or volatile compound mappers (VCMs). Thanks to the rapid progress in semiconductor technology, its use has been increased dramatically (Nordberg et al., 2000). Although individual sensors gives low specificity, relevant information can be obtained from a combination of several sensors (Nordberg et al., 2000; Rudnitskaya & Legin, 2008). It is possible to use the electronic sensors for monitoring in AD process with its sensitivity for gases and other volatile compounds (Nordberg et al., 2000).

The 29 VCMs used in the study were monitoring H₂ and total VFA off-line in the headspace of a CSTR, the results showed a high correlation for these two parameters (98 % and 93 % respectively) (Nordberg et al., 2000). While Buczkowska et al. (2010) used a novel flow-through array of solid state electrodes for online VFA and COD measurements in the liquid phase, the correlation coefficient between the predictions and real concentrations were 0.94-0.98 for COD and 0.75 for VFA. Provided a proper calibration method, the sensors can give reasonable predictions.

Their low price and high robustness make the sensor an attractive alternative hardware for complex process monitoring (Madsen et al., 2011). Although there is a big application potential, problems still exist in this type of sensors, such as fouling, degradation, and sampling issues.

1.3.4 Summary

Although acetic acid is the dominant acid produced in biogas digester, other individual VFAs are found to be also important as an online process indicator (i.e. propionate, butyrate and isobutyrate). The assumption (measuring acetic acid as total VFA) for the titrimetric methods limits their accuracy and the possibility for individual VFA measurements. Although the individual VFA prediction was not very satisfying, the NIR was able to measure acetate and propionate in the studies done by Jacobi et al. (2009) and Nordberg et al. (2000). However in most of the studies reviewed above, these techniques were only used to measure acetate or total VFA. Besides the advantages of each technique, they have certain drawbacks as well, for example, the requirements of manual sampling, pre-treatment, frequent maintenance, or chemical dosing. NIR was preferable for measuring the characteristics of slurry in a fermenter/digester, while MIR was used more often in liquid with lower solids content.

Although the titration and electronic sensors are less expensive, the FT-IR does not require any chemical dosage, and it is capable of online monitoring multiple parameters.

1.4 Mathematical calibration methods & relevant factors for IR technique

To extract quantitative information from spectroscopic signals, a calibration model should be built between explanatory observations (spectra) and the response values (reference). Usually, multivariate calibration models, such as multiple linear regression (MLR), principal component regression (PCR) and partial least squares (PLS), are applied for spectroscopic data (Beebe & Kowalski, 1987; Marbach, 2005; Thomas & Haaland, 1990).

The calibration model built for a specific analyte needs to be validated with external validation samples. After the validation, the calibration model will be able to be applied for unknown sample measurements.

However, due to the sensitivity of the infrared light (IR), the model can easily become invalid when the chemical or physical characteristics of the sample vary (Krapf et al., 2013). For instance, pH might fluctuate in the AD process, the pH has an impact on the hydrogen bonds of the analyte, which leads to a change in the IR spectra (Schenk et al., 2008). Since the calibration model is based on the relation between the spectra and the reference concentration, the predicted concentration will vary according to the change of the spectra.

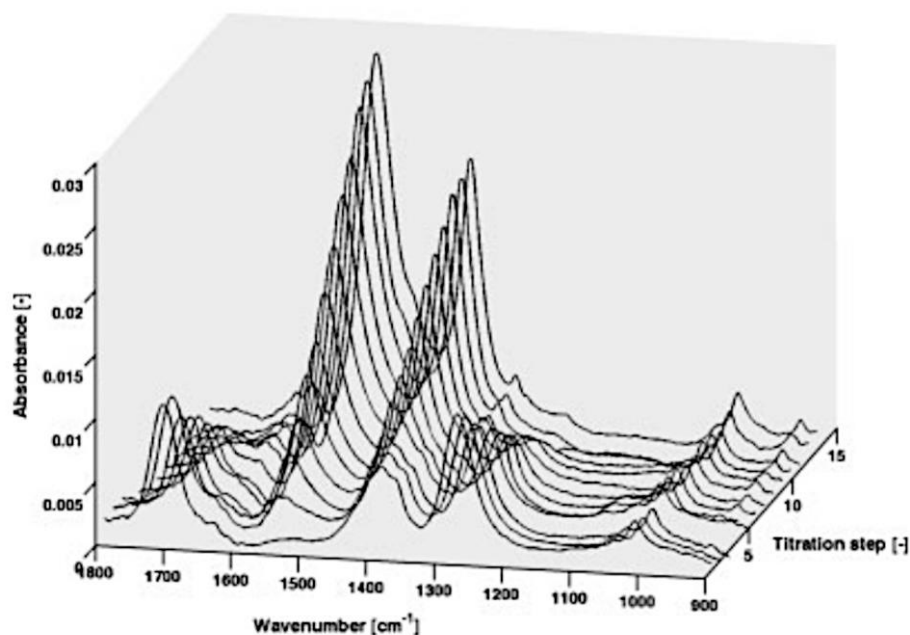


Figure 3 Spectrum of acetate under different pH (Schenk et al., 2008)

Besides pH, a few other relevant noises, such as temperature, and humidity, analyte concentrations might also influence the sensor performance (Jacobi et al., 2009; Krapf et al., 2013; Schenk et al., 2008). According to a recent study, the HCO_3^- and NH_4^+ also add to the adsorption peaks in the MIR wavelength range ($800 - 1800 \text{ cm}^{-1}$) (Bongards et al., 2014). The concentration of these two chemicals might affect the accuracy of IR measurements as well.

CHAPTER 2 RESEARCH QUESTIONS & OBJECTIVES

The OPTI-VFA project is aiming to develop a novel monitoring and controlling tool, the OPTI-VFA sensor, in order to improve the reliability, efficiency and profitability of the AD process. The VFA concentrations in AD processes are the main focus of this sensor. Calibration models of total VFA and 3 individual VFAs (acetate, propionate and butyrate) were built by our Finnish partner, the Technical Research Centre of Finland (VTT). A prototype with a specially designed software program was finished in April 2015.

With an impending need for a reliable online VFA monitoring system for the AD process, the research question of the study is whether the OPTI-VFA sensor is able to meet this demand. In more detail, is the sensor able to give reliable VFA concentration predictions, do the relevant factors (pH, temperature, HCO_3^- and NH_4^+) affect the sensor performance, and how can the sensor be improved?

Firstly, is the sensor able to give reliable predictions for total VFA, acetic acid, propionic acid and butyric acid concentrations under controllable laboratory conditions?

- To answer this question, a lab-scale validation needs to be done. The AD system should be operated under various conditions (pH, HRT and OLR) to create a dynamic VFA profile. Online VFA measurement by the sensor and a reference offline measurement by GC should be compared, in order to demonstrate the sensor's ability to predict the VFA concentration and follow the dynamics of the VFA concentrations. Other basic parameters indicating the system state, such as pH, COD and $\text{NH}_4\text{-N}$, should also be checked to support the conclusion.

Secondly, is the sensor able to give reliable predictions for total VFA, acetic acid, propionic acid and butyric acid under uncontrollable full-scale conditions?

- To answer this question, a full-scale validation needs to be done. To test the robustness of the sensor, a validation in a full-scale AD system should be carried out. In the full-scale treatment plant, measurement conditions are less controllable. The sensor will be exposed to a more fluctuating situation (i.e. a larger temperature/pH/flow rate range). By comparing with the reference GC measurements, the reliability of the sensor predictions in these conditions can be shown.

Thirdly, do the relevant factors affect the sensor performance?

- Manual sample matrices should be prepared to validate the sensor. Regarding the relevant factors such as pH, temperature, HCO_3^- and NH_4^+ , samples with a series of impact levels have to be made and measured in addition to the online measurements. Compared with a 0 impact level reference, the significance of these factors that are affecting the sensor performance can be concluded.

Fourthly, is it possible to improve the sensor if it is not giving reliable predictions?

- The relevant factors causing the inaccuracy of the prediction should be determined by analysing the spectra of the online predictions and batch tests. The relevant impact found in the prediction spectra should be excluded in order to improve the calibration model. Additionally, comparison of different calibration methods should be done to find a suitable calibration method.

Therefore, the main purpose is to evaluate the performance of the OPTI-VFA sensor under different conditions (high VFA concentrations, low VFA concentrations, and interference present). To gather the data to answer the research question, experiments were planned according to the four research questions presented above. Detailed explanations about the two-phase system and operations, monitoring methods and monitored parameters are given in Chapter 3.

3.1.2 Biowaste, leachate and inoculum

The biowaste, the leachate and the inoculum used in this research were collected from the full-scale biogas plant of Attero in Venlo, the Netherlands. Attero is a company using domestic remnant waste, organic waste and mineral waste to generate sustainable power, heat and gas. The biowaste used in the plant includes 75 % garden waste and 25 % kitchen waste of households (Figure 6). The undegradable waste was firstly picked out, and the rest was cut into small pieces to be hydrolysed in the hydrolysis tunnels for 7-9 days. The biowaste taken from the plant was again pre-treated, with slowly degradable part (i.e. twig) picked out. The leachate was collected from the storage tank where the hydrolysis water and the UASB effluent were mixed. The inoculum used for the anaerobic reactor was taken from the UASB. The biowaste and the leachate used to feed the reactors and the inoculum taken from the plant were kept in the fridge (0-4°C).



Figure 6 Biowaste (left), Leachate (middle), inoculum (right)

The characteristics of the biowaste, leachate and inoculum from Venlo are shown in Table 3.

Table 3 Characteristics of biowaste, leachate and inoculum for system start-up

	Biowaste	Leachate	Inoculum
TS (g/kg wt)	449.5	22.6	334.1
VS (g/kg wt)	262.6	11.4	120.7
TSS (g/L)	-	0.6	276.1
VSS (g/L)	-	0.6	83.6
tCOD (g O ₂ /L)	-	25.8	-
sCOD (g O ₂ /L)	-	20.6	-
TP (mg/L)	-	74.0	-
RP (mg PO ₄ -P/L)	-	23.4	-
TN (mg N/L)	-	2.0	-
NH ₄ -N (mg NH ₄ -N/L)	-	1.7	-

3.2 Experimental setup of the two-phase system

A two-phase AD system was chosen to achieve high VFA concentrations in the leaching bed reactor, and low VFA concentrations in the UASB reactor (near the discharge point).

The schematic of the two-phase system used in this study is shown in Figure 7, photography of the experimental setup is shown in Appendix E, Figure E1. This setup was established to mimic the full-scale biogas plant of Attero.

The first-phase, leaching bed reactor, was used for VFA production. In the leaching bed, biowaste was packed in a filter bag and then submerged in the liquid (Appendix E, Figure E2). The produced VFA diffused into the liquid, and the liquid was being re-circulated. The hydrolysis cycle ended after a certain operational period. The bag was replaced with a new bag of biowaste, and then a new cycle started. The working volume of the leaching bed was 5.5 L.

The second-phase, UASB reactor, was used for methane production. It had a working volume of 7 L. The VFA produced in the first-phase was fed to the UASB. During the start-up period, the storage tank was filled with leachate from the Venlo biogas plant, and the leachate was used to keep a stable OLR for the second-phase. The OLR was varied by the control software of CEIT during the later operation period.

The locations of the 5 pumps used for the two-phase system are indicated in Figure 7. Pump 1 is the first-phase water feeding pump; pump 2 is the second-phase feeding pump; pump 3 is the first-phase re-circulation pump; pump 4 is the first-phase production extraction pump; and pump 5 is the second-phase re-circulation pump.

Both reactors were operated under mesophilic conditions (35 °C), with a TC 16 water-bath from P.M. Tamson Instruments.

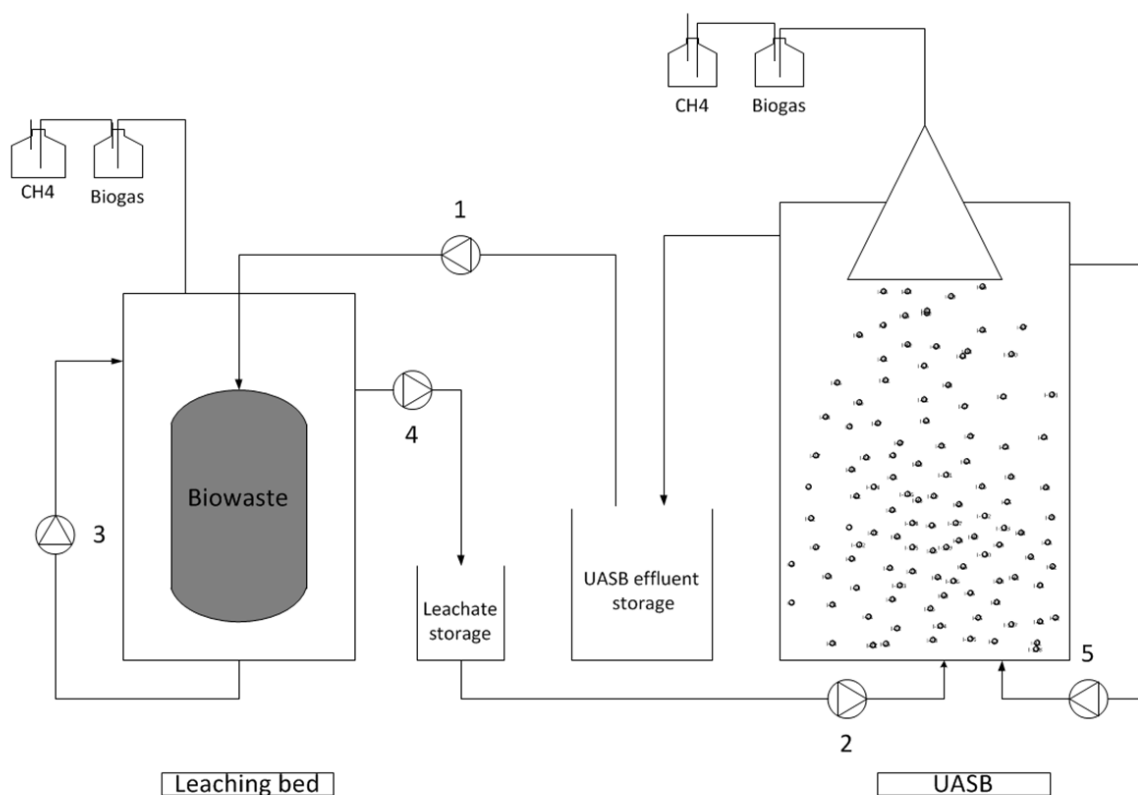


Figure 7 Two-phase anaerobic system

3.2.1 The leaching bed reactor

The first reactor was operated as a batch, with a cycle of various days (Table 4), each cycle had a different running time/liquid feeding rate to create variation in VFA concentrations. Therefore, a larger VFA span could be used for the sensor validation. The liquid feeding and discharging were equal in terms of flow rate. Tap water was fed to cycle 1, and UASB effluent was fed to cycle 2-6. The operation of 6 cycles were summarised in Table 4.

Table 4 Feeding strategy for leaching bed reactor

Cycle No.	Running time (days)	Biowaste (g)	Feeding rate (L/day)	Discharge rate (L/day)
1	4	1034.5	4	4
2	9	1035.7	2→0*	2→0*
3	5	1025.2	0	0
4	3	1024.4	0.5	0.5
5	14	1040.3	0.5	0.5
6	18	1026.5	0.5→0*	0.5→0*

(*: Feeding and discharging stopped on day 1 for cycle 2, and on day 4 for cycle 6)

3.2.2 The UASB reactor

The second reactor was operated continuously from April 2015 to July 2015. The substrate was the leachate from an Attero's full-scale biogas plant located in Venlo or from Water Lab at TU Delft. The up-flow velocity was also varied between 1 m/h and 2 m/h during the operational period. The information is given in Table 5.

Table 5 Feeding strategy for UASB reactor

Period (days)	Leachate from	Upflow velocity (m/h)
0-21	Venlo	2.0
22-26	Lab	2.0
27-30	Lab	1.5
31-33	Venlo	1.5
34-36	Lab	1.0
37-60	Venlo	1.0
61-78	Venlo	1.5
79-100	Venlo	1.5
100-105	Lab	1.5

3.2.3 Basic parameters measured

To track the system performance, basic parameters such solids contents, COD contents and ammonia contents were measured daily.

- TS/VS and TSS/VSS

The measurement of solids contents were determined following standard methods (Gaterell et al., 2000). About 10 g (or 10 ml) sample was kept in each aluminium dish at 103~105°C for 4 hours, in order to determine total solids content (TS). After the TS measurement, the sludge was put in the oven again at 500 °C for 2 hours to determine the volatile solids content (VS). The measurement of total suspended solid (TSS) was done firstly by filtrating the sample (around 10 mL) through a glass fibre filter, which has a pore size of 1.2 µm. Triplicate measurements were performed in parallel for each parameter; the averaged value was taken as the final result, and standard deviation of the triplicate as errors.

- **sCOD/tCOD, rP/tP, NH₄-N/tN**

Soluble COD (sCOD) and total COD (tCOD) contents were measured with test cells from HACH® LANGE LCK 014, reactive phosphorus (rP) and total phosphorus (tP) concentrations were measured with LCK 350 test cells, and ammonium (NH₄-N) and total nitrogen (tN) concentrations were measured with HACH® LANGE LCK 303 and Spectroquant® test cells. For tCOD, tP, and tN measurements, triplicate measurements were performed in parallel to get an average result. For sCOD, rP and NH₄-N measurements, the samples were first centrifuged at a speed of 12000 rpm for 15 minutes, and then filtered with syringe membrane filters (pore size 0.45 µm). Duplicates were measured in parallel. sCOD, tCOD and NH₄-N were measured every day (except Sunday) for both reactors.

Table 6 Cell kits used for variables measurement

Variables	Manufacturer	Kits number	Measuring range
COD	HACH® LANGE	LCK 014	1000-10000 mg O ₂ /L
Ammonia	HACH® LANGE	LCK 303	2-47 mg NH ₄ -N/L
Nitrogen	Spectroquant®	1.14563.0001	0.5-25.0 mg NO ₃ -N/L
Phosphorus	HACH® LANGE	LCK 350	2-20 mg PO ₄ -P/L 6-60 mg PO ₄ /L

- **PA/TA**

Partial alkalinity (PA) and total alkalinity (TA) are also important indicators since they represent the buffer capacity in the reactor. Titration method was employed using a 787 KF auto-Titrator developed by Metrohm AG to determine the alkalinity of effluents from both reactors. The sample used was 10 ml. PA and TA were expressed in the unit of gram calcium carbonate per litre. Two-point method was applied with a middle-point at pH 5.75 and an end-point at pH 4.3. PA and TA were calculated based on titration every four days for the UASB, and every day for the Leaching bed.



Figure 8 Metrohm AG 787 KF auto-Titrator

- **VFA**

An Agilent 7890A GC was employed for the VFA measurement. Before measuring with GC, samples were pre-treated in order to avoid a blocking of the GC injecting needle. The samples were firstly centrifuged with a Thermo Scientific Sorvall ST 16R centrifugal machine for 15 minutes, at a speed of 12000 rpm. 4°C was kept for centrifugation in order to avoid further consumption of VFA by the microorganisms. After centrifugation the samples were filtered with syringe membrane filters (with a pore size of 0.45 µm). The GC measurements were taken as a reference for the sensor validation.



Figure 9 Agilent 7890A GC

Table 7 Measure frequency for manual measurements

Parameters	Frequency	
	Leaching bed	UASB
TS/VS	-	-
TSS/VSS	-	-

sCOD/tCOD	Once per day	Once per day
rP/tP	-	-
NH₄-N/tN	Once per day	Once per day
PA/TA	Once per day	Once per four days
VFA	Once/twice per day	Once/twice per day

- **pH/Temperature**

The pH and temperature in the two-phase system were monitored with sensors online.

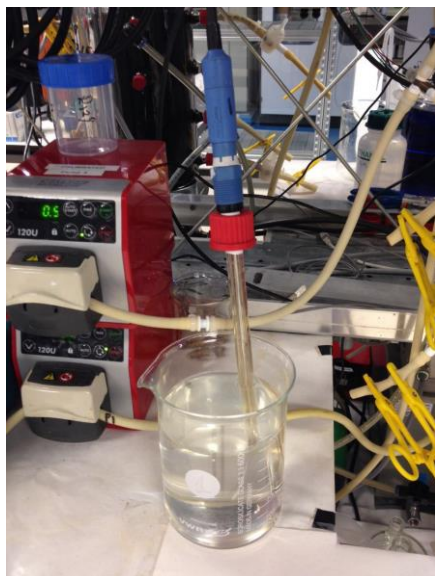


Figure 10 pH and temperature sensor

- **Biogas & Methane**

Biogas and methane production were monitored with Ritter® Apparatebau gas meter and they were recorded online.

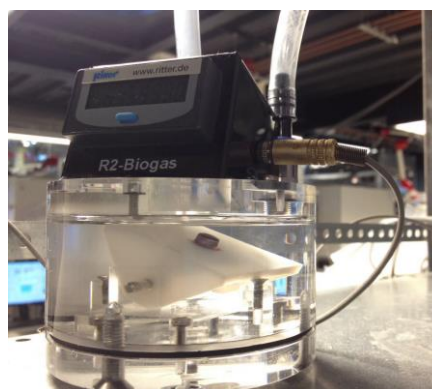


Figure 11 Gas meter

3.2.4 The OPTI-VFA sensor

The OPTI-VFA sensor was used to monitor the dynamic VFA profile in the liquid (in both phases). The measurements were compared with offline GC measurements. The hardware of the sensor is a commercial Bruker Matrix MF FT-IR and a 2-bounce diamond ATR fibre probe (27 cm) from Art

Photonics. The two components are connected by an optical fibre, and the length of the optical fibre is about 125 cm (see Figure 12).

During the measurements, the OPTI-VFA sensor was installed in the headspace of the reactor or submerged in the sample. MIR wavelengths were sent by the Bruker unit, and transmitted by the optical fibre to the ATR probe. The light intensity was measured both before reflected by the diamond tip and after. Software designed by VTT was installed on a PC to carry out the measurements. Parameters such as wavelength range, number of spectrum and number of measurements can be set. The measured spectra and VFA profile could also be shown on the user interface (Appendix E, Figure E3).

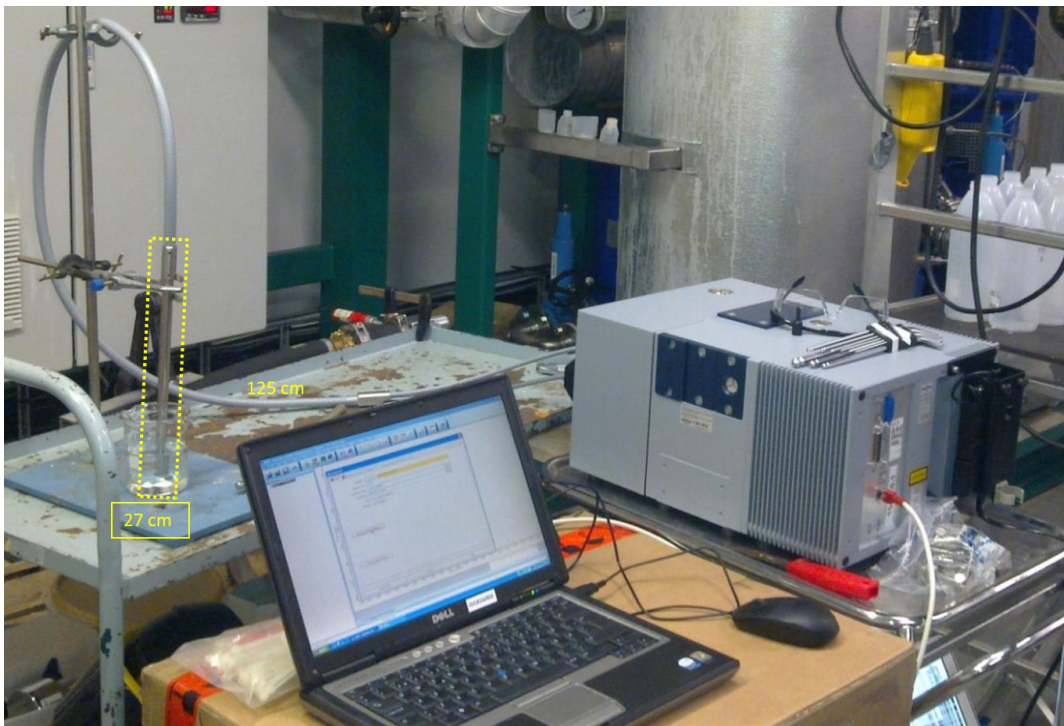


Figure 12 Bruker Matrix MF FT-IR system , and ATR fibre probe

3.3 In-process & off-process VFA measurements

3.3.1 Sensor validation in lab-scale

The VFA concentrations were measured in-process (inside the reactor) every 15 minutes during the night with the OPTI-VFA sensor (Figure 13a). During the day, 50 mL samples were collected in beakers

every 2 hours, and then measured off-process (Figure 13b). When measuring off-process, samples were kept in a water bath with the same temperature as that in the reactors, which were $35 \pm 0.1^\circ\text{C}$ for leaching bed and $33 \pm 0.1^\circ\text{C}$ for UASB, respectively. A background measurement was performed in demineralized water at the same temperature before measuring the samples. The measurements conducted in the same day were all based on this background.

The temperature was controlled using PMT TC 16 water bath combined with an IKA® ETS-D6 electronic contact thermometer (Appendix E, Figure E4). The electronic contact thermometer was equipped with an optimized PID control. Therefore, throughout the whole measurement, the temperature was kept stable to mimic practical measuring environment in reactors. VFA contents of each sample were measured 3 times (350 scans each time) with 5 minutes interval by the OPTI-VFA sensor. MIR wavelength range of $800\text{-}1800\text{ cm}^{-1}$ was selected.

After being measured by the OPTI-VFA sensor, the off-process samples were then pre-treated and measured by GC.

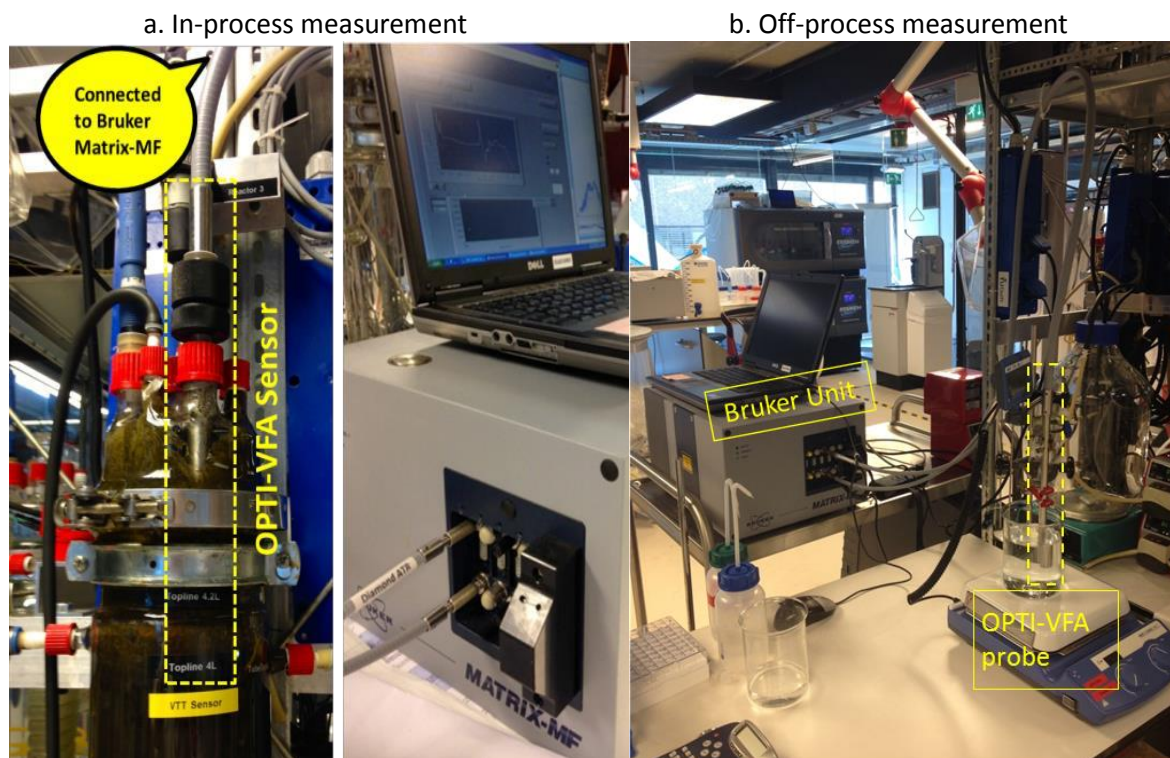


Figure 13 VFA profile monitoring with OPTI-VFA system

3.3.2 Sensor validation in full-scale

The OPTI-VFA system was brought to the full-scale treatment plant (Attero) in Venlo for validation in May 2015. The sensor was installed in the bypass pipelines to measure the VFA dynamic concentrations for both phases (see Figure 14 and 15). Before the installation, a background spectrum was measured in demi water at the process temperature.

The leachate samples and the UASB effluent samples were also collected in beakers every hour during the day. All the samples were kept in a fridge ($0\text{-}4^\circ\text{C}$) and sent back to the laboratory in TU Delft. The VFAs in the samples were measured by GC in the laboratory.

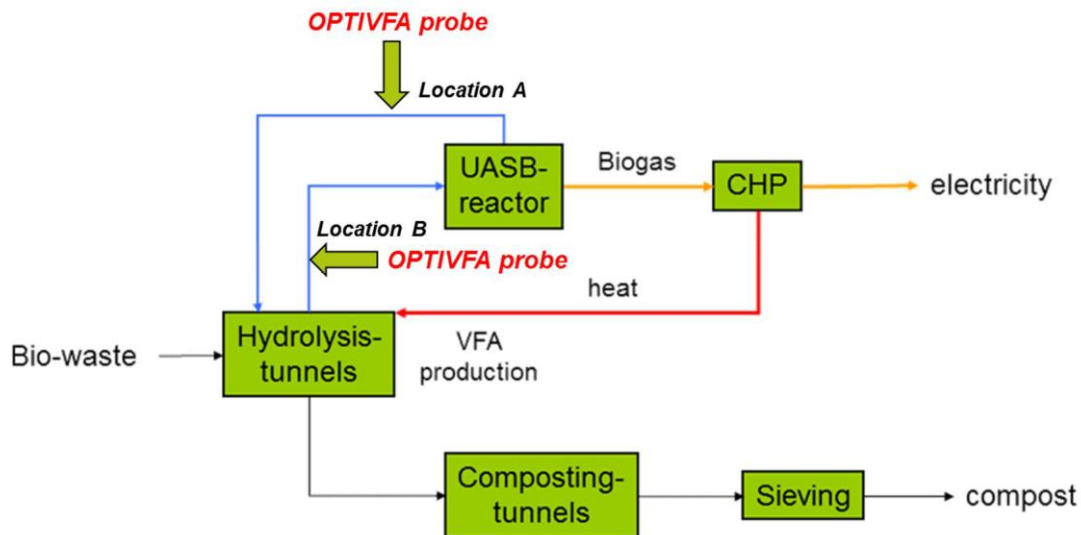


Figure 14 Installation point of OPTI-VFA sensor in the full-scale biogas plant



Figure 15 In-process measurement in Venlo

3.4 Batch tests

3.4.1 pH tests

Two sample matrices were used for the validation of the sensor, with varied pH values. The demi water matrix was spiked with analytical grade acetic acid, propionic acid and butyric acid solutions (Table 8). The leachate matrix was taken from the Venlo full-scale treatment plant.

The pH changes were adjusted by adding analytical grade NaOH and HCl solutions with high concentrations (Table 8). Conductivity and salinity after adjustments were also measured, with a

WTW LF 325 conductivity meter. The samples were measured both by GC and the OPTI-VFA sensor, and results were compared for sensor validation.

There were 7 samples with an initial pH around 2.6 in the demi water matrix, and 7 samples with an initial pH of 7.6 in the leachate matrix. The first samples with a subscript of 0 were without pH adjustments, while the pH in other samples was adjusted. It is shown in Table 9. The sample matrices were kept in a water bath where the temperature was controlled at $35 \pm 0.1^\circ\text{C}$, and measured with the OPTI-VFA sensor.

Table 8 Chemicals used for pH tests

Chemicals	Density (g/ml)	Purity (%)	Quality
Acetic acid	1.049	99.7	analytical grade
Propionic acid	0.993	99.5	analytical grade
Butyric acid	0.964	99.0	analytical grade
NaOH	1.370	33.0	analytical grade
HCl	1.200	37.0	analytical grade

Table 9 pH changes for sensor validation

Demi water matrix				Leachate matrix			
Sample	Original pH	Adjusted pH	Temperature	Sample	Original pH	Adjusted pH	Temperature
D ₀	2.6	2.6	26.4	L ₀	7.7	7.7	24.8
D ₁	2.6	3.9	26.0	L ₁	7.5	3.4	25.0
D ₂	2.6	5.0	25.8	L ₂	7.6	4.3	25.0
D ₃	2.6	6.2	24.8	L ₃	7.6	5.5	25.1
D ₄	2.7	7.0	24.9	L ₄	7.6	6.5	25.0
D ₅	2.7	7.7	25.0	L ₅	7.6	8.3	24.9
D ₆	2.7	9.1	25.0	L ₆	7.6	9.0	24.9

Table 10 pKa values of individual VFA

VFA	pK _a
Acetate	4.75
Propionate	4.87
Butyrate	4.81

The pH has an impact on the dissociation level of the VFAs. To study the impact of VFA dissociation on the sensor performance, the dissociation level (Equation 1) of the VFAs was calculated with the pH and pK_a values (Table 9 and 10) of each VFA.

Equation 1

$$\frac{[A^-]}{[HA]} = 10^{pH-pK_a}$$

3.4.2 Temperature tests

The same leachate sample L_0 from Venlo full-scale treatment plant was used in temperature tests. A background spectrum was measured at 35 °C, and the sample was then measured at various temperatures given in Table 11. The lowest temperature 33 °C was observed in the lab-scale UASB effluent, and the highest temperature 42.4 °C was observed in the full-scale Leaching bed reactor. This temperature span was selected to validate the sensor performance.

Table 11 Temperature variation for sensor validation

Sample	Measurement	Temperature (°C)
Demi water	Background	35
Leachate	T_0	35
Leachate	T_1	33
Leachate	T_2	36
Leachate	T_3	38
Leachate	T_4	40
Leachate	T_5	42
Leachate	T_6	44

3.4.3 Interference of HCO_3^- and NH_4^+

Four matrices (Table 12) were applied to examine the impact of these two ions. Each sample had a total volume of 30 mL, which was composed of $\text{NaHCO}_3/\text{NH}_4\text{Cl}$ solution and/or base matrix (demi water or UASB effluent). The concentration increases with the sample number, which are given in Table 13.

Table 12 Compositions of HCO_3^- and NH_4^+ Matrix

Base Matrix	Number	NaHCO_3 (mL)	Stock	Base Matrix (mL)	Number	NH_4Cl (mL)	Stock	Base Matrix (mL)
Demi-water	1	0.00		30.00	1	0.00		30.00
	2	10.00		20.00	2	10.00		20.00
	3	20.00		10.00	3	20.00		10.00
	4	30.00		0.00	4	30.00		0.00
UASB Effluent	1	0.00		30.00	1	0.00		30.00
	2	10.00		20.00	2	10.00		20.00
	3	20.00		10.00	3	20.00		10.00
	4	30.00		0.00	4	30.00		0.00

Table 13 HCO₃⁻ / NH₄⁺ concentrations in each sample

Matrix	Sample number	NaHCO ₃ (g/L)	NH ₄ Cl (g/L)	Sample number	NaHCO ₃ (g/L)	NH ₄ Cl (g/L)
Demi-water	1	0	0.0	1	0.0	0.0
	2	14.3	0.0	2	0.0	7.5
	3	28.6	0.0	3	0.0	15.6
	4	42.8	0.0	4	0.0	22.6
UASB Effluent	1	13.4	6.9	1	13.4	6.9
	2	26.7	6.9	2	13.4	13.9
	3	40.5	6.9	3	13.4	21.6
	4	52.0	6.9	4	13.4	30.5

3.5 Methods for OPTI-VFA sensor improvements

3.5.1 Two calibration methods applied

In this study, two types of calibration models were applied and evaluated for the OPTI-VFA system, with the spectra and GC references collected. They are multivariate partial least squares (PLS) regression model, and spectral matched filter (SMF) calibration model (or science based calibration model (SBC)). These models are expressed in mathematical equations below. Before building the calibration model, all the data were analysed qualitatively by principal component analysis (PCA) method. Root mean square error (RMSE) and coefficient of determination (R²) were calculated to compare the model performance.

Equation 2 PLS model (VTT, 2015)

$$X = TP^T + E$$

$$y = Tq + f$$

The n*p matrix **X** is the independent observations, which is decomposed into orthogonal n*p matrix **T** and non-orthogonal p*j matrix **P**. Thus the covariance between **T** and **y**, the n*1 reference values, can be maximised. While **q** is the y-loadings (j*1), **E** and **f** are the model residuals. PLS model searches for the latent variables that are meaningful for predicting results (**y**) from measurements (**X**). And the latent variable j determines the complexity of the model.

Equation 3 SMF model (Marbach, 2002; VTT, 2015)

$$X^T = y \cdot g^T + X_n^T$$

$$b = (\Sigma^{-1} \cdot g) / (g^T \cdot \Sigma^{-1} \cdot g)$$

Matrix **X^T** is the measured spectrum. Matrix **y** is the reference value. The matrix **g^T** represents the response spectrum of the analyte of interest and **X_n^T** represents the noise in the measured spectrum, such as instrumental error and interfering spectra. SMF model is aiming to find an optimal regression

vector that optimizes the signal-to-noise ratio of the output. Such a regression vector \mathbf{b} can be found when the multivariate signal response \mathbf{g} and noise Σ^{-1} are known a priori.

The calibration models of total VFA, acetic acid, propionic acid and butyric acid were built with these two methods. The validation dataset collected in this study were used to validate and improve these models.

3.5.2 Re-measurement of the calibration samples

The concentrations of individual VFAs in the calibration samples should be uncorrelated, in order to create an ideal situation to study their responses separately. However, the analysis of GC results showed that a natural correlation existed between VFA species. Spiking samples to break down this natural correlation should be done, thus to ensure the calibration model only react to the concentration changes of the targeted VFA.

The leachate and the UASB effluent samples from Venlo were shipped to Oulu, and used to build a first calibration model for acetic acid, propionic acid, butyric acid and total VFA. Due to a less accurate VFA concentration reference (caused by i.e. VFA variation during the shipment from Delft to Oulu, errors in pipetted volumes), the predictions given by the sensor showed a 200 mg/L root mean square error of calibration (RMSEC). To modify the calibration curve, these calibration samples were sent back to TU Delft laboratory and re-measured by both OPTI-VFA sensor and GC. The samples are listed in Table 14. Under the same sample name, there are two samples with/without pH adjustment.

Table 14 List of Spiked calibration samples with reference VFA concentrations

Order	Name	Acetic acid	Propionic acid	Butyric acid	pH	Adjusted pH
		(mg/L)	(mg/L)	(mg/L)		
Base VFA	UASB effluent	15	2.5	0	8.05	-
1	222	2007	2001	1500	7.02	7.89
2	132	15	4000	1500	7.00	7.97
3	213	2007	2.5	3000	7.08	7.98
4	121	15	2001	0	7.49	7.97
5	233	2007	4000	3000	6.71	7.98
6	211	2007.5	2.5	0	7.37	7.99
7	321	4000	2001	0	6.91	7.97
8	222	2007	2001	1500	6.89	7.99
9	323	4000	2001	3000	6.62	7.96
10	332	4000	4000	1500	6.64	7.99
11	112	15	2.5	1500	7.60	7.96
12	312	4000	2.5	1500	6.91	7.97
13	231	2007	4000	0	6.93	7.98
14	123	15	2001	3000	7.19	7.96
15	222	2007.5	2001	1500	7.03	7.97
16	111	15	2.5	0	8.05	-
17	333	4000	4000	3000	6.02	8.00
18	113	15	2.5	3000	7.10	7.99
19	331	4000	4000	0	6.39	8.02
20	122	15	2001	1500	7.03	7.99
21	322	4000	2001	1500	6.71	8.01
22	131	15	4000	0	7.16	7.99
23	313	4000	2.5	3000	6.83	8.00
24	133	15	4000	3000	6.89	8.01
25	311	4000	2.5	0	7.03	7.99
26	212	2007	2.5	1500	7.15	8.00
27	232	2007	4000	1500	6.84	7.98
Base VFA	Leachate	1993	1067	161	7.62	-
1	133	1993	3000	1000	6.98	7.57
2	222	2746	2033	580	7.65	7.65
3	111	1993	1067	161	7.66	-
4	131	1993	3000	161	7.14	7.60
5	313	3500	1067	1000	6.97	7.62
6	113	1993	1067	1000	7.42	7.60
7	311	3500	1067	161	7.12	7.62
8	331	3500	3000	161	6.86	7.60
9	333	3500	3000	1000	6.77	7.60
10	114	1993	1067	4161	6.80	7.60
11	411	5993	1067	161	6.75	7.60
12	141	1993	5067	161	6.82	7.60

CHAPTER 4 RESULTS & DISCUSSION

4.1 System performance

The overall performance of the lab-scale two-phase system is presented in this section.

4.1.1 Leaching bed reactor

Six hydrolysis cycles were performed in the study. During each cycle, parameters such as COD, VFA, NH_4^+ , and alkalinity were measured manually. Cycle 1, 2, 4 and 5 served for producing leachate for the UASB (details in Appendix A1). Only Cycle 3 and 6 were monitored with the OPTI-VFA sensor throughout the whole cycle, thus the validation was carried out mainly in these two cycles. Results of the basic parameters from the two cycles are presented below.

- **COD**

Figure 16 shows the COD results of these two cycles. The two cycles started with an initial tCOD of about 5200 mg/L and sCOD about 4800 mg/L. Feeding with UASB effluent, the leaching process maintained a constant pH of around 7.4-7.5 during these two cycle.

The operation strategy with no liquid feeding (only recirculation) in cycle 3 showed the highest tCOD concentrations (peak tCOD was 14500 mg/L), and a higher tCOD increasing speed (1600 mg COD/L·d) than other . The COD concentration kept increasing during the 5 days cycle.

While in cycle 6, the concentration peak (about 10500 mg/L) and the increasing rate for the first 5 days (1000 mg COD/L·d) were lower. The COD concentration became relatively stable during day 5 and 11, and started to decrease after day 11. Probably the hydrolysis process was sufficient in 5 days this is in agreement with Wang's study (Wang et al., 2002). Besides, the effect of COD consuming bacteria did not show up before day 11, thus the COD concentration was constant. After day 11, the VFA was significantly consumed (as shown in Figure 17b), so the COD concentration decreased.

Regarding the sCOD content in the total COD, it increased in the first 5 days, and then started to decrease. The highest sCOD percentage was 89.7 % in cycle 3. In cycle 6, 88.9 % COD was soluble in the leachate on day 7, but it reduced to only 81.8 % on day 17. Combining with Figure 17, it can be seen that the sCOD content varied according to the VFA concentrations. The increased sCOD mainly consisted of VFAs.

By adding UASB effluent to the leaching bed reactor, the alkalinity could be reused, so there was no need to adjust the leachate pH before using it as the substrate for the UASB, but it also caused a reduction in COD concentration after 10 days. To keep a high tCOD concentration in the leachate, a running time of less than 10 days for the process was required.

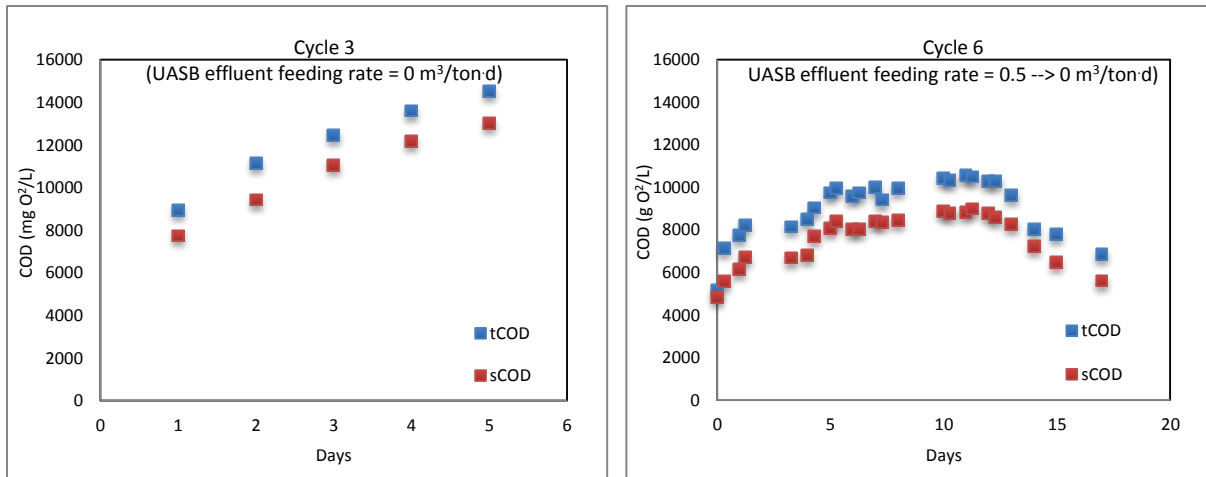


Figure 16 COD results of cycle 3 and cycle 6

- **VFA**

The VFA results of the two cycles are shown in Figure 17. The VFA concentrations showed the same trend as the COD concentrations. With the constant pH of 7.4-7.5, production of alcohols was prevented and the VFA production was improved.

In cycle 3, the leaching process continued for 5 days, the methanogens were not able to play a role in this short time period. The total VFA increased with time, from around 1000 mg/L on day 1 to 6500 mg/L on day 5. Under this operation strategy, the biowaste showed a VFA production rate of 1100 mg/L/d.

In cycle 6, the VFAs increased from around 60 mg/L to 3600 mg/L, and then decreased to 340 mg/L at the end of the cycle. The lower VFA peak in this cycle might be caused by a larger amount of methanogens in the UASB effluent, which was fed to the cycle 6. Thus the VFA consumption was higher than in cycle 3 during day 0-5. The VFA concentration was almost constant during day 7-10, it might be both the hydrolysis and acidification process were sufficient within 10 days.

The VFA concentrations were always much lower than the sCOD concentrations. On day 1 the VFA/sCOD ration was about 1:4-1:6, and it was about 1:2-1:3 at the peak concentrations. This might be caused by the production of some other long chain/mid chain fatty acids, or the presence of inorganic compounds (i.e. sulphide).

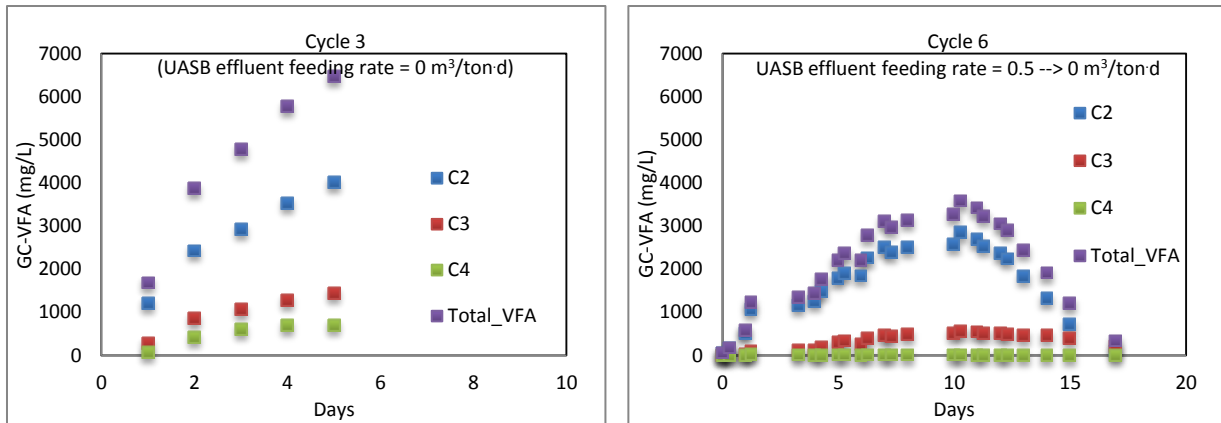


Figure 17 VFA results of cycle 3 and cycle 6

- $\text{NH}_4^+\text{-N}$

The ammonia concentration in both cycles was constant. In cycle 3, the ammonia concentration was around 1500 mg $\text{NH}_4\text{-N/L}$. In cycle 6, it was around 1700 mg $\text{NH}_4\text{-N/L}$. Since the ammonia accumulated in the UASB, the concentration in the effluent that fed to cycle 6 was higher than that fed to cycle 3. The ammonia concentration contributed to the buffer capacity, which helped to keep a constant pH in the leaching bed reactor.

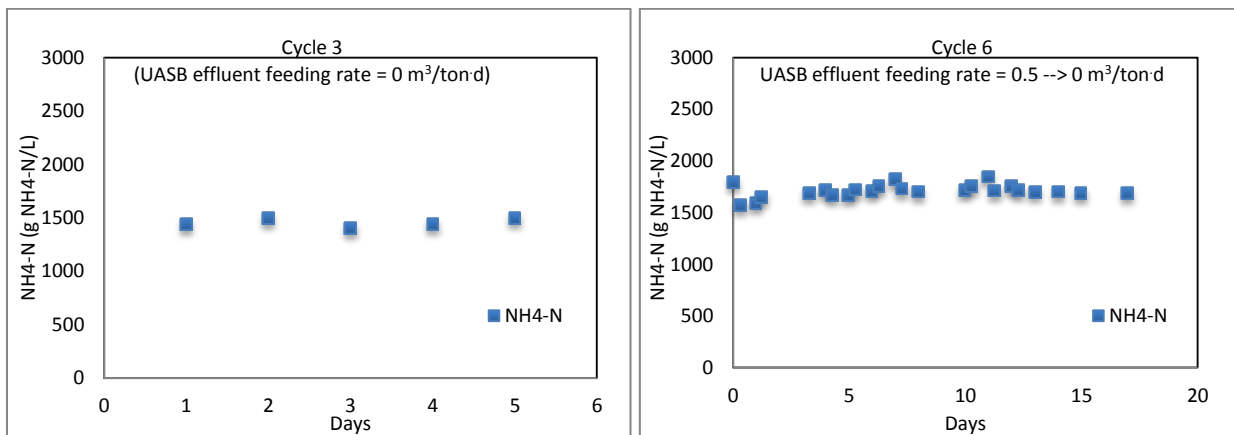


Figure 18 Ammonia results of cycle 3 and cycle 6

- PA/TA

Alkalinity was measured only for samples from cycle 5 and cycle 6, which is shown in Figure 19.

On the left panel of Figure 19, the blue marks stand for PA, which is the measure of bicarbonate and ammonia concentrations; the red marks stand for TA, which includes the bicarbonate, ammonia, and VFA concentrations.

The TA remained around 8 g $\text{CaCO}_3\text{/L}$ in cycle 5, and around 9 g $\text{CaCO}_3\text{/L}$ in cycle 6. The buffer capacity in the UASB reactor increased, thus the TA also increased in the leaching bed reactor. PA varied according to the VFA producing rates and the concentrations, but with a delay of 1-2 days. As we can see in cycle 5, the lowest peak of PA was on day 3 and day 7, while the highest VFA producing

rate was on day 3 and the highest VFA concentration was on day 6. Similar situation could be found in cycle 6, where the lowest PA peaks were on day 1 and day 12, and the peak of VFA producing rate was on day 1, the peak of VFA concentration was on day 10.

Generally, the high buffer capacity was able to maintain a constant pH under fluctuated VFA concentrations in these two cycles.

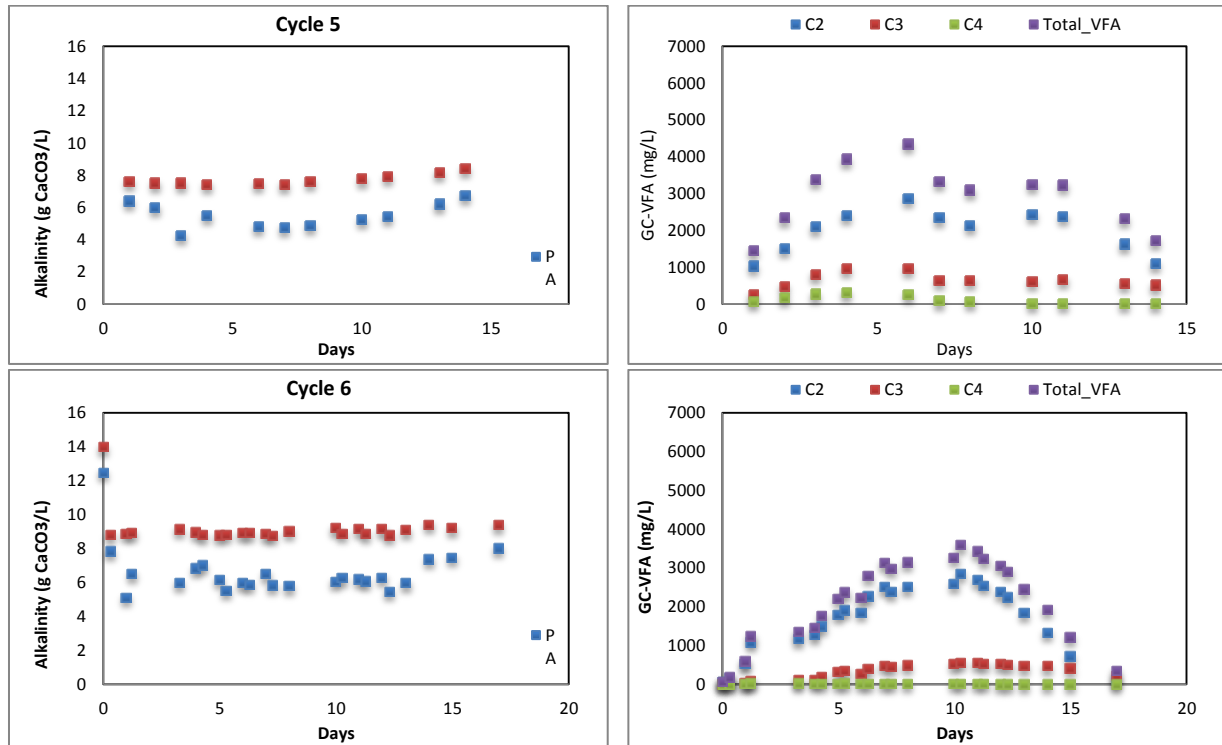


Figure 19 Alkalinity and VFA results of cycle 5 and cycle 6

4.1.2 UASB performance

The UASB was running for 105 days, the overall performance of the reactor is shown in Figure 20.

There were 8 sub-periods in the whole operation period of the UASB, which were divided by the OLR. The feeding was manually controlled to reach a steady state during the first 3 sub-periods (start-up period). In sub-period 4-8, the OLR was controlled by the CEIT control software, in order to develop an automatic control strategy for the AD systems (results are shown in Appendix A2).

- **Temperature & pH**

The temperature in the UASB was controlled at 35 °C by a water bath in sub-period 1-7. On day 100, the control stopped, and the temperature in the reactor dropped gradually from 35 °C to 25 °C. Because the OLR was lower than 10 kg/m³d during the whole period, the system did not suffer from significant overloads when temperature dropped. Only the VFA concentration in the effluent increased slightly due to the less active methanogenesis. As can be seen from the pH results, it remained around pH 7.6-7.7 due to high buffer capacity (Figure 20d). With the constant pH, the VFA

concentration in the effluent was constantly low after day 40. This pH range might be preferable for the methane production.

- **COD & COD removal**

The COD concentrations in the effluent fluctuated with the OLR, and the fluctuation was in the range of 3000-7000 mg O₂/L. A biomass washed-out appeared on day 15-19, under an OLR of 5 kg/m³.d. Due to the large quantity of fine inorganic crystals (mostly struvite) in the inoculum, the amount of biomass was small (TSS = 26.5 g/L, VSS = 8.0 g/L, see section 3.1.2). Furthermore, the inoculum was stored at 4 °C for a week and the system was operated for merely two weeks, which gives the reason to believe that the sludge was not very active.

The removed COD was mainly VFA. The variation of COD removal was in agreement with that of the VFA concentrations in the influent (data not shown).

- **Biogas and methane production**

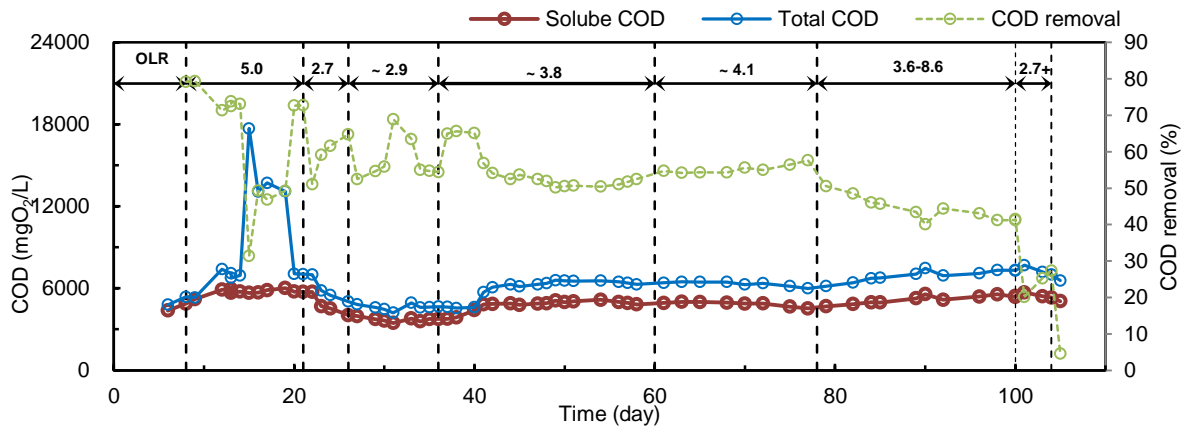
The biogas production increased with the OLR, i.e. in sub-period 2, the biogas production was around 257 L CH₄/kg COD_{added} at a OLR of 5 kg/m³.d, and it was only 158.7 L CH₄/kg COD_{added} in sub-period 7 when OLR was 3.6 kg/m³.d. During day 20 and 30, a significant drop of biogas production was observed, this might be caused by the flush out of biomass in sub-period 2.

The biogas production was quite sensitive to the OLR, peaks can be observed when organic loading pulses in sub-period 4-7 were applied(details can be found in Appendix. A2).

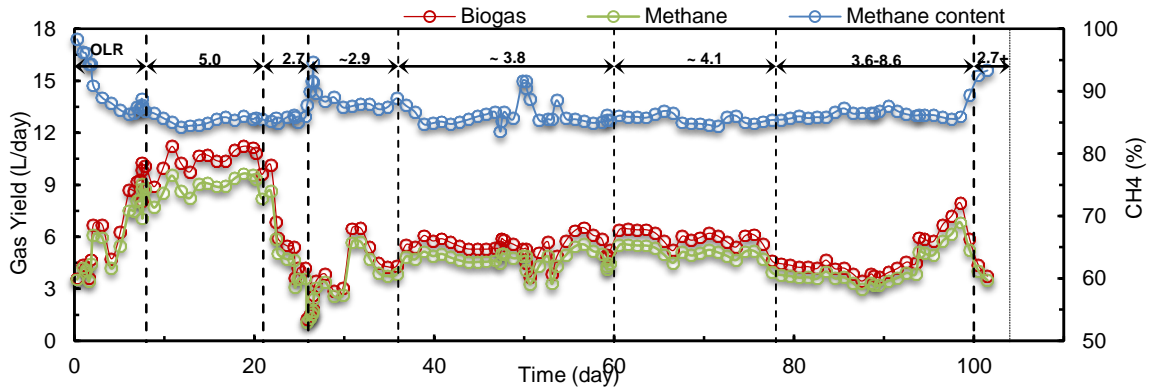
- **VFA**

The total VFA in the UASB effluent reduced from 1.5 g/L to less than 100 mg/L after 40 days. On the same day when the UASB reactor suffered from a biomass washed-out (high tCOD concentration in sub-period 2), the acetic acid started to accumulate in the system, and the consumption of propionic acid was stopped (see Figure 20c). Two other small VFA peaks on day 50-60 and day 100-104, showed a change in system balance. Nevertheless, the concentration was too low to give a notable indication of the process deterioration.

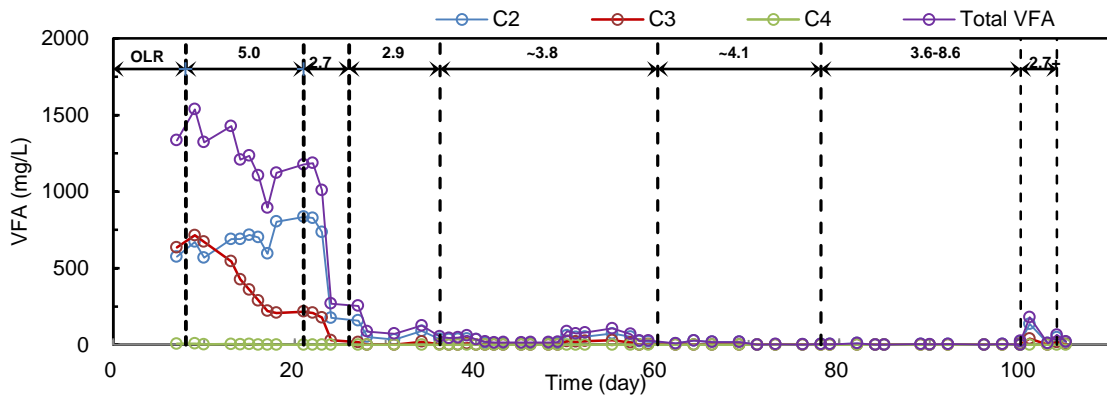
Despite an almost constant sCOD of 5000 mg/L in the effluent after day 40, the total VFA was barely 50 mg/L. There might be other inorganic/organic compounds present, such as alcohols and sulphide, which also contributed to COD measurements. In the UASB reactor, inoculum was adapted to simplified substrates (i.e. VFA), thus organic molecules with high molecular weight might not be degraded. However, the alcohols in the samples were analysed by GC, and the results showed that no alcohols were present in the UASB reactors. Probably the concentration of sulphide was high in the leachate.



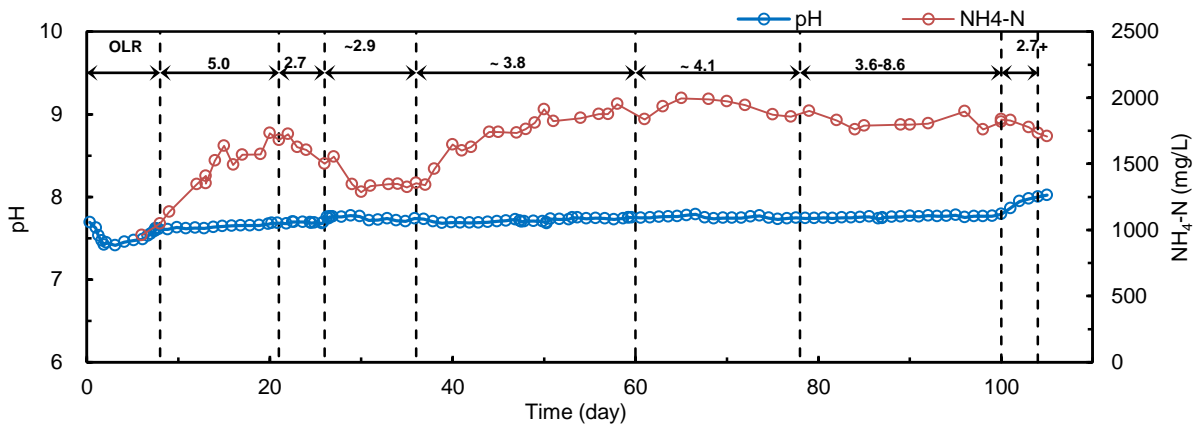
a



b



c



d

Figure 20 UASB performance during the whole experimental period

- **PA/TA**

The total alkalinity increased from 8 g CaCO₃/L to 10 g CaCO₃/L. This might be related with the increase in ammonia concentration. 1 g NH₄-N is 7.1 g alkalinity (in terms of CaCO₃), thus with the NH₄⁺ increased from 1.4 g/L to 1.7 g/L (Figure 20d, from day 38 to day 80), the alkalinity increased about 2.0 g/L, which is in consistent with the observation (Figure 21).

However, a significant fluctuation of PA was observed during day 70 and 90, while the VFA concentration did not change dramatically. The reason of this phenomenon was not very clear. It could be the error of sampling or the titrator.

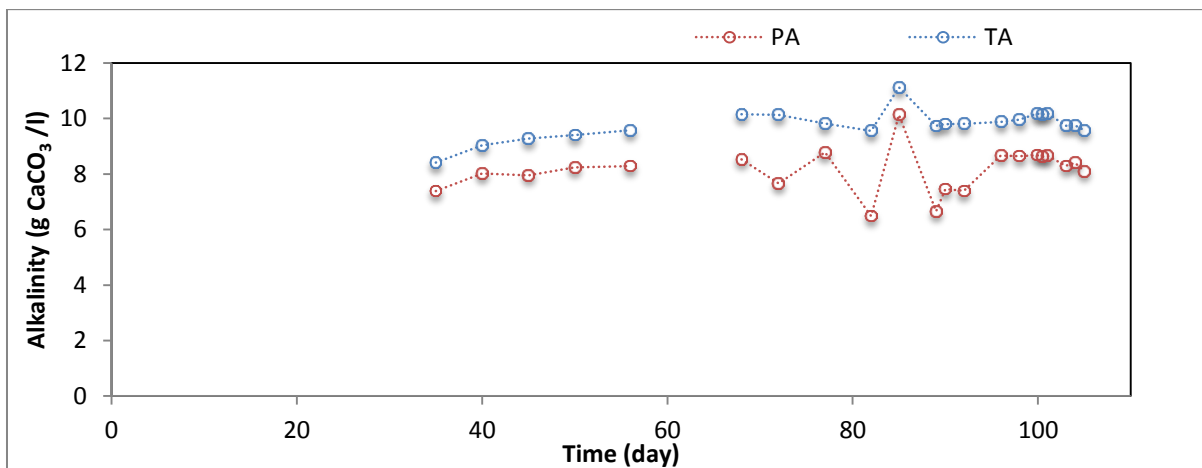


Figure 21 Results of partial and total alkalinity

- **NH₄⁺**

The ammonia concentration in the effluent was equal to that in the influent.

- **Summary**

It was found that the COD removal and VFA concentrations could be the early indicators for the imbalance in an UASB reactor. Biogas production was not very sensitive in this case. Due to the high buffer capacity, pH was not able to give information about the imbalanced process state. When the VFA concentration is low (<100 mg/L), the COD removal could be used as a process indicator for biogas production.

4.2 Validation

4.2.1 In-process measurements & Off-process measurements

- **Lab-scale leachate**

In Figure 22 and Figure 23 the VFA concentration predicted by the OPTI-VFA sensor are compared with GC references. These are the results from the Cycle 3 and Cycle 6 of the leaching reactor.

Although there was a positive offset of 500-1000 mg/L, the sensor could show the total VFA profile as showed by the GC references.

Compared with the GC references, the prediction of acetic acid (C2) by the OPTI-VFA sensor were rather good (Figure 22b), both the in-process and off-process predictions were very close to the reference values. At the end of the monitoring, one C2 concentration measured off-process showed a larger offset (800 mg/L). This might be caused by a fluctuation in the measuring conditions, for instance, the temperature in the water bath was not stable during the spectrum measurement.

The predictions of propionic acid (C3) and butyric acid (C4) concentrations by the sensor were not good enough (Figure 22c and 22d). There was a large deviation of 500-1000 mg/L between the C3 sensor prediction and GC values. The deviation for C4 measurement was smaller, about 500 mg/L. And the OPTI-VFA sensor was able to show the increasing trend of C4. Although C3 has a higher concentration, the sensor had a slightly better performance in predicting the C4 concentrations. The reason was not very clear.

Considering the high total VFA concentration, the 1000 mg/L offset was more acceptable than that in C3 and C4 measurements.

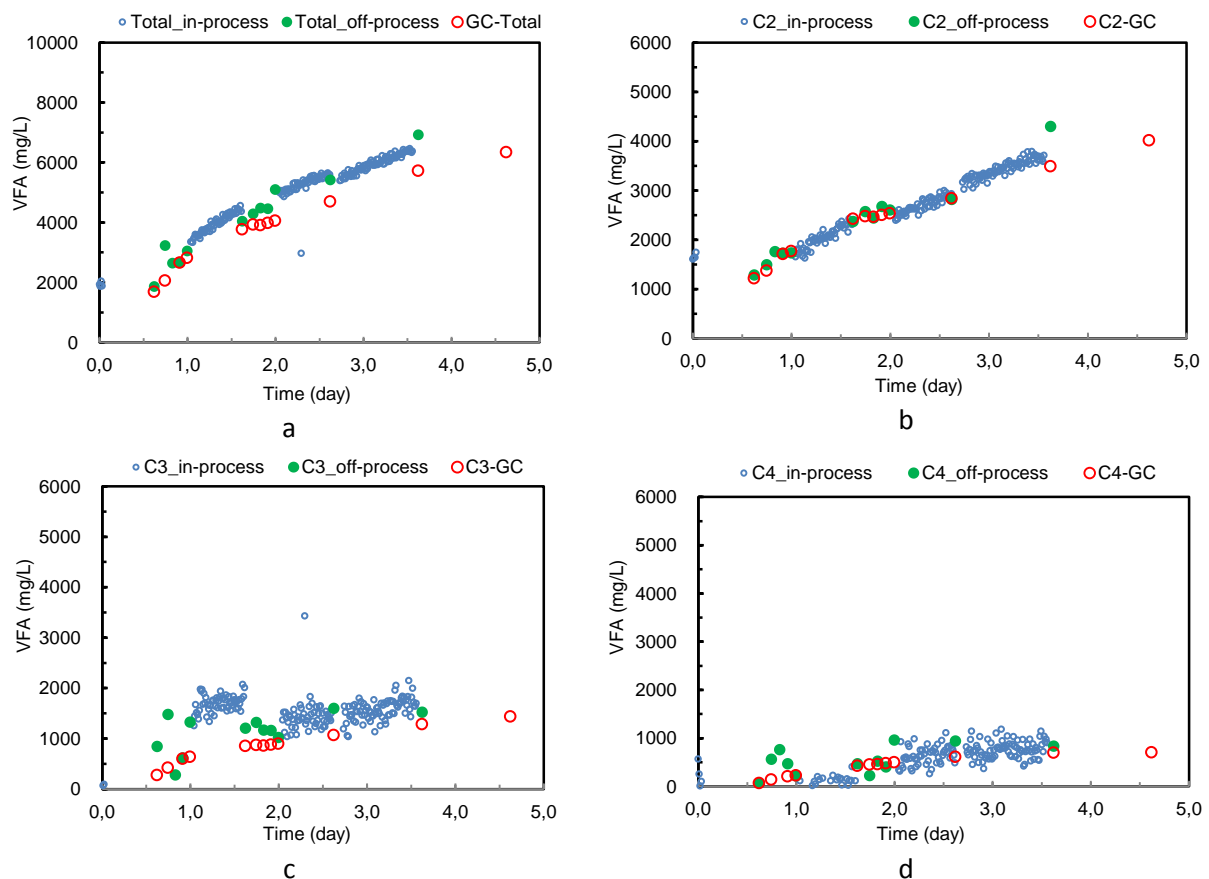


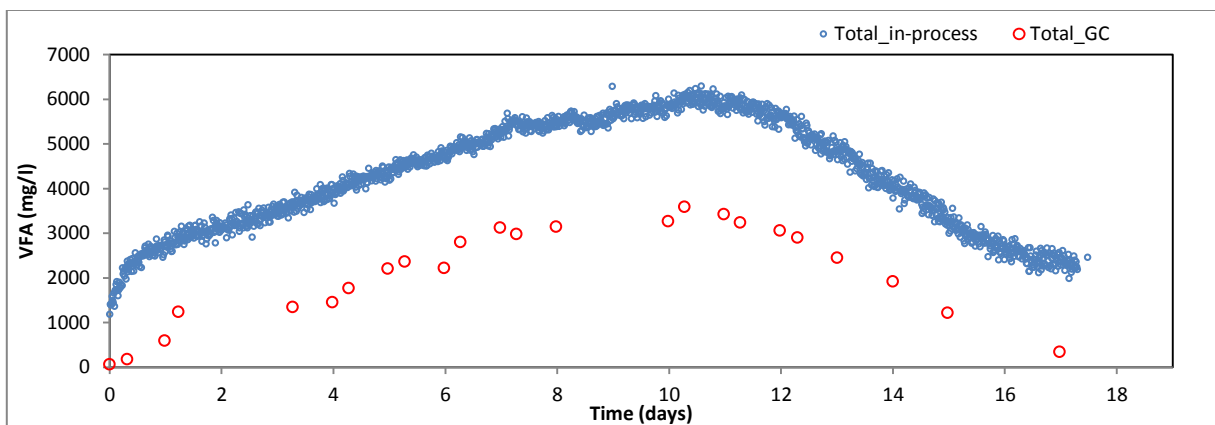
Figure 22 Results of online monitoring in the lab leachate (Cycle 3)

In cycle 6 (Figure 23), the in-process total VFA predictions showed a 1500-2000 mg/L offset from the reference measurements. But the variation of total VFA concentration was perfectly indicated, i.e. the dramatic increase in day 0-1, and the slightly decrease in day 7-10. The larger offset than in cycle 3

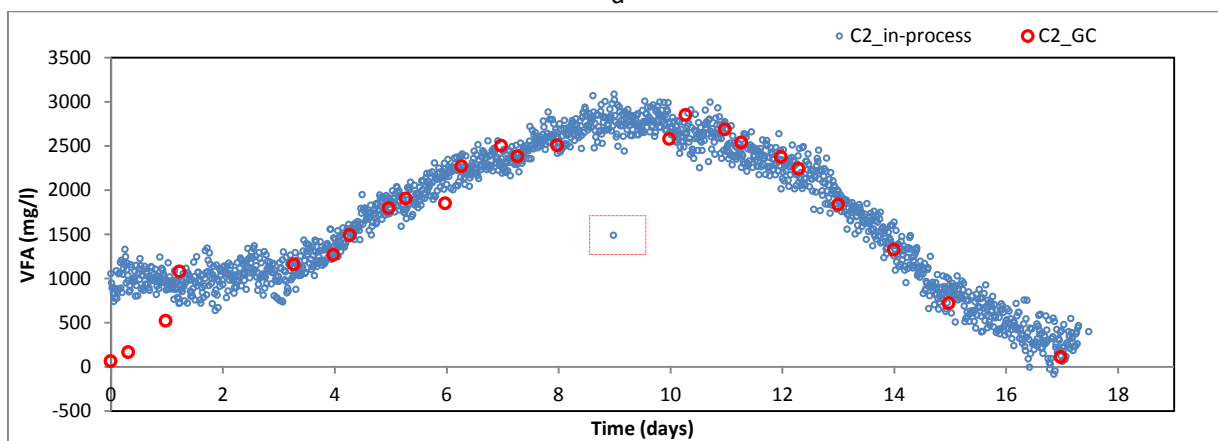
might be caused by a lower total VFA concentration, thus the relevant factors (i.e. HCO_3^- and NH_4^+) showed a more significant influence. But it could be compensated by further improving the model.

For C2 measurements, the sensor predictions were quite accurate after day 2 (less than 500 mg/L noises). The variation of the C2 concentration was also well predicted. The C2 concentration was low on day 1 and day 17, but sensor was only able to indicate the low concentration on day 17. Probably it is because the high alkalinity was taken into account as C2 concentration on day 0-1. Or the sensor needed one day to stabilize in the beginning of the monitoring, since the larger deviation during the first day was also observed in the results of cycle 3. There were some large offsets during the continuous online monitoring, as shown in the red squares in Figure 23b and 23d. These offsets were more likely caused by the fluctuation in the light source.

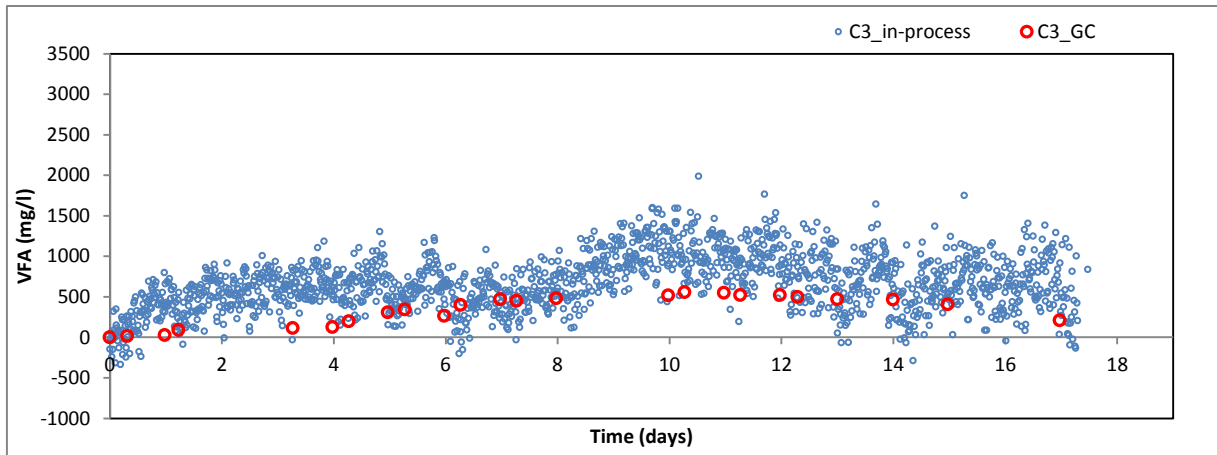
The in-process measurement of C3 showed a positive offset of 500-1000mg/L, while the C4 measurements by the OPTI-VFA sensor showed a negative offset of 500-1500 mg/L. Since the measurements gave a larger noise, the dynamic concentration of C3 and C4 was not well indicated by the sensor. That might be related to the low concentrations in the process, the MIR was not sensitive enough for these low concentrations.



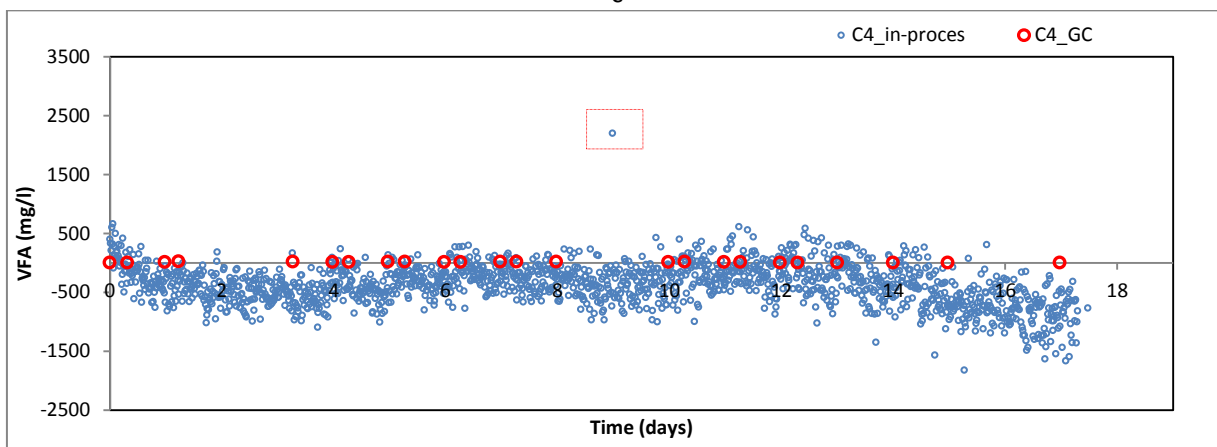
a



b



C



d

Figure 23 Results of online monitoring in the lab leachate (Cycle 6)

- **Full-scale Leachate**

Figure 24 is the result of online VFA monitoring in the leachate of the full-scale treatment plant in Venlo, with GC measurements as a reference.

The total VFA and C2 concentrations were more fluctuated than in the lab reactor, but they were within a much smaller range (4000-4500 mg/L for total VFA, 2000-3000mg/L for C2). Compared to the results from the lab, the accuracy of the sensor measuring in full-scale was less, but still reliable. The predictions were able to follow the trend of VFA concentrations measured by GC.

The cause for this slight disparity in the accuracy might be the high flow rate of the leachate. In the lab-scale leaching bed reactor, the maximum flow rate was 7 L/h, which was the recirculation flow rate. Compared to the high flow rate of 100-1000 m³/h at full-scale, the sensor was almost measuring in a steady environment in the lab reactor.

The measurements of C3 and C4 again showed a larger noise than that of total VFA and C2, which is the same as the results from the lab. The concentration of C3 and C4 remained stable at about 1000

mg/L and 100 mg/L respectively, but the sensor was again not able to give a good prediction. It is likely that low concentrations of C3 and C4 and the high flow rate led to this result.

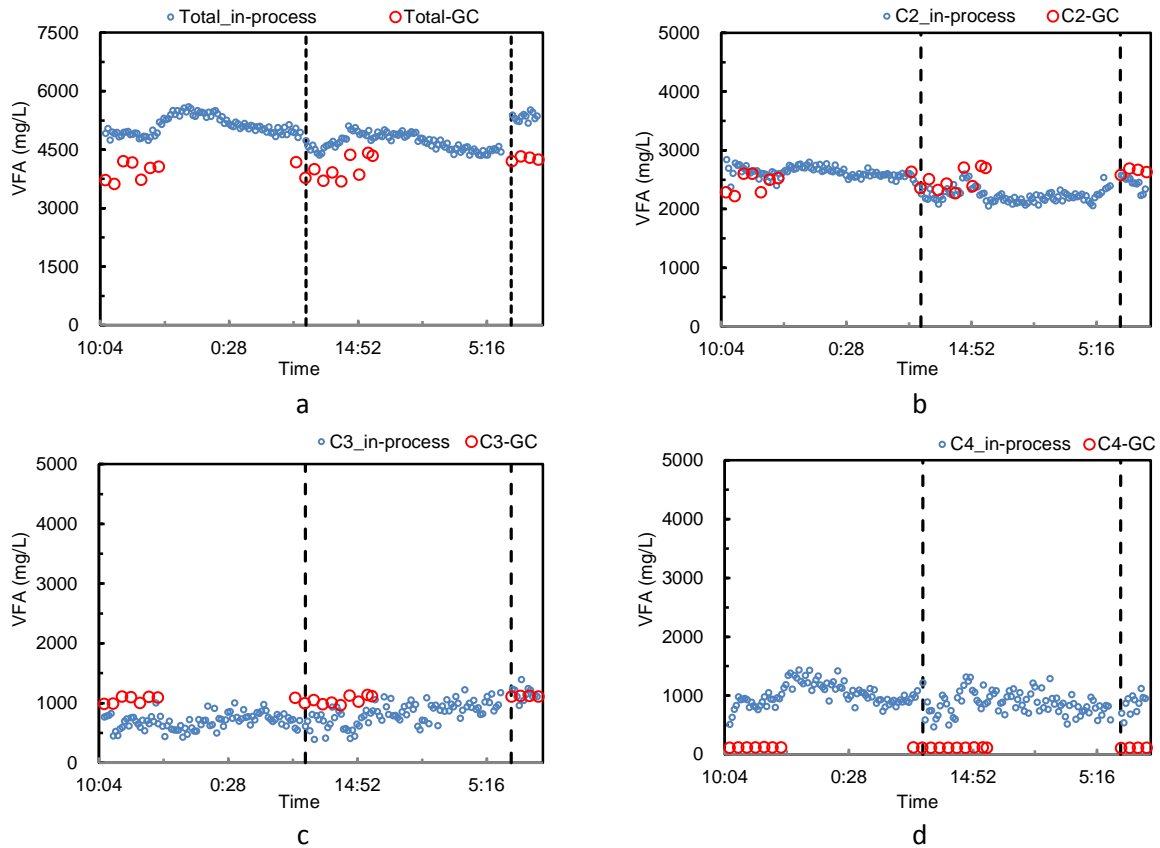


Figure 24 Results of online monitoring in Venlo leachate

- **Full-scale UASB effluent**

The total VFA concentration in UASB effluent was below 30 mg/L, about 65 % was C2 and 35 % was C6. The VFA concentrations were very low, as can be seen in Figure 25. In this situation, the OPTI-VFA sensor was unable to monitor the VFA profile. There was a positive offset of 500 mg/L for total VFA measurements, and a negative offset of 200-600 mg/L for C2 measurements. While for C3 and C4, there were only random offsets. Probably it is because of the insufficient MIR sensitivity, or other relevant factors (i.e. HCO_3^- and NH_4^+) influenced the sensor performance significantly under low VFA concentrations.

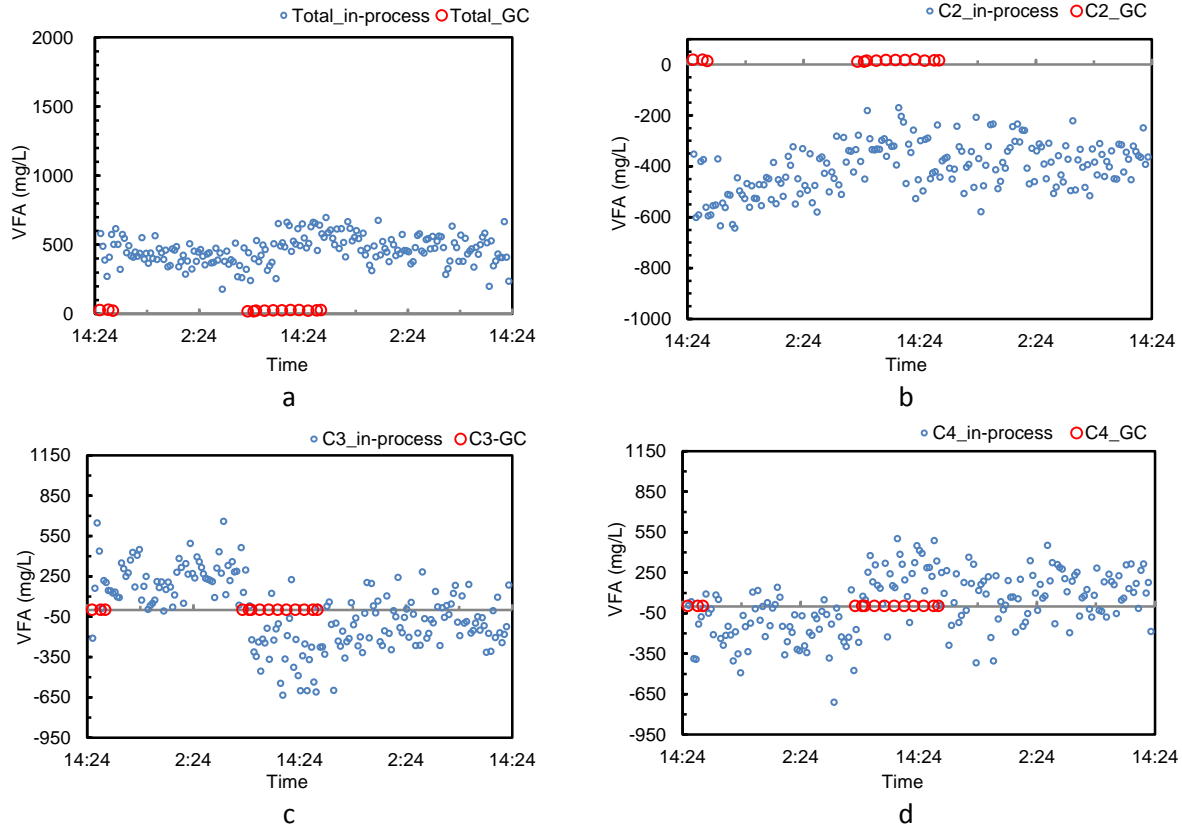


Figure 25 Results of online monitoring in Venlo UASB effluent

- **Baseline spectra in Laboratory and Full-scale**

The baseline spectra (measured in demi water) were flatter in lab measurements (wavelength range $800\text{--}1800\text{ cm}^{-1}$). The baseline spectra were significantly tilted in full-scale measurements, as shown in Figure 26b. When the temperature was $40\text{ }^{\circ}\text{C}$, it was more difficult to maintain a stable temperature for the background measurement. The tilted baseline might be one of the reasons that the sensor prediction was less accurate in the full-scale validation.

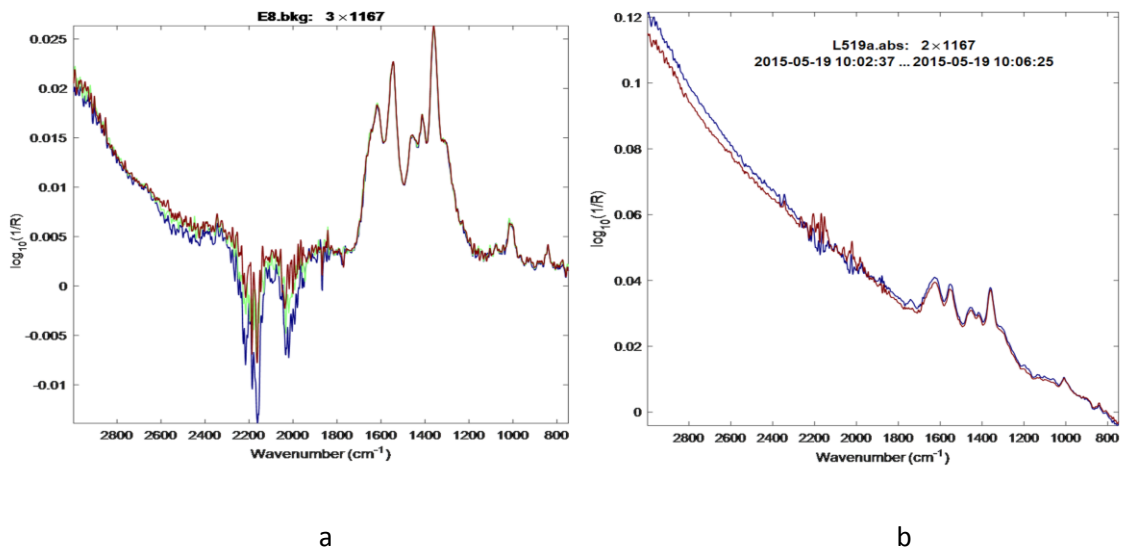


Figure 26 Comparison of baseline spectra measured in laboratory and full-scale (a: baseline spectra measured in the lab; b: baseline spectra measured in full-scale)

- **Discussion**

Comparing all the results shown above, the prediction for acetic acid was acceptable, while for total VFA, propionate and butyrate, the calibration should be further improved. The less controlled measurement environment in the full-scale led to a less accurate prediction of the sensor.

The sensor showed a better performance when total/individual VFA concentration was higher than 2000 mg/L. Below this concentration, the sensor seemed to be affected more significantly by other parameters. For example, the substances like HCO_3^- and NH_4^+ presented in the measuring media (find details in section 4.2.4), as well as pH, temperature and flow rate in the measuring environment (find details in section 4.2.3). Unfortunately, the examination of flow rate impact was not carried out.

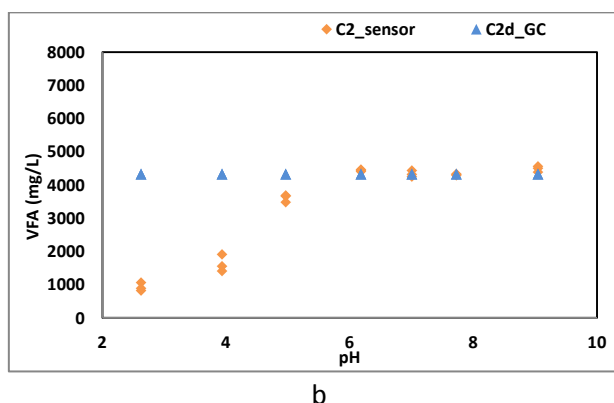
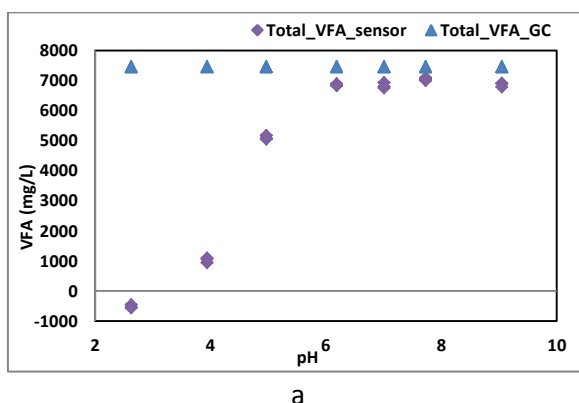
4.2.2 pH test

The results of pH tests are given in Figure 27 and 28.

- **Demi water matrix**

As we can see from Figure 27, in the pH range of 6-9, the sensor predictions were very close to the GC reference. The offset of the sensor predictions for individual VFAs was within 250 mg/L. The smallest difference was 13.58 mg/L for acetic acid, and 403.66 mg/L for total VFA at pH 8 (Appendix B Table B1).

The sensor predictions deviated largely from the GC values under a pH below 6. The dissociation level of VFA decreases with the pH, the spectrum changes as the VFA form (dissociated & un-dissociated) changes. The current calibration curve was based on calibration samples within a pH range of 6-8, it is possible that the un-dissociated VFA at low pH was not well detected. Which probably caused the large deviation at pH 3-5 in Figure 27.



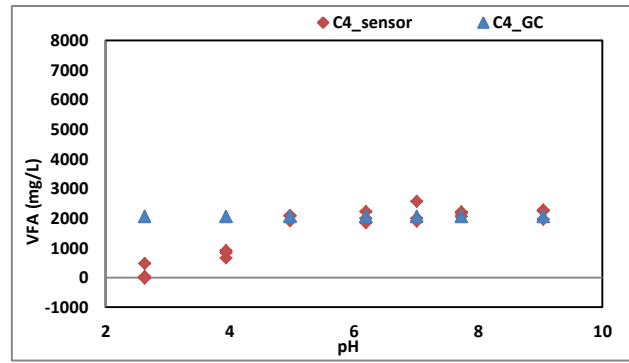
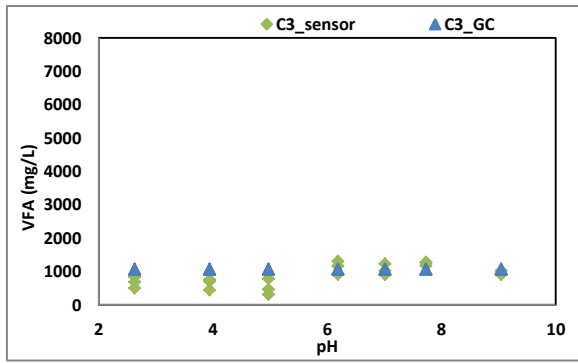


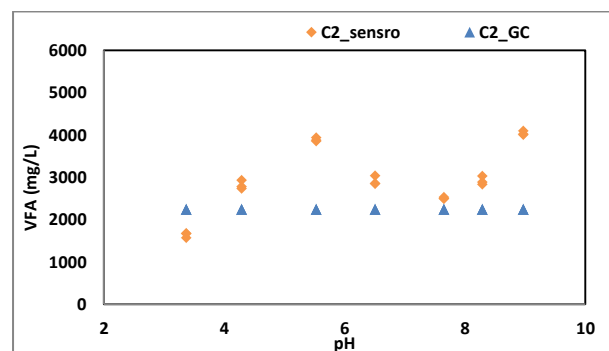
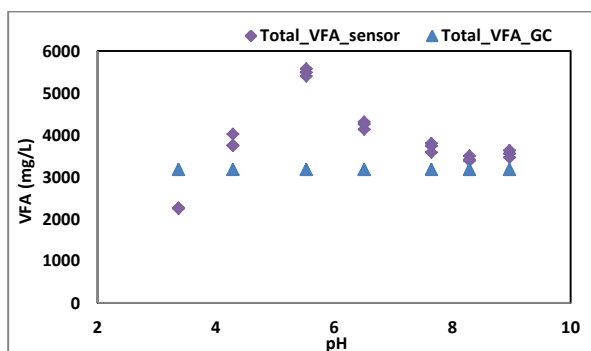
Figure 27 Results of pH test (demi water matrix)

- Leachate matrix

For the leachate matrix, the sensor predictions were less satisfying than that of demi water matrix. In Figure 28, the prediction gave a smaller difference from GC values under a pH between 6-8. However, the offsets were still above 200 mg/L (Appendix B. Table B2). Generally, the sensor had a better performance under pH 7-8, which is similar as seen in results of the demi water matrix.

The higher accuracy of the sensor results in demi water matrix could be explained by two reasons. One is that the VFA concentrations in the demi water matrix were much higher (about 2 times) than that in the leachate matrix; and secondly, only VFA was present in the demi water matrix, without any other Interfering substances.

Take the total VFA prediction as an example (Figure 28a), the low pH and bicarbonate concentration introduced a negative offset, while ammonia concentration introduced a positive offset (Figure 27a, 31-a1, and 32-a1). At pH 3, although HCO_3^- was stripped out as CO_2 ($\text{HCO}_3^- + \text{H}^+ \rightarrow \text{CO}_2 + \text{H}_2\text{O}$), the VFA was un-dissociated, thus the prediction was still lower than the reference (negative offset caused by low pH). When pH increased to 5, the VFA dissociated, so the prediction also increased. The impact of HCO_3^- and NH_4^+ was minimized when pH was above 7 ($\text{HCO}_3^- + \text{OH}^- \rightarrow \text{CO}_3^{2-} + \text{H}_2\text{O}$; $\text{NH}_4^+ + \text{OH}^- \rightarrow \text{NH}_3 + \text{H}_2\text{O}$), and the VFAs were fully dissociated, therefore the sensor prediction became more reliable.



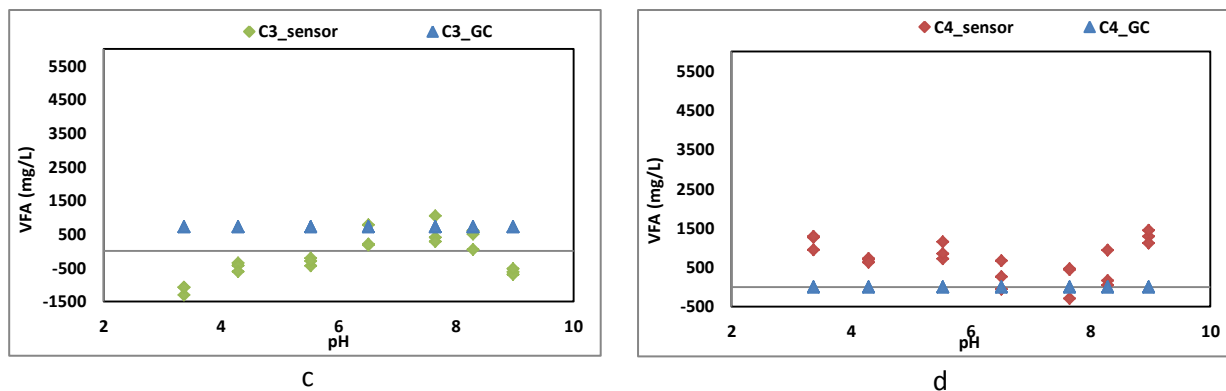


Figure 28 VFA results of pH test (leachate matrix)

- **Conductivity and salinity**

The conductivity of demi water samples was in the range of 0.5-8.2 mS/m, and the salinity was in the range of 0.0-4.6 g/kg (Table 15). For leachate samples, the conductivity was in the range of 23.1-31.8 mS/m, and the salinity was in the range of 14.0-19.8 g/kg (Table 15).

The difference in conductivity/salinity between samples (in the same matrix) was small, thus the impact of the conductivity/salinity was considered low on the sensor performance.

Table 15 Conductivity and salinity of the two sample matrices

Demi water matrix				Leachate matrix			
Sample	Conductivity (mS/m)	Salinity	Temperature	Sample	Conductivity (mS/m)	Salinity	Temperature
D0	0.49	0.0	23.7	L0	23.1	14.0	23.0
D1	1.76	0.7	23.1	L1	31.3	19.4	22.8
D2	5.35	2.8	22.8	L2	31.8	19.8	22.7
D3	6.92	3.8	22.7	L3	28.9	17.8	22.6
D4	8.18	4.6	22.7	L4	25.9	15.8	22.6
D5	7.25	4.0	22.9	L5	23.4	14.2	22.7
D6	7.32	4.0	23.5	L6	24.9	15.2	23.2

- **VFA dissociation level**

In Figure 29, the dissociation level of VFAs in both matrices increased with pH. The dissociation level went above 10^1 at a pH around 6, 10^2 at pH 7, 10^3 at pH 8 and 10^4 at pH 9. Details can be found in Appendix B, Table B4.

It is clear that in the demi water matrix, the sensor performance improved accordingly with the increasing of VFA dissociation (Figure 29). In the leachate matrix, the sensor performance improved when the dissociation level was between 10^2 and 10^3 . In both matrices, the sensor did not perform better when the individual VFA dissociation level went up to 10^4 .

When the dissociation level of individual VFAs was between 10^2 and 10^3 , the sensor could give a better prediction of VFA concentrations. Probably because the calibrations samples were in the range of 6-8, thus the spectra in this range were used as a reference to build the mathematical model.

When the dissociation level increased with the pH, the spectra shape changed (Schenk et al., 2008), thus the difference between the measured spectra and background spectra were different, and the calculated concentrations were not as accurate as in the lower dissociation level.

The pH did not have a direct impact on the sensor performance, however, it has an impact on the measured spectra. To improve the sensor performance for a specific AD system, the calibration model should be built within the system pH range.

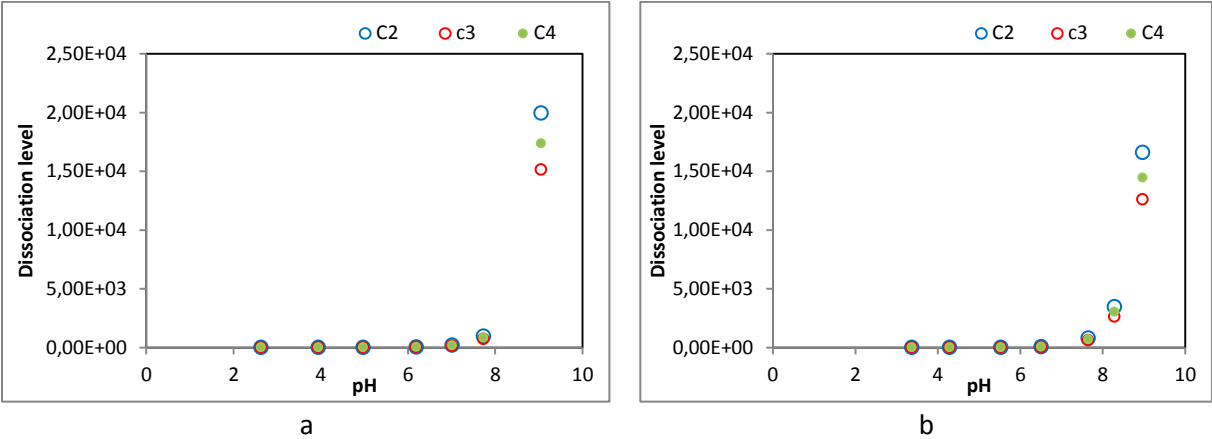
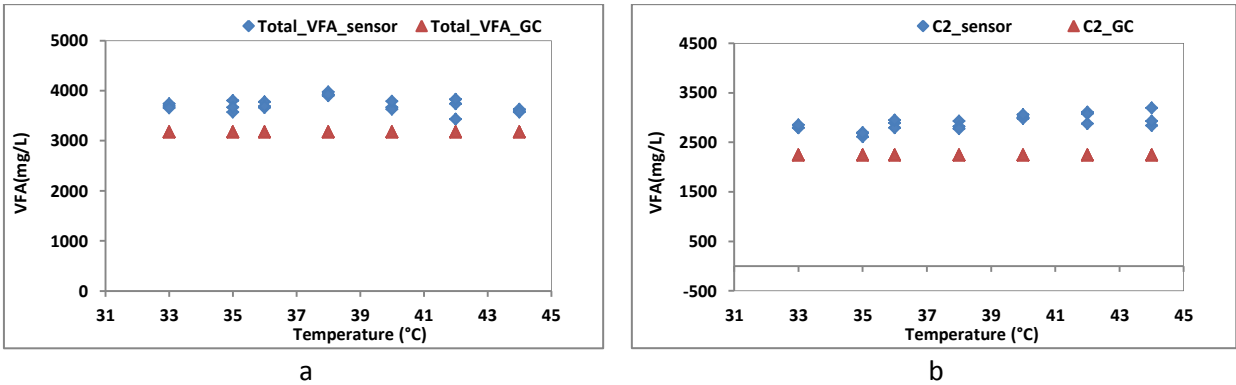


Figure 29 VFA dissociation level under different pH
a: Demi-water matrix; b: Leachate matrix

4.2.3 Temperature test

In Figure 30, the VFA concentrations predicted by the OPTI-VFA sensor under a temperature range of 33-44 °C are shown. For total VFA, the sensor predictions were quite stable, the change in temperature did not give a significant impact. For C2 and C3, the offset between sensor and GC values increased with the temperature difference (between measuring temperature and background temperature 35 °C). For C4, the sensor predictions varied between 100 and 500 mg/L (Appendix B Table B3), while the GC value was 0 mg/L, and no trend with the temperature changes can be seen.

The minimal offset between the two measurements was observed at a temperature of 35 °C. That means, a background temperature, which is close to the sample temperature, should be selected during the measurement.



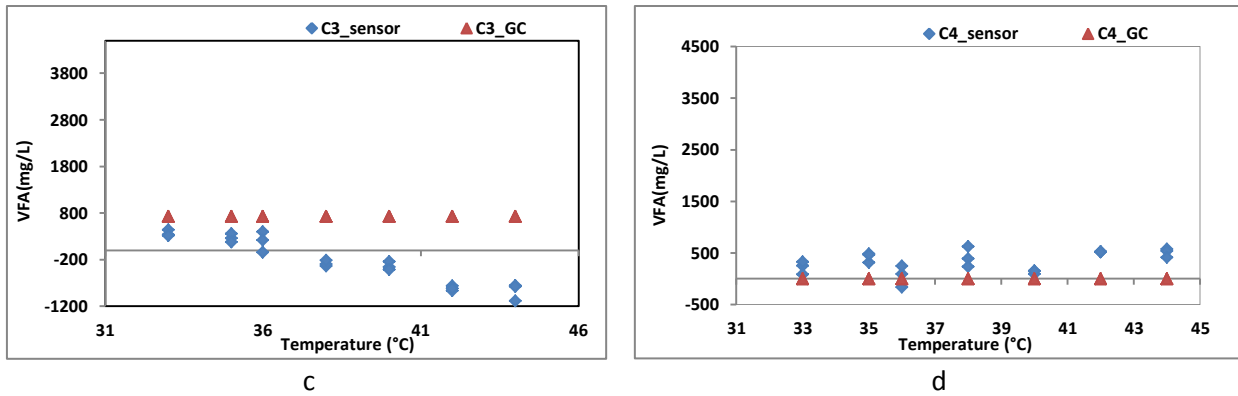


Figure 30 VFA results of temperature test

- **Discussion**

When measuring in a full-scale treatment plant, the sample temperature in the bypass can be significantly affected by the ambient temperature. Therefore, the temperature range can be much larger than the selected range. To ensure the robustness of the sensor, it should be validated in a larger temperature span.

4.2.4 Interference of HCO_3^- and NH_4^+

- **Impact of HCO_3^-**

The concentration of NH_4^+ in the demi water matrix was 0 g $\text{NH}_4\text{Cl/L}$, and VFA concentration was 0 mg/L. In the UASB effluent matrix, NH_4^+ concentration was 6.9 g $\text{NH}_4\text{Cl/L}$, total VFA concentration was 20 mg/L (C2 = 20 mg/L, C3 = C4 = 0 mg/L). The NaHCO_3 concentration increased from 0 g/L to 42.8 g/L in demi water matrix, and from 13.4 g/L to 52.0 g/L in UASB effluent matrix.

A negative correlation between VFA prediction and NaHCO_3 concentration could be observed in total VFA (Figure 31-a1 and 31-b1), C2 (Figure 31-a2 and 31-b2) and C3 predictions (Figure 31-b3). On the other hand, a positive correlation was observed in C4 predictions (Figure 31-b4). The impact of the HCO_3^- on C3 and C4 predictions in demi water matrix was not clear.

When the sensor was used to predict total VFA, the predicted concentration decreased from 1000 mg/L to -6000mg/L in both matrices. In sample 1, where the NaHCO_3 concentration was the lowest, the sensor prediction was most close to the real value. A similar trend can be found when predicting C2. However, the best prediction (closest to 0 mg/L) was found in sample 2 results, where the NaHCO_3 concentration was 14.3 g/L and 26.7 g/L respectively.

In demi water matrix sample 2, the predictions of C3 and C4 were also most close to 0 mg/L. But this phenomenon was not found in the UASB effluent matrix.

As shown in Figure 31, the sensor predictions deviated largely from the real value when the NaHCO_3 concentration was below 10 g/L and above 40 g/L.

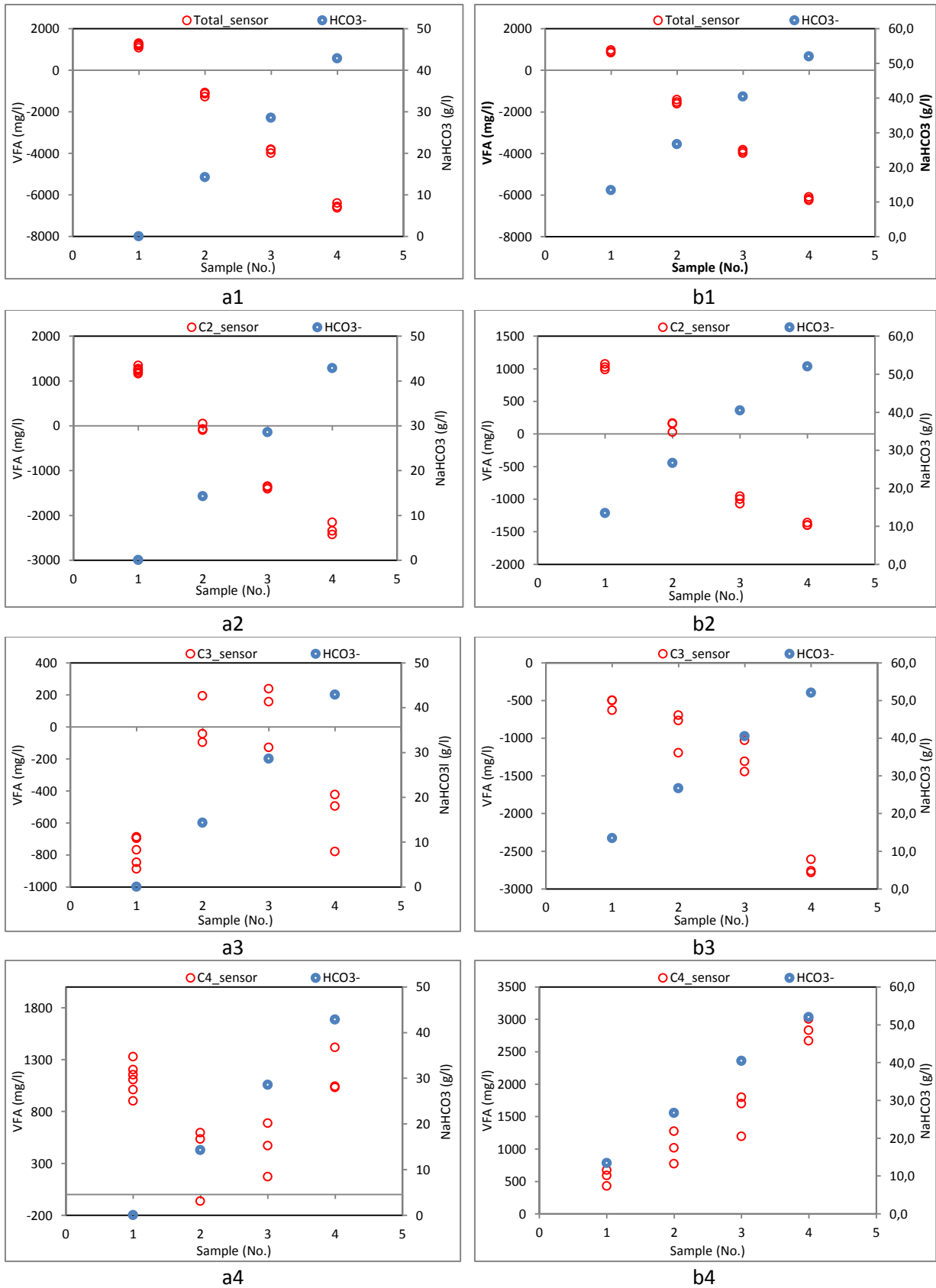


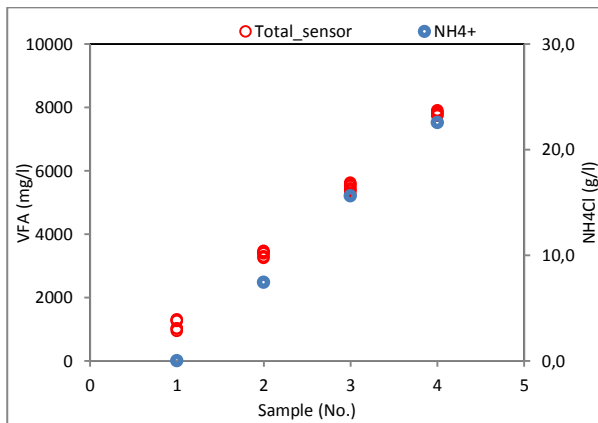
Figure 31 Sensor performance under different HCO₃⁻ concentrations

*(a1-4: results of Demi water matrix; b1-4: results of UASB effluent matrix)

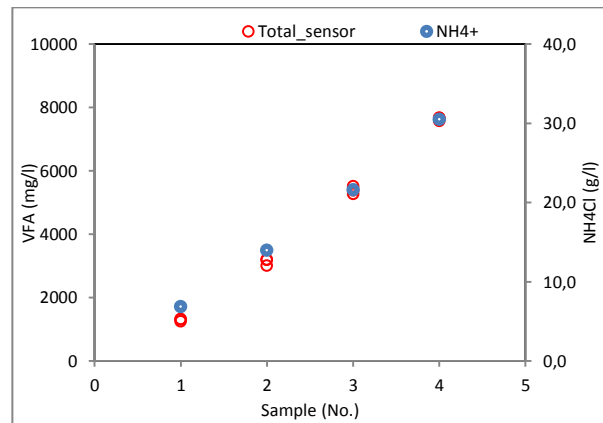
- **Impact of NH_4^+**

The concentration of NaHCO_3 was 0 g NaHCO_3/L in the demi water matrix, and 13.4 g NaHCO_3/L in UASB effluent matrix. The concentration of VFA was 0 mg/L in demi water matrix and 20 mg/L ($\text{C}_2 = 20 \text{ mg/L}$, $\text{C}_3 = \text{C}_4 = 0 \text{ mg/L}$) in UASB effluent matrix. The NH_4Cl in demi water matrix increased from 0 to 22 g/L, and increased from 6.9 to 30.5 g/L in UASB effluent matrix.

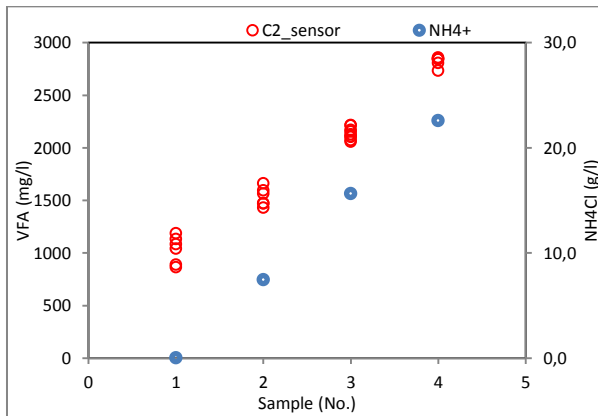
A positive correlation between VFA prediction and NH_4Cl concentrations was shown in total VFA and C_2 (Figure 32-a1, 32-b1 and 32-a2, 32-b2), whereas a negative correlation was shown in C_3 predictions (Figure 32-a3 and 32-b3). For C_4 predicted by OPTI-VFA sensor, the impact of NH_4Cl was not significant (Figure 32-a4 and 32-b4).



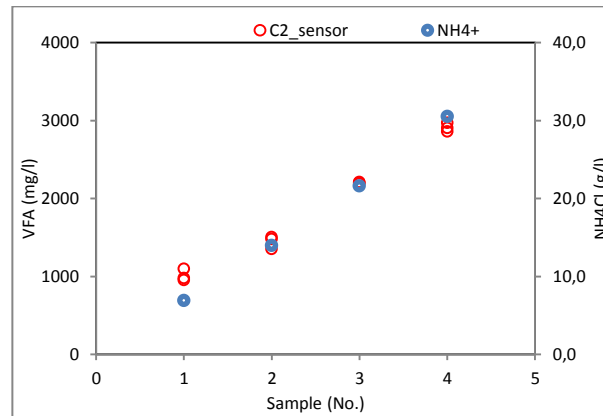
a1



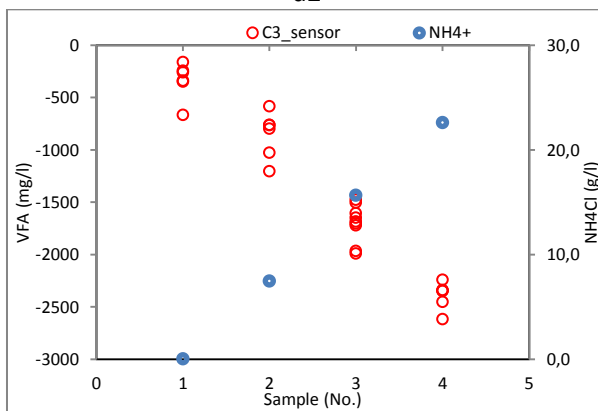
b1



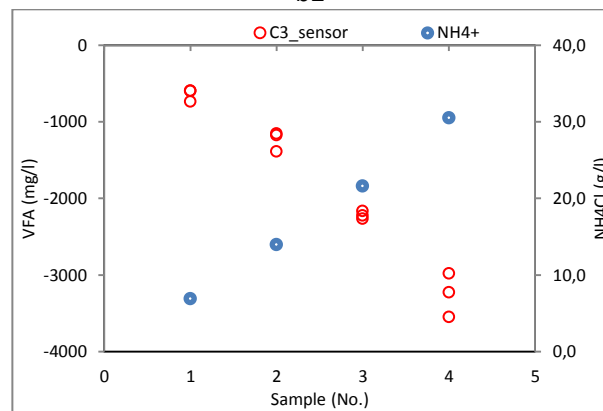
a2



b2



a3



b3

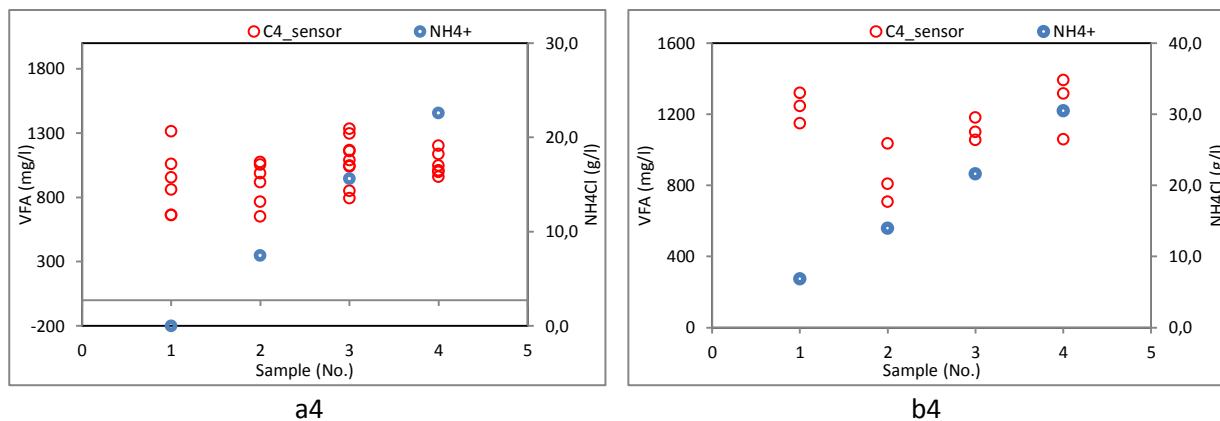


Figure 32 Sensor performance under different NH_4^+ concentrations

*(a1-4: results of Demi water matrix; b1-4: results of UASB effluent matrix)

- **Correlation coefficient between the interference and $\text{HCO}_3^-/\text{NH}_4^+$ concentrations**

In the demi water matrix, the variation in NaHCO_3 concentration was highly correlated to the sensor performance in measuring total VFA and C2. But the increase in NaHCO_3 concentration did not show a big impact in measuring C3 and C4. The correlation coefficient between the change in NH_4Cl concentration and the sensor performance in measuring total VFA, C2 and C3 was (\pm) 1, while it was smaller in measuring C4 (Table 16).

In the UASB effluent matrix, high correlation between NaHCO_3 concentration and sensor performance was found for all VFAs measurements (correlation coefficient > 0.9). Similarly to results of the demi water matrix, the correlation coefficient between the change in NH_4Cl concentration and the sensor performance in measuring total VFA, C2 and C3 was also (\pm) 1 (Table 16). But the impact of NH_4Cl concentration was much smaller in C4 measurements.

Table 16 Correlation coefficient between the interference and $\text{HCO}_3^-/\text{NH}_4^+$ concentration

HCO_3^-	Demi water matrix	UASB effluent matrix
Total VFA	-1.00	-1.00
C2	-1.00	-0.99
C3	0.20	-0.92
C4	0.07	0.96
NH_4^+	Demi water matrix	UASB effluent matrix
Total VFA	1.00	1.00
C2	1.00	1.00
C3	-1.00	-1.00
C4	0.85	0.25

- **Spectra**

The spectra of HCO_3^- and NH_4^+ are shown in Figure 33. A single spectrum of HCO_3^- and NH_4^+ was compared with the spectrum of C2 on the left, and the spectra from cycle 1 were given on the right.

The absorption peaks of HCO_3^- were in the wavelength of $1600\text{-}1700\text{ cm}^{-1}$ and $1300\text{-}1400\text{ cm}^{-1}$, the absorption main peak of NH_4^+ were in the wavelength of $1400\text{-}1500\text{ cm}^{-1}$, this is consistent with the study of Bongards et al. (2014). It is most likely that the NH_4^+ absorption peak was included as the total VFA absorption peak (Figure 33b), and its concentration was the most important contribution to the positive offset in total VFA prediction.

These peaks could be distinguished from the VFA peaks in the wavelength of 1400 cm^{-1} and 1550 cm^{-1} . Namely, calibration curves could be built for these two ions. It is possible to have more accurate VFA measurements (excluding the concentration of HCO_3^- and NH_4^+ from VFA measurements), and to use the same sensor to online monitor these two parameters at the same time.

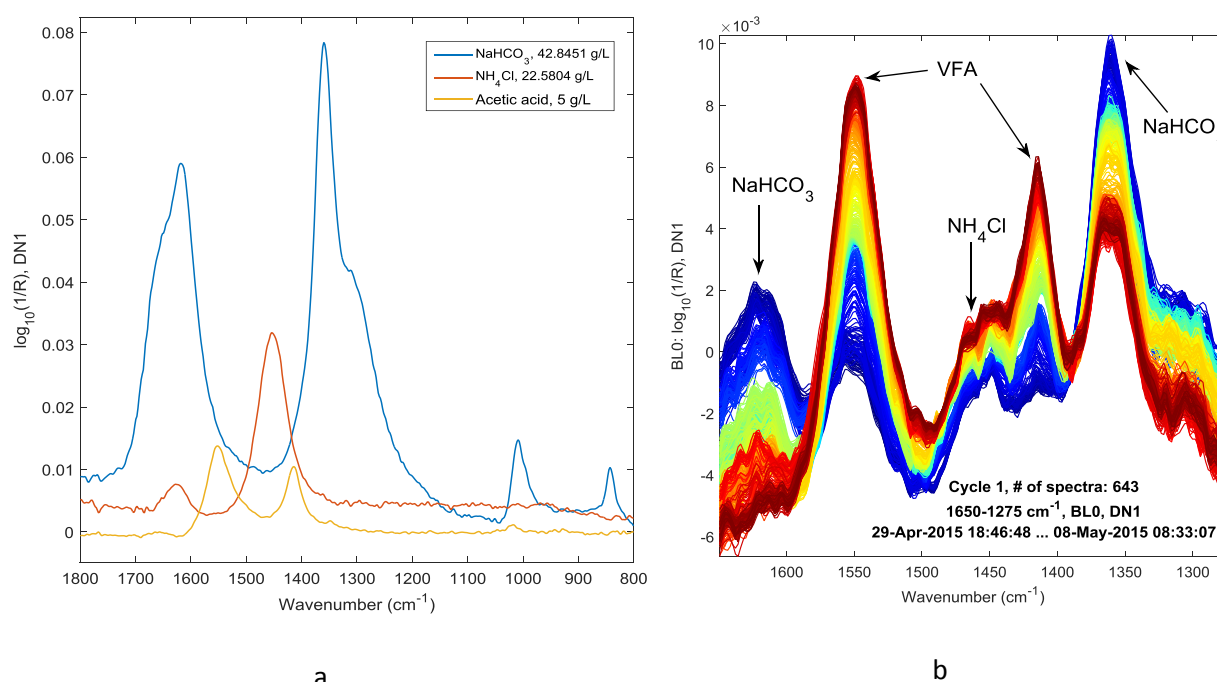


Figure 33 Absorption peaks of HCO_3^- and NH_4^+

- **Discussion**

Since the VFA concentration in both matrices was low, the sensor performance was not reliable even when there was no interference. However, if the non-interference situation (sample no.1 in this case) is taken as a reference, the sensor performance under interference-present situation can be examined. The blank demi water matrix can also be used as a reference for the UASB effluent matrix.

As indicated in Table 16, regarding on C3 and C4 measurements, the impact of the two interferences differed in the two matrices. The optical spectroscopy is sensitive to variations in the physical and chemical properties of sample matrix, so the difference might be caused by the different properties between these two matrices.

Regarding on total VFA and C2 measurements, the difference of the impact in the two matrices was very small. This means the interference of NaHCO_3 and NH_4Cl was much larger than other properties (i.e. color, solids content). It could be the cause of the offset in the online total VFA and C2 measurements (discussed in section 4.2.1).

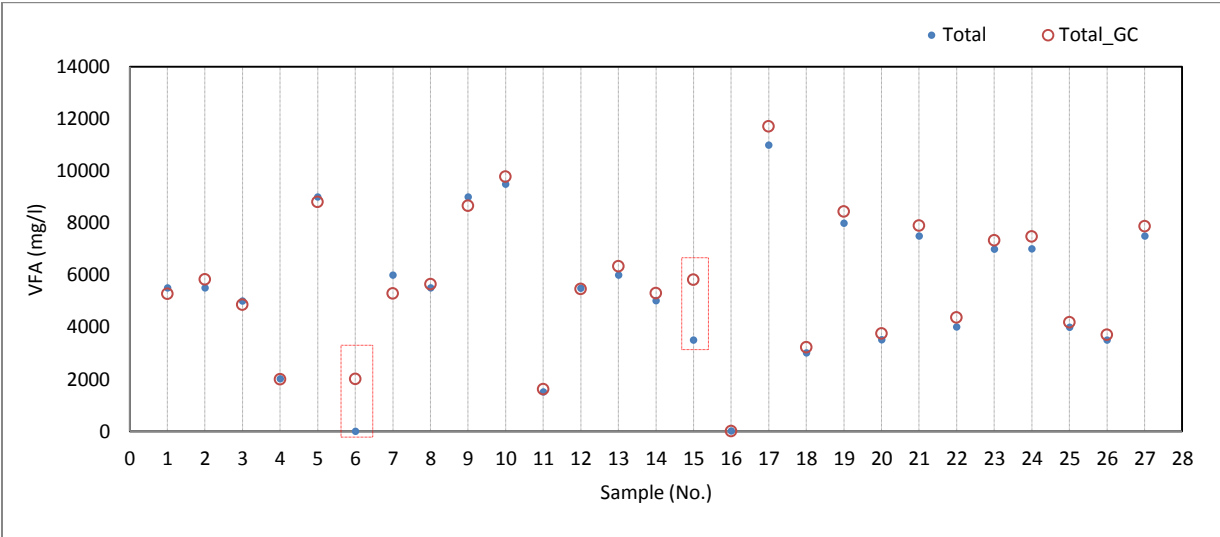
The interference of HCO_3^- and NH_4^+ could be removed, since they have distinguishable absorption peaks than VFAs. And the online monitoring of these two parameters could also be included in the OPTI-VFA sensor in the future.

4.2.5 Remeasurement of the calibration samples

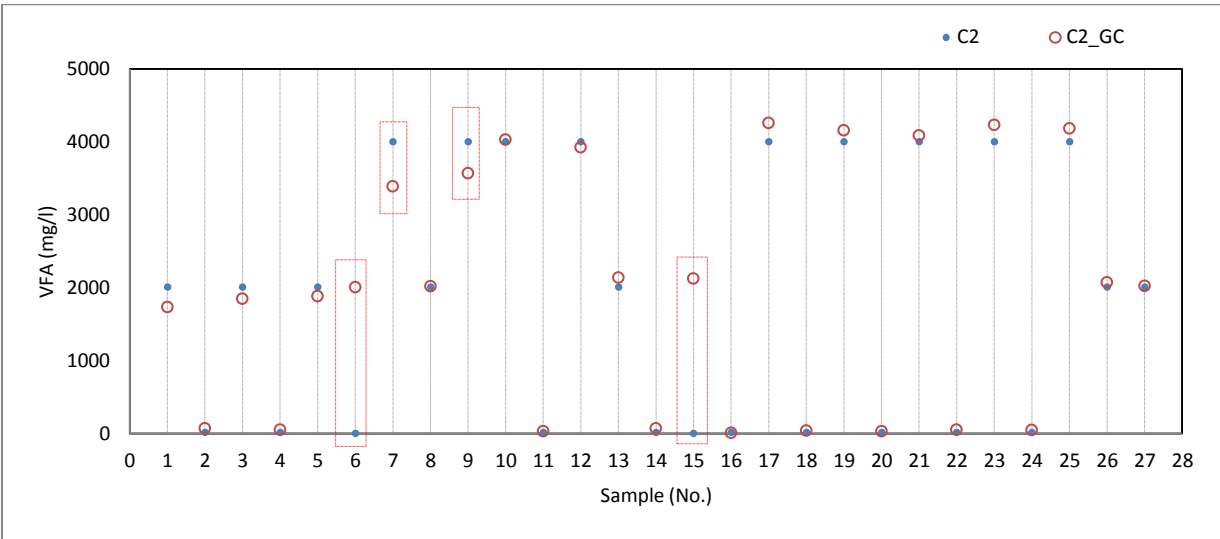
As shown and discussed in section 4.2, the calibration model was not very satisfying in C3 and C4 measurements. To get a more reliable reference concentration for these 77 calibration samples, they were re-measured by GC. Some differences between the two reference concentrations were found and shown in Figure 34 and 35, the exact values of GC measurement are given in Appendix C. Table C1.

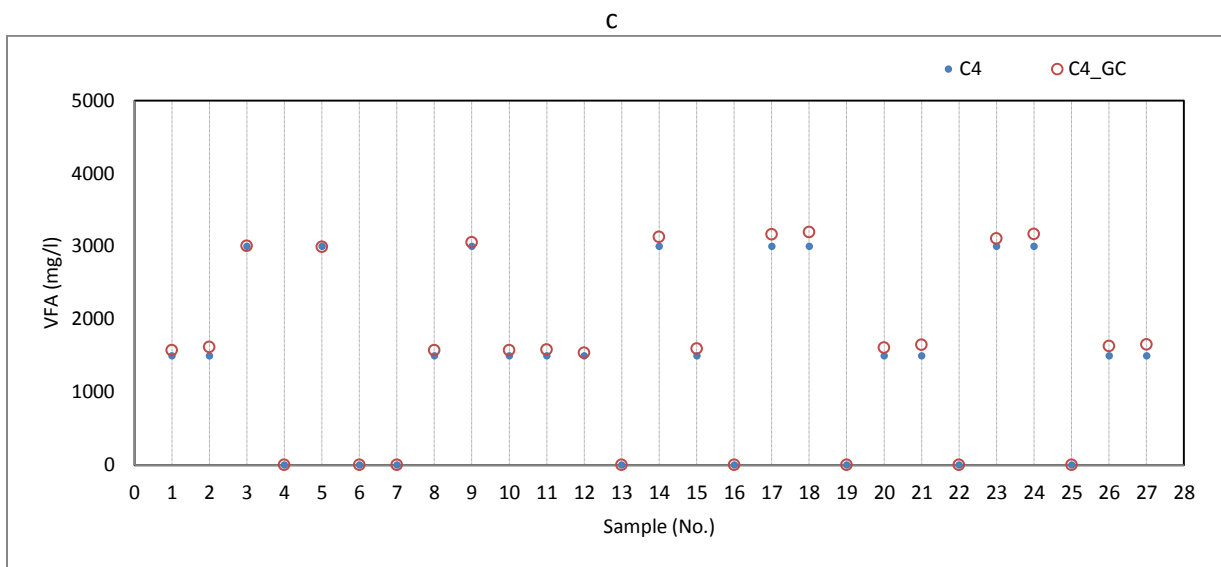
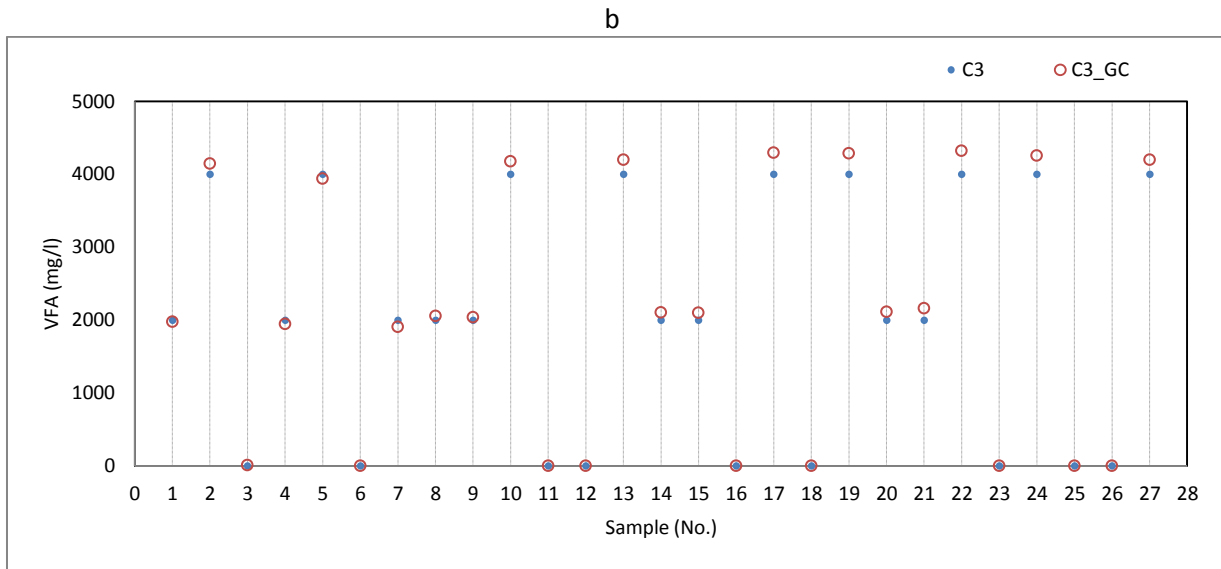
- Spiked UASB effluent samples

The red square markers in Figure 34a and 34b indicate a offset that is more than 200 mg/L. In sample 6 and 15, the offset in acetate was 2000 mg/L. While the biggest offset in C3 and C4 was only about 150 mg/L in four samples, and in the rest samples, this disparity was within 100 mg/L.



a





d

Figure 34 Comparison of two reference concentrations in UASB matrix

- **Spiked leachate samples**

Due to the existence of the base VFA concentrations in the leachate, the reference concentrations of these samples deviated further from the GC values (Figure 35). Generally, 500 – 800 mg/L offset in total VFA concentration, and 400 mg/L offset in C2 concentration could be found in every sample. The red square markers indicate an offset that is larger than 1000 mg/L.

Excluding the sample 2, 3 and 12, the average offset in the two reference values was smaller for C3 and C4 concentrations.

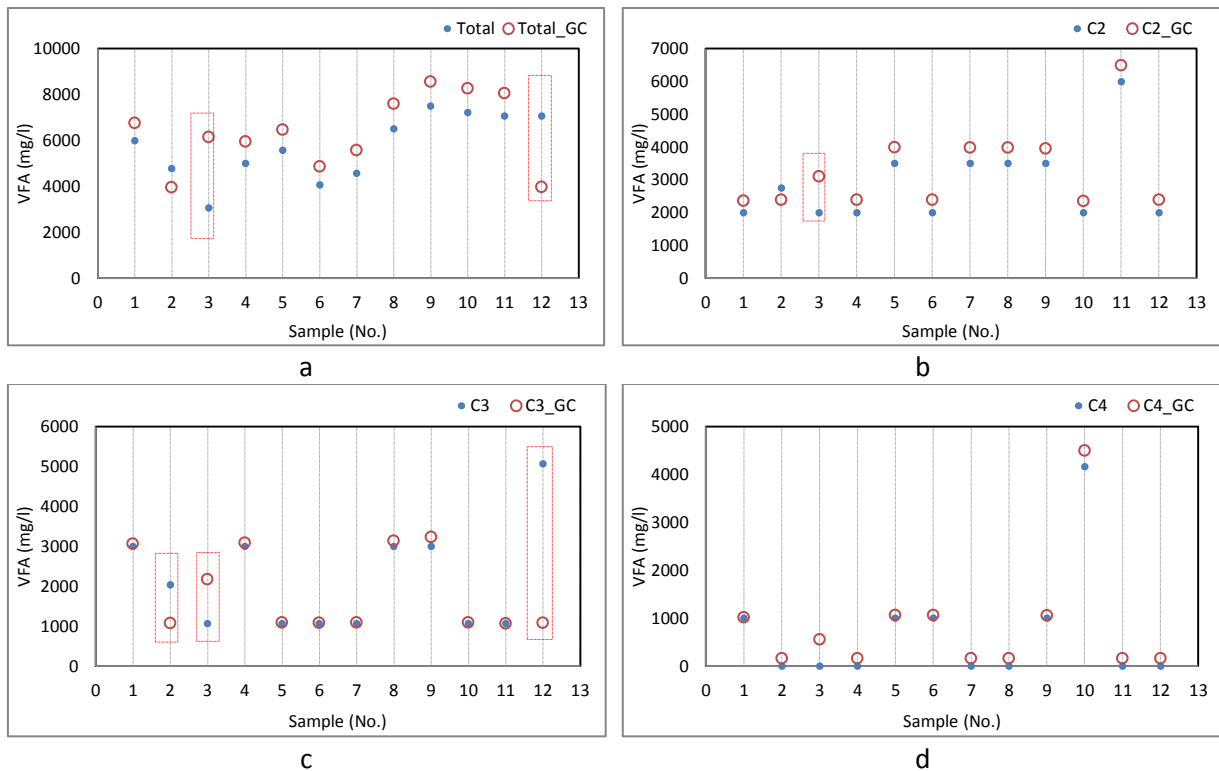


Figure 35 Comparison of two reference concentrations in leachate matrix

- **Discussion**

The results shown in Figure 34 and 35 indicated that, the inaccuracy of C3 and C4 models was not caused by the error in the reference concentrations. The offsets in C2 and total VFA concentrations did not show a notable impact on the predictions.

In the spiked UASB effluent calibration samples, the concentration of C2 and C3 was randomised among 0, 2000 and 4000 mg/L and C4 concentration was among 0, 1500 and 3000 mg/L. In the spiked leachate calibration samples, C2 concentration was randomised mainly among 2000 and 4000 mg/L, C3 concentration among 1000 and 3000 mg/L, and C4 among 0 and 1000 mg/L. Compared to C3 and C4, the C2 concentrations in the lab-scale and full-scale samples were more similar to the calibration samples. In this case, the C2 model was well tuned for measuring the specific type of effluent.

The C3 and C4 concentrations in a stable AD process are always much lower than C2 concentrations. As observed in this study, C3 was about 1000 mg/L and C4 was about 100 mg/L. Spiking the lower C3 and C4 concentrations for calibration dataset could be a solution for improving the models for these two compounds.

4.3 Dataset analysis

4.3.1 Noise of ambient humidity

The measured spectra were first analysed with PCA method, the loading weight of the acetic acid (PC1), propionic acid (PC2) and butyric acid (PC3) spectra are shown in Figure 36. The two peaks of

individual VFA could hardly be observed with the highly fluctuating noises. The noise has the same variation pattern as the ambient humidity (minima at 7:00 A.M. and maxima at 7:00 P.M.), with a cycle of 24 h. The ambient humidity was the most important source that contributed to this noise.

The cause of this noise might be the impact of ambient humidity on the Brucker unit components (i.e. light source or light transition component). However, the desiccant in the Brucker unit was not enough to remove this effect. To eliminate or attenuate the interference of the ambient humidity, the collected spectra should be processed before applied for VFA prediction.

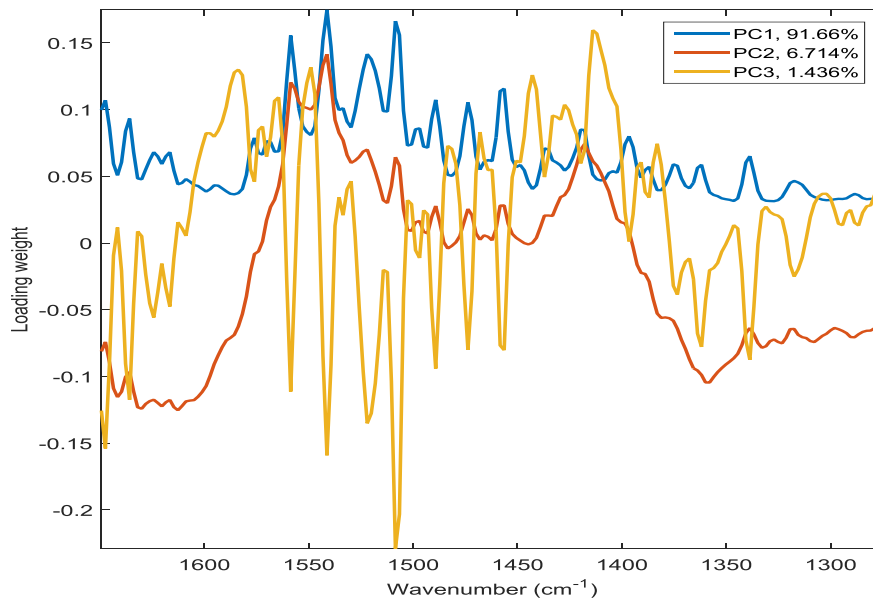


Figure 36 Measured spectrum with ambient humidity noise

4.3.2 Difficulties in improving of individual VFA calibration curve

As shown in Figure 37, the main peaks of C2, C3, and C4 (in the wavelength of 1350-1600 cm^{-1}) are very close under the same concentration. Especially for C3 and C4, even the small absorption peaks are really close (see the red squares in Figure 38). Usually, the concentrations of C3 and C4 are much lower than 5g/L, the absorption peaks will be more difficult to detect. Therefore, it was very difficult for the calibration model to differentiate between these two individual VFAs, which caused the inaccuracy of C3 and C4 measurements.

One solution is to use more calibration samples with a broader concentration range, in order to have a better calibration curve. However, this method is costly. Since the calibration curves have to be rebuilt for each specific treatment plant, the investment for applying the OPTI-VFA sensor would increase.

Another solution is to increase the light intensity, thus to be able to differentiate the spectra of the individual VFAs. With a more distinct spectrum shape, the calibration model can be more accurate, and the sensitivity of the sensor will be improved.

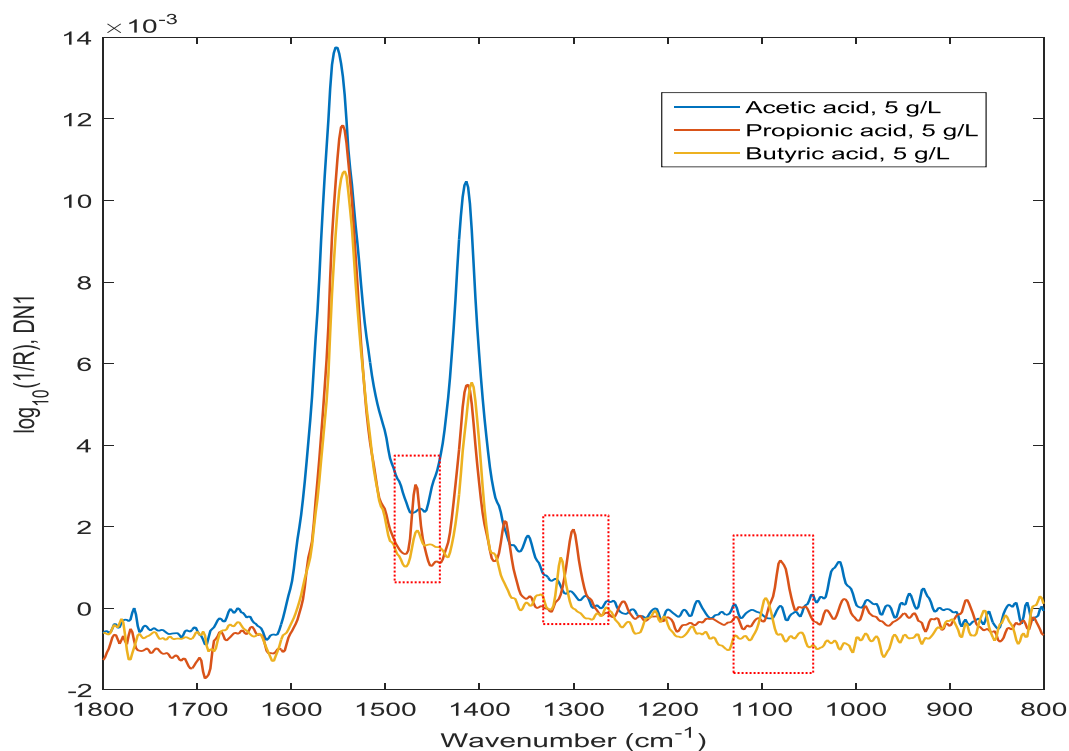


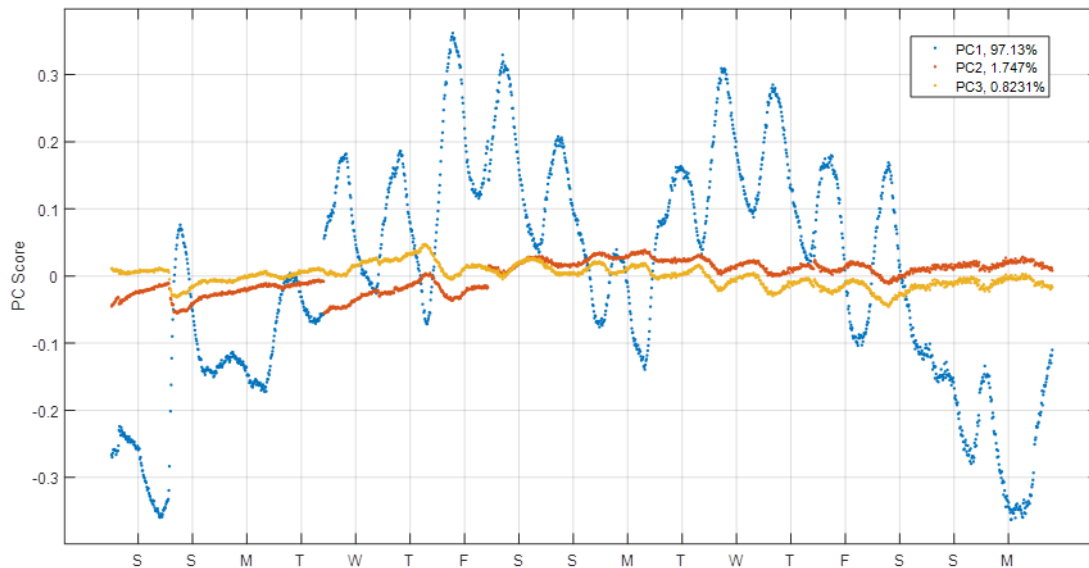
Figure 37 Spectrum of individual VFAs

4.4 Calibration model improvement

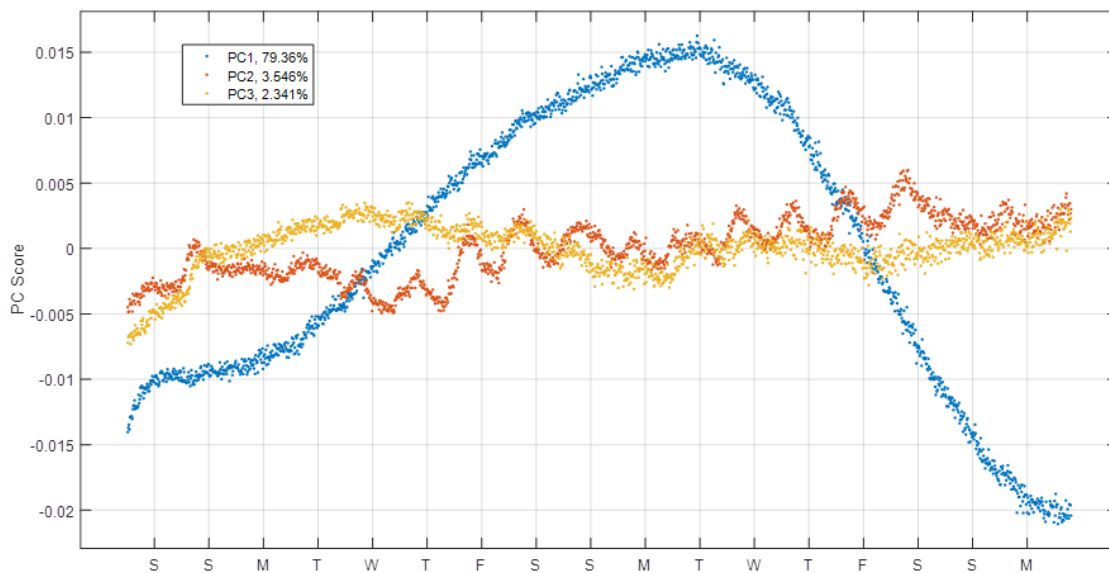
4.4.1 Improvement after removal of ambient humidity noise

The spectra measured in cycle 6 were processed, in order to compare the prediction before and after ambient humidity noise removal. Before removing the ambient humidity noise, the prediction of acetic acid (PC1 in Figure 38a) was fluctuating significantly, and the concentration peak was not shown compared to the GC reference of cycle 6 (Figure 17). While after the noise removal, the sensor predictions could well follow the dynamic C2 variations (PC1 in Figure 38b).

However, the ambient noise was still observed in the propionic acid predictions (Figure 38b, PC2). It shows that the noise removal was not complete, and it might be caused by the nonlinearity of the data.



a



b

Figure 38 Improvement of C2 prediction after removal of ambient humidity

Note: x-axis is the time in days, y-axis is the PC Score. (Data processed by VTT)

4.4.2 Improvement by applying SMF calibration model

The in-process and off-process total VFA predictions by PLS and SMF calibration model were compared in Figure 39 for Cycle 3 and 6.

For cycle 3, the difference between the in-process predictions (blue dots) by the two models was negligible. When comparing with the GC results (red diamond), the off-process predictions (red dots) predicted by SMF model had a lower noise, but this was not significant either. As a result, both calibration models were applicable for the OPTI-VFA system. However, it was found that less dataset is required to build the SMF model (195 spectra for PLS model and 153 spectra for SMF model).

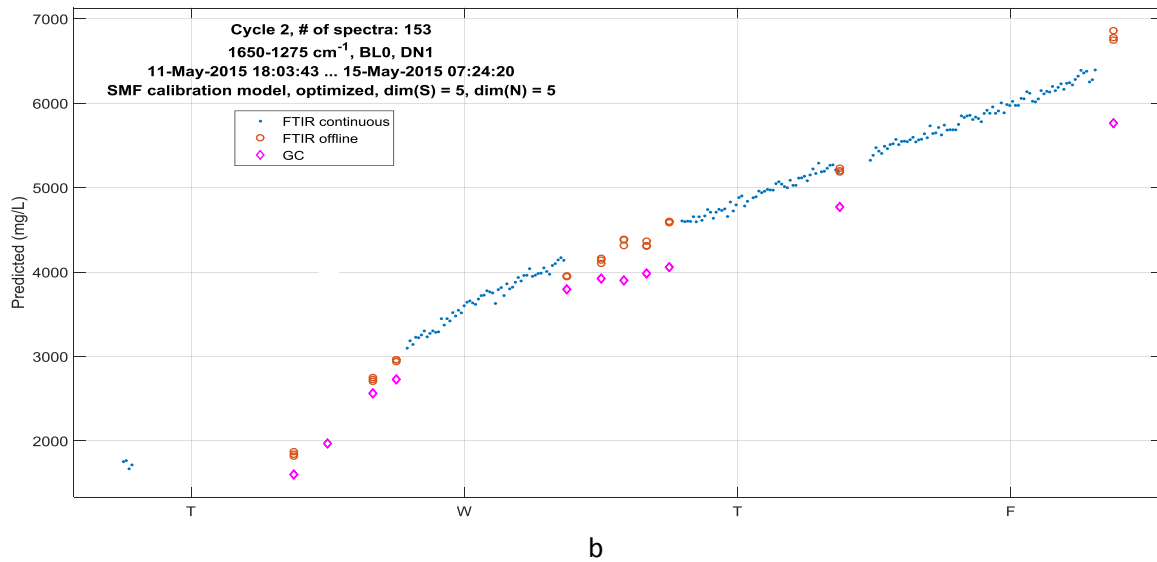
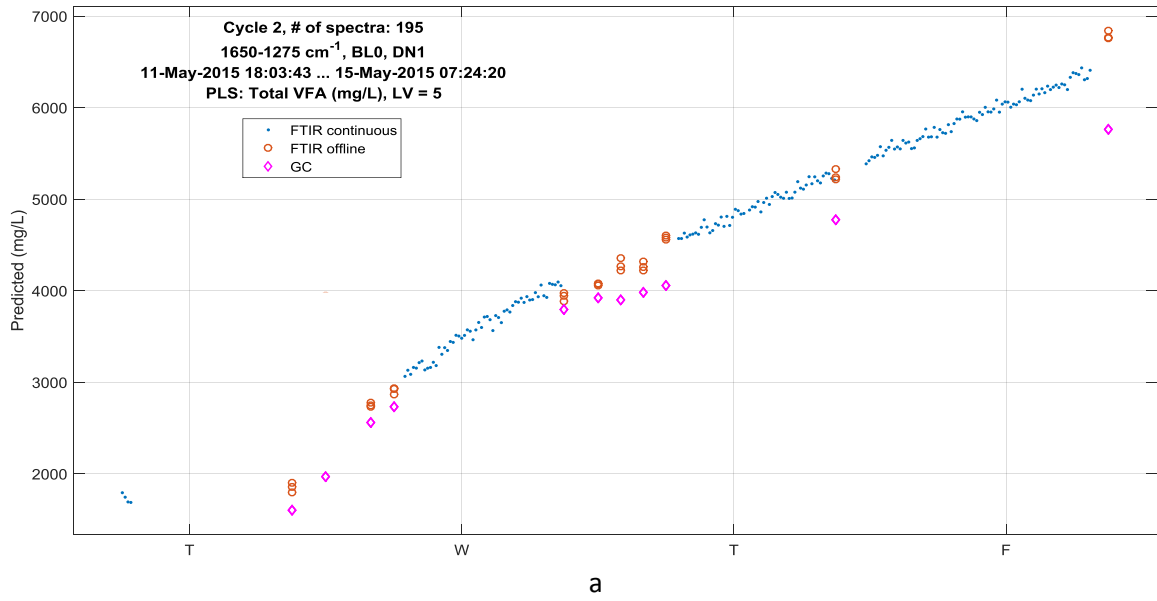
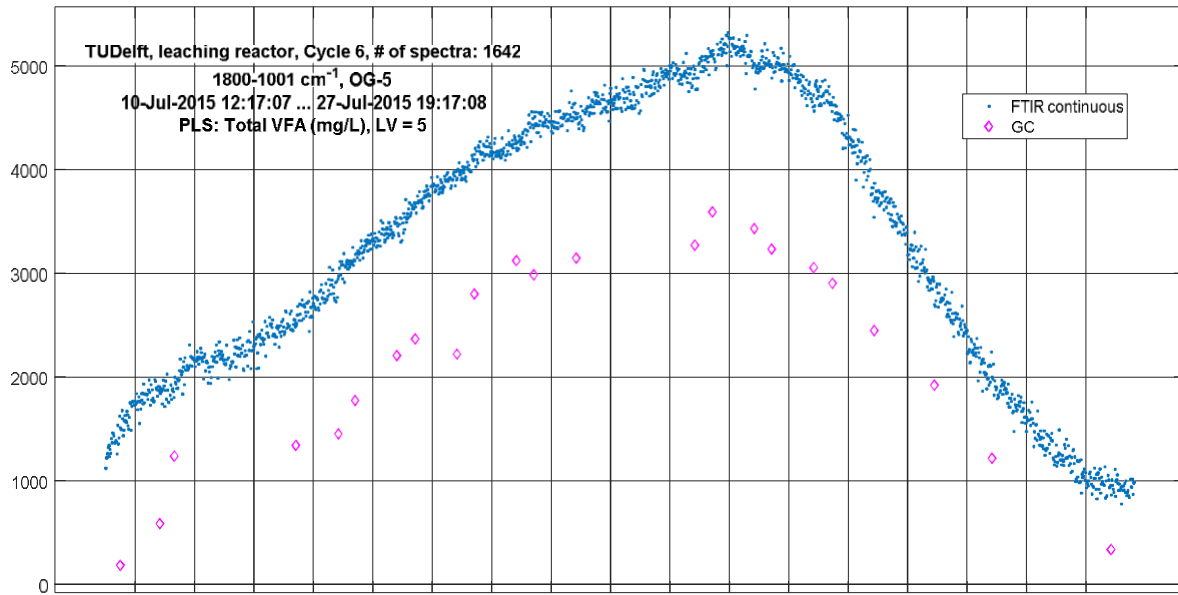


Figure 39 Comparison of three different calibration models

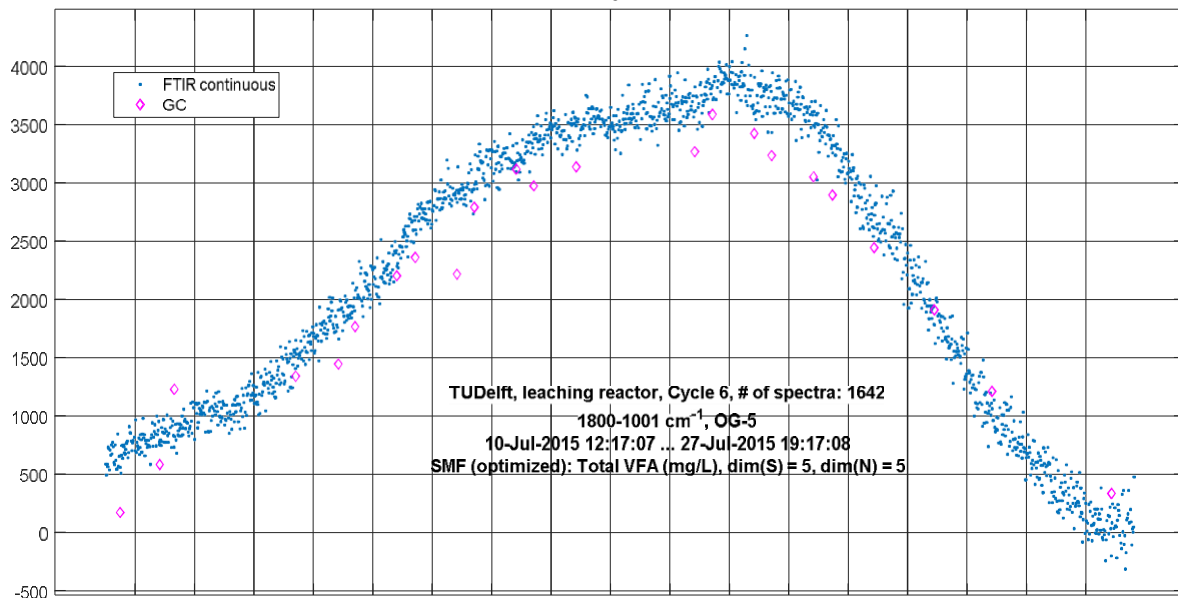
(a: PLS calibration model; b: SMF calibration model)

Note: x-axis is the time in days, y-axis is the VFA concentration. (Data processed by VTT)

For cycle 6, the total VFA concentration span (60-3600 mg/L) was smaller than that in cycle 3 (1000-6500 mg/L). In this situation, the SMF model gave a better prediction. As shown in Figure 40, although the noise of SMF predictions were slightly higher, the offset was much smaller than the PLS predictions (500 mg/L and 1500-2000 mg/L respectively).



a



b

Figure 40 Total VFA profile predicted by PLS and SMF models

Note: x-axis is the time in days, y-axis is the VFA concentration. (Data processed by VTT)

CHAPTER 5 CONCLUSION & RECOMMENDATION

5.1 Two-phase system performance

The first-phase leaching bed reactor was operated batch-wise, 6 cycles were carried out, with different liquid feeding rates and running times. It was found that the reactor was able to hydrolyse the biowaste sufficiently in approximately 5 days, while it took about 6-10 days to reach the peak VFA concentration. The peak VFA concentration was about half of the peak sCOD concentration, which indicated the insufficiency of the acidification. The VFA concentration in the leachate could be controlled by adjusting the liquid feeding rate and the running time of each cycle. The operation strategy without continuous liquid feeding gave the most efficient VFA production rate (1100 mg/L/d).

Because of the high alkalinity in the UASB effluent, the pH in the leaching bed could be maintained around 7 during the whole cycle. It prevented the production of alcohols and improved the VFA production. However, the negative effect of this recycling is that, the methanogens in the UASB effluent consumed part of the VFA produced in the first-phase.

The second-phase UASB reactor was operated for 105 days. The reactor functioned perfectly in conversion of VFA into methane, since the VFA concentration in the effluent remained constantly below 100 mg/L after day 40. The VFA concentration in the effluent was 100-250 times less than the soluble COD concentration, there might have been some other heavier organic molecules and/or a high concentration of sulphide present in the UASB effluent.

The COD removal and dynamic VFA profile were found to be early indicators for the system's imbalance. Although biogas production was sensitive to the variation of the OLR, it had a delay in indicating the deterioration of the system. The pH could not be used as an effective indicator either.

5.2 Sensor performance

The OPTI-VFA sensor was able to give an acceptable performance for online monitoring of the VFA concentration in the lab-scale leaching bed reactor. For acetic acid in the range of 1000 to 4000 mg/L, a good prediction was observed. The prediction of total VFA showed a constant offset of 1000 mg/L, but was still acceptable in a range of 2000 to 7000 mg/L. The propionic acid and butyric acid concentrations predicted by the sensor were not very reliable due to a concentration below 1000 mg/L.

By online monitoring of VFA concentration in Attero's full-scale biogas plant, the OPTI-VFA sensor demonstrated its potential in providing reliable predictions in the first-phase, although it could not indicate the low VFA concentrations in the second-phase. When monitoring in the first-phase, the sensor performance was similar to that in the lab-scale first-phase, with good predictions of total VFA and acetic acid yet inaccurate propionic acid and butyric acid predictions. The sensor could be applied in less controllable full-scale conditions for monitoring VFA production. However, it is still challenging to use the sensor for monitoring biogas production, where the VFA concentration is low.

A demi water matrix and a leachate matrix, with a pH range of 3-9, were applied for the sensor validation. With a high VFA concentration in the demi water matrix (a total VFA concentration of 7000 mg/L), the sensor was able to give a good prediction in a pH range of 6-9. But in the leachate matrix, the sensor could only give an acceptable prediction in the pH range of 7-8.

One leachate sample was measured by the OPTI-VFA sensor under a temperature range of 33-44 °C. The sample temperature in a mesophilic range did not significantly affect the performance of the OPTI-VFA sensor.

The sensor was also validated in four matrices with increasing levels of bicarbonate and ammonia concentrations. These two compounds could influence the sensor's performance in measuring total VFA, acetic acid and propionic acid. This interference was more significant than other physical or chemical properties of the sample.

5.3 Dataset analysis

The spectral data collected in the online monitoring, batch tests, and re-measurement of calibration samples was processed mathematically. From the analysis results, it can be concluded that the most likely cause of the positive offset in total VFA prediction was the presence of bicarbonate and ammonia. While the inaccuracy of propionic acid and butyric acid predictions was caused by a combination of their low concentrations, the presence of interference, and the similarity in their spectra.

On the one hand, the accuracy of total VFA (sum of the individual VFAs) prediction could be easily improved due to the similarity in individual VFA absorption peaks. On the other hand, it is challenging to establish an accurate calibration model for individual VFAs prediction, especially for propionic acid and butyric acid.

Additionally, the ambient humidity was found to introduce a periodic noise to the measured spectra, and it leads to a significant deterioration in the accuracy of VFA prediction.

5.4 Improvements and potentials

The ambient humidity noise can be partially removed with a mathematical method. Removing the ambient humidity noise could significantly improve the performance of PLS calibration model.

After comparing the predictions of the PLS and SMF models it can be concluded that the models could give similar performance in predicting high VFA concentrations. Therefore, either model can be used as a calibration method for the OPTI-VFA sensor. However, the SMF method requires less data for developing the VFA calibration models and it gave better predictions when the VFA concentrations were lower than 4000 mg/L for total VFA.

Since the bicarbonate and ammonia have distinct absorption peaks, which are different from that of the VFAs, it is possible to separate them from VFA measurements. By building calibration models for bicarbonate and ammonia, the accuracy of total VFA predictions can be improved and the sensor will give information of the process state.

5.5 Recommendations

Based on the conclusions, some recommendations are summarised for the application and improvement of OPTI-VFA system in the future.

1. Use the sensor for controlling VFA production instead of biogas production

The sensor was more accurate when measuring high concentration VFAs. Although the results were not very accurate, the sensor was able to predict the variations in VFA concentration. In the biogas production process, the VFA concentrations will be too low to be accurately detected by the OPTI-VFA sensor. To achieve a reliable performance, this sensor with improved models would be more interesting for monitoring and controlling the VFA production.

2. Include HCO_3^- and NH_4^+ measurements in the sensor's function

HCO_3^- and NH_4^+ contribute significantly to the buffer capacity in the AD process. The buffer capacity is also considered as a good indicator for the process state. Since these two ions have distinct absorption peaks in the same wavelength range used for VFA measurement, it is possible to build separate calibration models for them. In this case, the sensor will be able to monitor multiple parameters simultaneously. By online monitoring both VFA and alkalinity, OPTI-VFA sensor will be able to give more information about the process state, which certainly adds value to the OPTI-VFA system.

3. Verify the fouling potential in long-term operation

In our study, the leachate contained mainly VFA and no fouling or scaling was observed during the leachate measurements. The sensor did not need to be cleaned for 18 days of continuous in-process monitoring. Although foaming occurred during the online monitoring in UASB reactor, the diamond tip of the probe was not affected.

However, the long-term effect of in-process monitoring on the diamond tip could not be studied yet. The fouling might lead to a lower permeability, thus decreasing the accuracy of the sensor. Additionally, when the sensor is applied in high lipid-containing samples, the fouling potential can be much higher. To study the robustness of the OPTI-VFA sensor, validations under these conditions are recommended.

4. Shorten optical fibre

The (polycrystalline infrared) optical fibre connecting the light source and the probe was expensive (about EUR 1000 per metre) and it absorbs infrared light during the light transportation. In a full-scale treatment plant, it is possible to create a by-pass, where the probe could be easily installed. In this case, the length of the optical fibre can be shortened. It will be beneficial for reducing system cost and increasing the light transmission, thus improving the sensitivity of the system for low VFA concentration predictions.

Reference

- Ahring, B.K., Sandberg, M., Angelidaki, I. 1995. Volatile fatty acids as indicators of process imbalance in anaerobic digestors. *Appl Microbiol Biotechnol*, **43**, 559-565.
- Anderson, G.K., Yang, G. 1992. Determination of bicarbonate and total volatile acid concentration in anaerobic digesters using a simple titration. *Water environment research*, **64**(1), 53-59.
- Angelidaki, I., Alves, M., Bolzonella, D., Borzacconi, L., Campos, J.L., Guwy, A.J., Kalyuzhnyi, S., Jenicek, P., van Lier, J.B. 2009. Defining the biomethane potential (BMP) of solid organic wastes and energy crops: a proposed protocol for batch assays. *Water science and technology : a journal of the International Association on Water Pollution Research*, **59**(5), 927-34.
- Battimelli, A., Carrere, H., Delgenes, J.P. 2009. Saponification of fatty slaughterhouse wastes for enhancing anaerobic biodegradability. *Bioresource technology*, **100**(15), 3695-700.
- Beebe, K.R., Kowalski, B.R. 1987. An introduction to multivariate calibration and analysis. *Analytical Chemistry*, **59**(17), 1007A-1017A.
- Bisogni, J.J., Witzmann, S.W., Stedinger, J.R. 1998. A simple method for determination of volatile acid concentration with corrections for ionic strength. *Water environment research*, **70**(7), 1303-1306.
- Boe, K., Batstone, D.J., Steyer, J.P., Angelidaki, I. 2010. State indicators for monitoring the anaerobic digestion process. *Water research*, **44**(20), 5973-80.
- Bongards, M., Gaida, D., Trauer, O., Wolf, C. 2014. Intelligent automation and IT for the optimization of renewable energy and wastewater treatment processes. *Energy, Sustainability and Society*, **4**(1), 19.
- Bouallagui, H., Ben Cheikh, R., Marouani, L., Hamdi, M. 2003. Mesophilic biogas production from fruit and vegetable waste in a tubular digester. *Bioresource technology*, **86**, 85-89.
- Bouvier, J.C., Steyer, J.P., Delgenes, J.P. 2002. *On-line titrimetric sensor for the control of VFA and/or alkalinity in anaerobic digestion processes treating industrial vinasses*. IWA.
- Buczowska, A., Witkowska, E., Gorski, L., Zamojska, A., Szewczyk, K.W., Wroblewski, W., Ciosek, P. 2010. The monitoring of methane fermentation in sequencing batch bioreactor with flow-through array of miniaturized solid state electrodes. *Talanta*, **81**(4-5), 1387-92.
- Cobb, S.A., Hill, D.T. 1991. Volatile fatty acid relationships in attached growth anaerobic fermenters. *Transactions of the ASAE*, **34**(6), 2564-2572.
- Costello, D.J., Greenfield, P.F., Lee, P.L. 1991a. Dynamic modelling of a single-phase high-rate anaerobic reactor-II. Model verification. *Water research*, **25**(7), 859-871.
- Costello, D.J., Greenfield, P.F., Lee, P.L. 1991b. Dynamic modelling of a single-phase stage high-rate anaerobic reactor-I. Model derivation. *Water research*, **25**(7), 847-858.
- Demirel, B., Yenigun, O. 2002. Two-phase anaerobic digestion processes: a review. *Journal of Chemical Technology & Biotechnology*, **77**(7), 743-755.
- Dias, A.M., Moita, I., Alves, M.M., Ferreira, E.C., Pascoa, R., Lopes, J.A. 2008. Activated sludge process monitoring through in situ near-infrared spectral analysis. *Water science and technology : a journal of the International Association on Water Pollution Research*, **57**(10), 1643-50.
- Directive, E.W.F. 2008. European Union Waste Framework Directive.
- Falk, H.M., Reichling, P., Andersen, C., Benz, R. 2015. Online monitoring of concentration and dynamics of volatile fatty acids in anaerobic digestion processes with mid-infrared spectroscopy. *Bioprocess and biosystems engineering*, **38**(2), 237-49.
- Feitkenhauer, H., von Sachs, J., Meyer, U. 2002. On-line titration of volatile fatty acids for the process control of anaerobic digestion plants. *Water research*, **36**(1), 212-218.
- Ganesh, R., Torrijos, M., Sousbie, P., Lugardon, A., Steyer, J.P., Delgenes, J.P. 2014. Single-phase and two-phase anaerobic digestion of fruit and vegetable waste: comparison of start-up, reactor stability and process performance. *Waste management*, **34**(5), 875-85.
- Gaterell, M.R., Gay, R., Wilson, R., Gochin, R.J., Lester, J.N. 2000. An Economic and Environmental Evaluation of the Opportunities for Substituting Phosphorus Recovered from Wastewater

- Treatment Works in Existing UK Fertiliser Markets. *Environmental Technology*, **21**(9), 1067-1084.
- Ghosh, S., Henry, M.P., Christopher, R.W. 1985. Hemicellulose conversion by anaerobic digestion. *Biomass*, **6**(4), 257-269.
- Grimberg, S.J., Hilderbrandt, D., Kinnunen, M., Rogers, S. 2015. Anaerobic digestion of food waste through the operation of a mesophilic two-phase pilot scale digester--assessment of variable loadings on system performance. *Bioresource technology*, **178**, 226-9.
- Gujer, W., Zehnder, A.J.B. 1983. Conversion processes in anaerobic digestion. *Water science and technology : a journal of the International Association on Water Pollution Research*, **15**, 127-167.
- Hasson, M., Nordberg, A., Sundh, I., Mathisen, B. 2002. Early warning of disturbances in a laboratory-scale MSW biogas process. *Water science and technology : a journal of the International Association on Water Pollution Research*, **45**(10), 255-260.
- Held, C., Wellacher, M., Robra, K., Gubitz, G.M. 2002. Two-phase anaerobic fermentation of organic waste in CSTR and UFAF-reactors. *Bioresource technology*, **81**(1), 19-24.
- Holm-Nielsen, J.B., Lomborg, C.J., Oleskowicz-Popiel, P., Esbensen, K.H. 2008. On-line near infrared monitoring of glycerol-boosted anaerobic digestion processes: evaluation of process analytical technologies. *Biotechnology and bioengineering*, **99**(2), 302-13.
- Ince, O., Anderson, G.K., Kasapgil, B. 1995. Control of organic loading rate using the specific methanogenic activity test during start-up of an anaerobic digestion system. *Water research*, **29**(1), 349-355.
- Jacobi, H.F., Moschner, C.R., Hartung, E. 2009. Use of near infrared spectroscopy in monitoring of volatile fatty acids in anaerobic digestion. *Water science and technology : a journal of the International Association on Water Pollution Research*, **60**(2), 339-46.
- Khalid, A., Arshad, M., Anjum, M., Mahmood, T., Dawson, L. 2011. The anaerobic digestion of solid organic waste. *Waste management*, **31**(8), 1737-44.
- Khanal, S.K. 2008. *Anaerobic biotechnology for bioenergy production: principles and applications*. first ed. John Wiley & Sons USA.
- Kim, M., Ahn, Y., Speece, R.E. 2002. Comparative process stability and efficiency of anaerobic digestion: mesophilic vs. thermophilic. *Water research*, **36**(17), 4369-4385.
- Kleybocker, A., Liebrich, M., Verstraete, W., Kraume, M., Wurdemann, H. 2012. Early warning indicators for process failure due to organic overloading by rapeseed oil in one-stage continuously stirred tank reactor, sewage sludge and waste digesters. *Bioresource technology*, **123**, 534-41.
- Kondusamy, D., Kalamdhad, A.S. 2014. Pre-treatment and anaerobic digestion of food waste for high rate methane production – A review. *Journal of Environmental Chemical Engineering*, **2**(3), 1821-1830.
- Krapf, L.C., Nast, D., Gronauer, A., Schmidhalter, U., Heuwinkel, H. 2013. Transfer of a near infrared spectroscopy laboratory application to an online process analyser for in situ monitoring of anaerobic digestion. *Bioresource technology*, **129**, 39-50.
- Kuba, T., Furumai, H., Kusuda, T. 1990. A kinetic study on methanogenesis by attached biomass in a fluidized bed. *Water research*, **24**(11), 1365-1372.
- Labib, F., Ferguson, J.F., Benjamin, M.M., Merigh, M., Ricker, N.L. 1992. Anaerobic butyrate degradation in a fluidized-bed reactor: effects of increased concentrations of hydrogen and acetate. *Environmental science & technology*, **26**(2), 369-376.
- Lahav, O., Shlafman, E., Morgan, B.E., Loewenthal, R.R., Tarre, S. 2002. *Accurate on-site volatile fatty acids (VFA) measurement in anaerobic digestion-verification of a new titrative method*.
- Lee, W.S., Chua, A.S.M., Yeoh, H.K., Ngoh, G.C. 2014. A review of the production and applications of waste-derived volatile fatty acids. *Chemical Engineering Journal*, **235**, 83-99.
- Li, L., He, Q., Wei, Y., He, Q., Peng, X. 2014. Early warning indicators for monitoring the process failure of anaerobic digestion system of food waste. *Bioresource technology*, **171**, 491-4.

- Li, W. 2014. Novel monitoring for dynamic VFA production from anaerobic kitchen waste digestion. in: *Sanitary engineering* Vol. Master, Technonology University of Delft. Delft, pp. 77.
- Lin, J., Zuo, J., Gan, L., Li, P., Liu, F., Wang, K., Chen, L., Gan, H. 2011. Effects of mixture ratio on anaerobic co-digestion with fruit and vegetable waste and food waste of China. *Journal of Environmental Sciences*, **23**(8), 1403-1408.
- Lissens, G., Vandevivere, P., De Baere, L., Biey, E.M., Verstraete, W. 2001. Solid waste digestors: process performance and practice for municipal solid waste digestion. *Water science and technology : a journal of the International Association on Water Pollution Research*, **44**(8), 91-102.
- Madsen, M., Holm-Nielsen, J.B., Esbensen, K.H. 2011. Monitoring of anaerobic digestion processes: A review perspective. *Renewable and Sustainable Energy Reviews*, **15**(6), 3141-3155.
- Marbach, R. 2005. A new method for multivariate calibration *Journal of Near infrared Spectroscopy*, **13**(5), 241.
- Marbach, R. 2002. On Wiener filtering and the physics behind statistical modeling. *Journal of biomedical optics*, **7**(1), 130-47.
- Mata-Alvares, J. 1987. A dynamic simulation of a two-phase anaerobic digestion system for solid wastes. *Biotechnology and bioengineering*, **30**, 844-851.
- Mata-Alvares, J., Llabres, P., Cecchi, F., Pavan, P. 1992. Anaerobic digestion of the Barcelona central food market organic wastes: experimental study. *Bioresource technology*, **39**, 39-48.
- Melikoglu, M., Lin, C.S.K., Webb, C. 2013. Analysing global food waste problem: pinpointing the facts and estimating the energy content. *Central European Journal of Engineering*, **3**(2), 157-164.
- Molina, F., Castellano, M., García, C., Roca, E., Lema, J.M. 2009. Selection of variables for on-line monitoring, diagnosis, and control of anaerobic digestion processes. *Water Science & Technology*, **60**(3), 615.
- Moosbrugger, R.E., Wentzel, M.C., Ekama, G.A. 1993a. A 5 pH point titration method for determining the carbonate and SCFA weak acid/bases in anaerobic systems. *Water science and technology : a journal of the International Association on Water Pollution Research*, **28**(2), 237-245.
- Moosbrugger, R.E., Wentzel, M.C., Loewenthal, R.E., Ekama, G.A., Marais, G. 1993b. Alkalinity measurement: Part 3-A 5 pH point titration method to determine the carbonate and SCFA weak acid/bases in aqueous solution containing also known concentration of other weak acid/bases. *Water SA-PRETORIA-*, **19**, 29-29.
- Mouneimne, A.H., Carrère, H., Bernet, N., Delgenès, J.P. 2003. Effect of saponification on the anaerobic digestion of solid fatty residues. *Bioresource technology*, **90**(1), 89-94.
- Nielsen, H., Uellendahl, H., Ahring, B. 2007. Regulation and optimization of the biogas process: Propionate as a key parameter. *Biomass and Bioenergy*, **31**(11-12), 820-830.
- Nizami, A.S., Murphy, J.D. 2011. Optimizing the operation of a two-phase anaerobic digestion system digesting grass silage. *Environ Sci Technol*, **45**(17), 7561-9.
- Nordberg, A., Hansson, M., Sundh, I., Nordkvist, E., Carlsson, H., Mathisen, B. 2000. Monitoring of a biogas process using electronic gas sensors and near-infrared spectroscopy (NIR). *Water science and technology : a journal of the International Association on Water Pollution Research*, **41**(3), 1-8.
- Osborne, B.G., Fearn, T., Hindle, P.H. 1993. *Practical NIR spectroscopy with applications in food and beverage analysis*. Longman Scientific and Technical, Harlow, UK.
- Palmowski, L., Simons, L., Brooks, R. 2006. Ultrasonic treatment to improve anaerobic digestibility of dairy waste streams. *Water Science & Technology*, **53**(8), 281.
- Pavan, P., Battistoni, P., Cecchi, F., Mata-Alvares, J. 2003. Two-phase anaerobic digestion of souce sorted OFMSW (organic fraction of municipal solid waste): performance and kinetic study. *Water science and technology : a journal of the International Association on Water Pollution Research*, **41**(3), 111-118.
- Penaud, V., Delgenes, J.P., Torrijos, M., Moletta, R., Vanhoutte, B., Cans, P. 1997. Definition of optimal conditions for the hydrolysis and acidogenesis of a pharmaceutical microbial biomass. *Process Biochemistry*, **32**(6), 515-521.

- Ripley, L.E., Boyle, W.C., Converse, J.C. 1986. Improved alkametric monitoring for anaerobic digestion of high-strength wastes. *Water pollution control federation*, **58**(5), 406-411.
- Rudnitskaya, A., Legin, A. 2008. Sensor systems, electronic tongues and electronic noses, for the monitoring of biotechnological processes. *Journal of industrial microbiology & biotechnology*, **35**(5), 443-51.
- Schenk, J., Marison, I.W., von Stockar, U. 2008. pH prediction and control in bioprocesses using mid-infrared spectroscopy. *Biotechnology and bioengineering*, **100**(1), 82-93.
- Schober, G., Schafer, J., Schmid-Staiger, U., Trosch, W. 1999. One and two-phase digestion of solid organic waste. *Water research*, **33**(3), 854-860.
- Shin, H.S., Han, S.K., Song, Y.C., Lee, C.Y. 2001. Performance of UASB reactor treating leachate from acidogenic fermenter in the two-phase anaerobic digestion of food waste. *Water research*, **35**(14), 3441-3447.
- Sonakya, V., Raizada, N., Kalia, V.C. 2001. Microbial and enzymatic improvement of anaerobic digestion of waste biomass. *Biotechnology Letters*, **23**(18), 1463-1466.
- Spanjers, H., Bouvier, J.C., Steenweg, P., Bisschops, I., Gils, W.v., Versprille, B. 2006. Implementation of in-line infrared monitor in full-scale anaerobic digestion process. *Water Science & Technology*, **53**(4-5), 55.
- Steyer, J.P., Bouvier, J.C., Gras, C.P., Harmand, J., Delgenes, J.P. 2002. On-line measurements of COD, TOC, VFA, total and partial alkalinity in anaerobic digestion processes using infra-red spectrometry. *Water science and technology : a journal of the International Association on Water Pollution Research*, **45**(10), 133-138.
- Thomas, E.V., Haaland, D.M. 1990. Comparison of multivariate calibration methods for quantitative spectral analysis. *Analytical Chemistry*, **62**(10), 1091-1099.
- Van Lier, J.B., Mahmoud, N., Zeeman, G. 2008. Anaerobic wastewater treatment. *Biological Wastewater Treatment: Principles*, 401-442.
- VTT. 2015. OPTI-VFA User interface and database for calibration.
- Wang, J.Y., Xu, H.L., Tay, J.H. 2002. A hybrid two-phase system for anaerobic digestion of food waste. *Water science and technology : a journal of the International Association on Water Pollution Research*, **45**(12), 159-165.
- Yu, H.W., Samani, Z., Hanson, A., Smith, G. 2002. Energy recovery from grass using two-phase anaerobic digestion. *Waste management*, **22**(1), 1-5.
- Zhu, B., Gikas, P., Zhang, R., Lord, J., Jenkins, B., Li, X. 2009. Characteristics and biogas production potential of municipal solid wastes pretreated with a rotary drum reactor. *Bioresource technology*, **100**(3), 1122-9.

Appendix

A. System performance

- **A1. Results of other 4 cycles.**

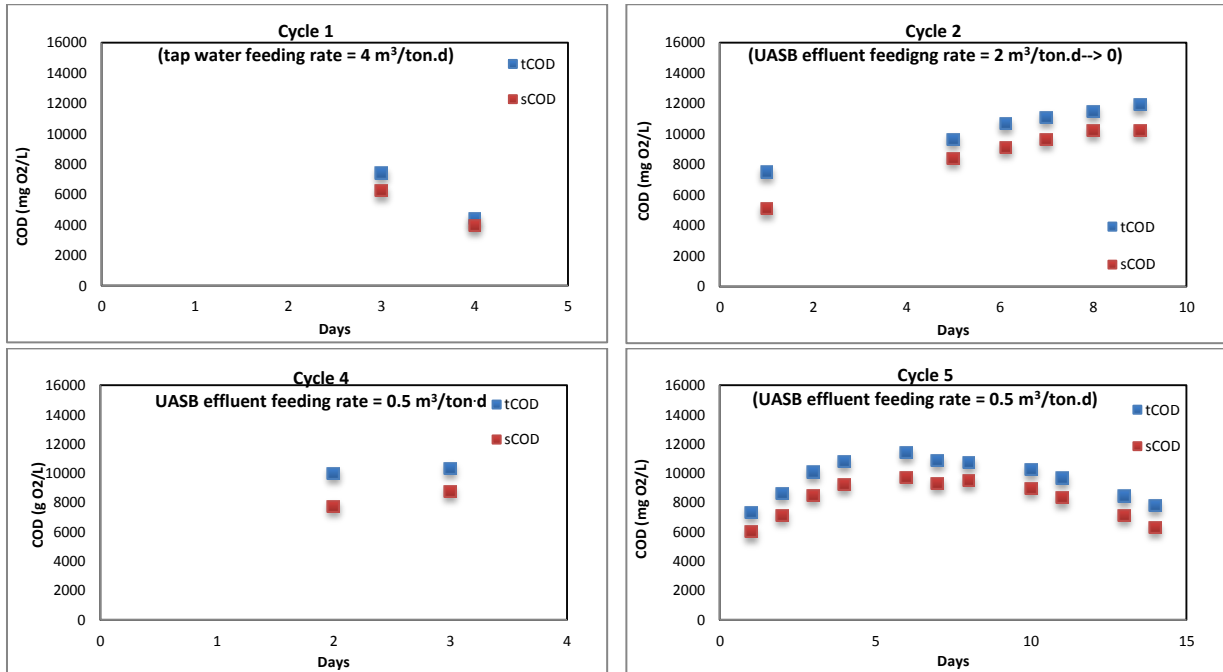


Figure A1.1 COD results

During the first cycle, there was only recirculation on day 0-2 to achieve biomass growth. On day 3 a continuously liquid feeding started. Two samples were taken on day 3 and day 4. Due to the high feeding and discharging speed (4 m³/ton·d) of tap water, the total COD in the leachate did not exceed 8 g/L, and started to decrease on day 4. A pH drop from 7 to 5 was observed, probably the low pH inhibit the hydrolysis process. Therefore, the COD concentration started to decrease on second day with tap water feeding.

The feeding and discharging was lowered to 2 m³/ton·d and stopped on day 5 during the second cycle, in order to achieve a higher COD concentration. In addition, the effluent from UASB (the second-phase) was used to replace tap water. The total COD overreached 12 g/L on day 9, the end of the cycle.

The feeding and discharging speed for cycle 5 was only 0.5 m³/ton·d. And this was kept throughout the whole cycle. There were 14 days in cycle 5, total COD raised from 7.3 g/L on day 1, to 11.4 g/L on day 6. But it started to decrease after reaching its peak. On day 14, the total COD was only 7.8 g/L.

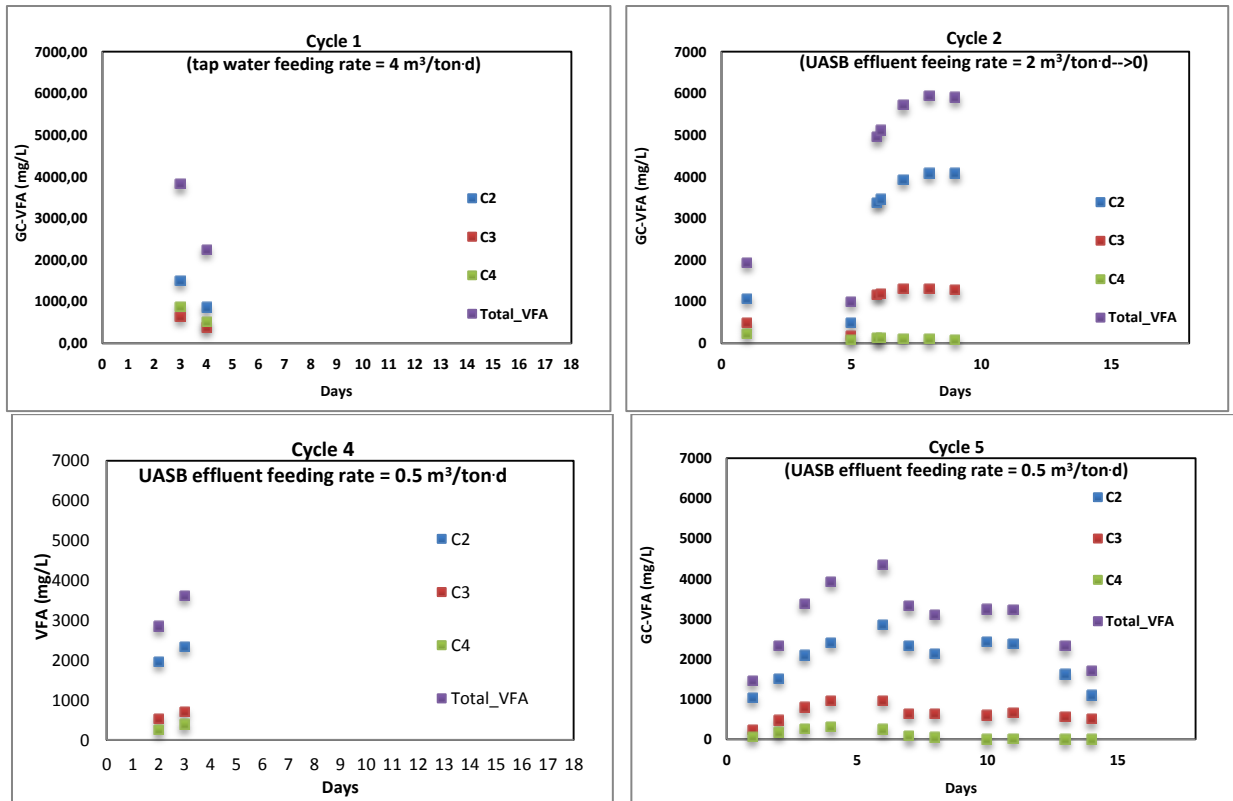


Figure A1.2 VFA results

VFA concentrations had a similar trend as the CODs under different liquid feeding rates. With a high liquid feeding rate for one day in cycle 1, the highest total VFA concentration was only 4000 mg/L.

In cycle 2, VFA concentration kept dropping when the feeding rate was halved, and decreased to 1000 mg/L on day 5. To increase the VFA concentration in the leaching bed, liquid feeding was stopped after day 5. The maximal total VFA concentration of 6000 mg/L was reached on day 8.

With a continuous liquid feeding rate of 0.5 m³/ton·d during cycle 5, the maximal total VFA level was observed on day 6, which was only about 4500 mg/L. Besides continuous liquid feeding, the lower VFA concentration in cycle 5 might also be caused by the microbial activities in the biowaste.

The VFA concentration in the leachate could be controlled by adjusting the liquid feeding rate. Under a low feeding rate in cycle 5, the total VFA concentration increased to 4500 mg/L. And the highest concentration of 7000 mg/L was achieved when there was no continuously liquid feeding in cycle 3.

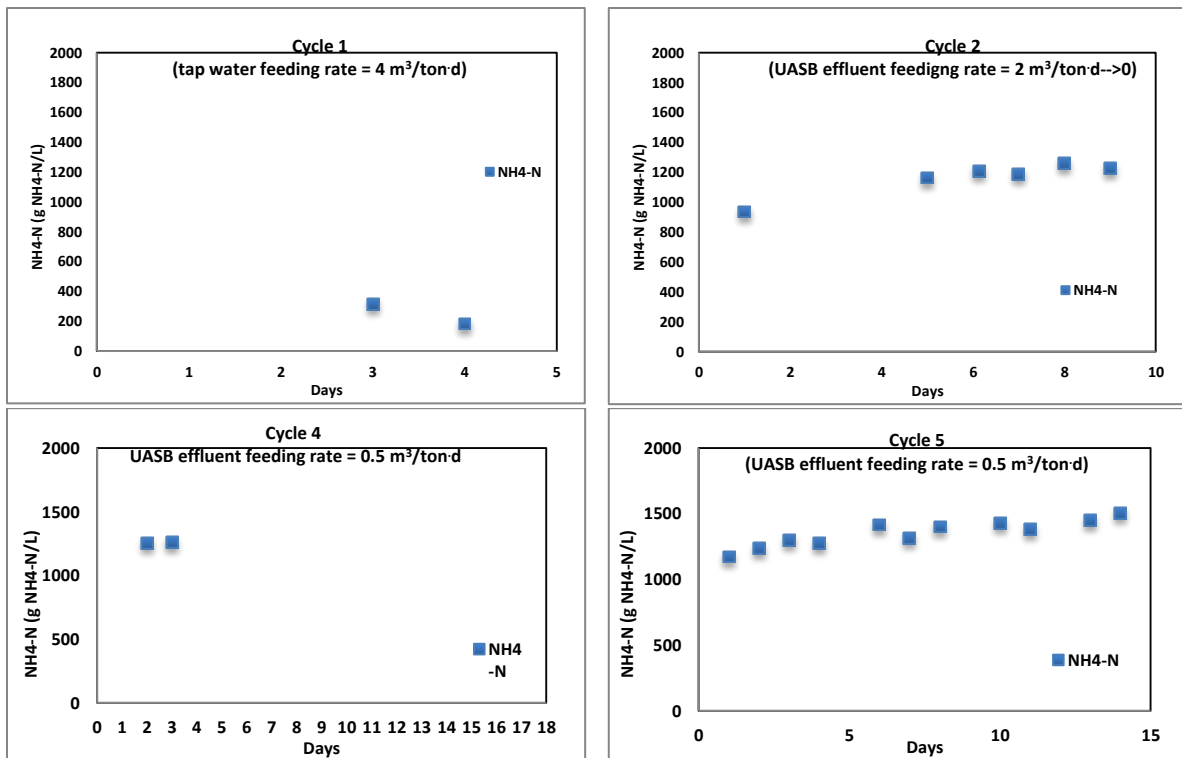


Figure A1.3 NH₄-N results of 4 cycles

The Ammonium concentration in the sample taken from the Venlo treatment plant was 1696 mg NH₄-N/L. During cycle 1, the concentration was only around 400 mg NH₄-N/L, because it was diluted by tap water.

Ammonium had accumulated in the UASB reactor, thus it increased in the UASB effluent, which had been added into the leaching bed during cycle 2-6. So a higher ammonium concentration was observed in the later cycles.

- **A2. Biogas responses to the feeding pulses**

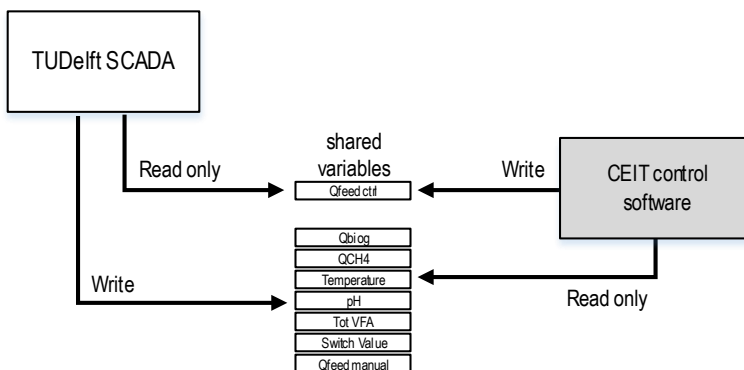


Figure A2.1 The two control systems of the UASB reactor

As can be seen in Figure A2.1, the 'conventional mode' was controlled by TUDelft SCADA system, by manually set a feeding flow rate ($Q_{\text{feed manual}}$). While in the 'control mode', $Q_{\text{feed ctrl}}$ was set automatically by CEIT control software.

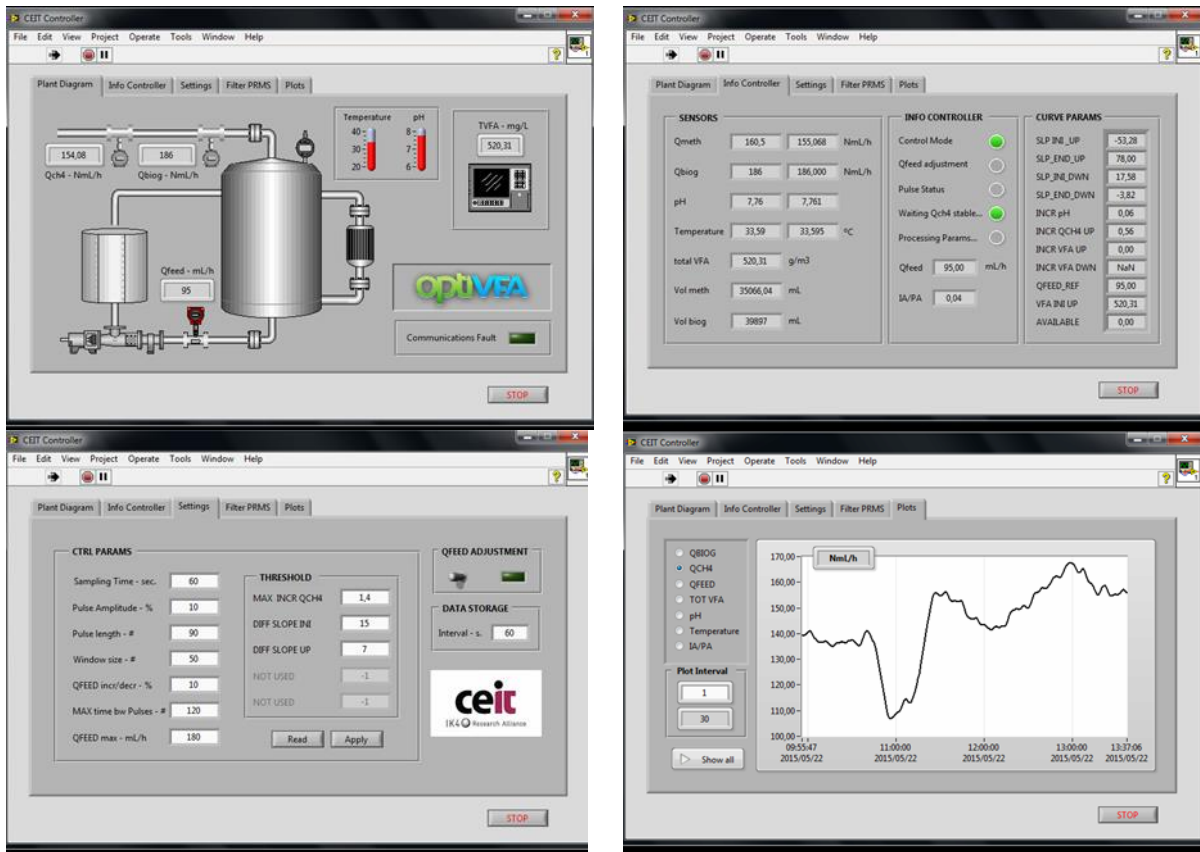
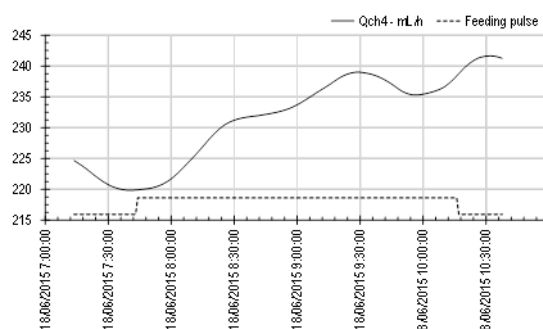
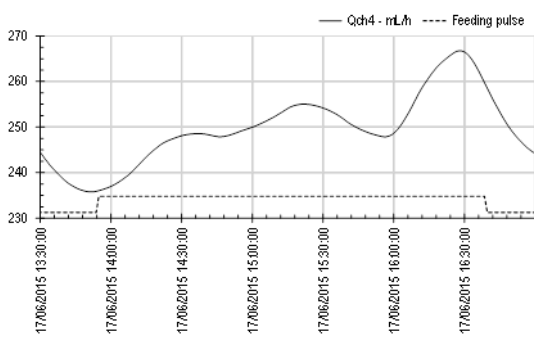


Figure A2.2 User interface of CEIT control software

Figure A2.2 shows the four main user interfaces of the control software. The first interface shows the layout of the reactor. Real time values of the ‘shared variables’, and the indicators calculated from them are shown on the second interface. Whether the process is at its maximum treatment capacity can be observed on this interface. On the third interface, control parameters such as sample frequency, length an amplitude of the pulse can be set by the controller. And the dynamics of all ‘shared variables’ can be visualized on the last interface.

The CEIT control software was validated by observing the correlation of dynamic methane signals and Q_{feed} pulses. A few trials were done, and it was found that, the real-time CH_4 signals were highly fluctuated. Therefore, 15 % amplitude of the Q_{feed} and 3 h pulse length were selected to minimize the negative impact, and to increase the reliability of the correlation as well.

The results of the tuning and validation are shown in Figure A2.3 (June 2015) and Figure A2.4 (July 2015).



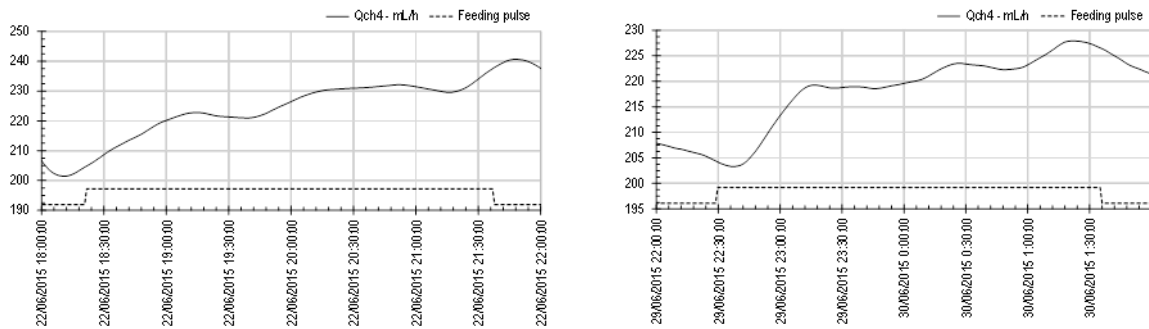


Figure A2.3 Methane flow-rate time response to feeding pulses applied in the UASB reactor (June 2015)

In June 2015, feeding pulses were regularly applied. The CH₄ responses shown in Figure A2.3 were quite sensitive to the pulses, however, it revealed the demand of a filter to smoothen the fluctuation in the response.

As a result, CEIT add a new indicator (to indicate overload situations) and installed a new algorithm into the software. The new control strategy was activated in July. In Figure A2.4 (a), Q_{feed} increased step-wise from 95 mL/h to 125 mL/h in two days, the overall increase of Q_{feed} was about 31%. The methane production rate showed similar trend, which rose from 140 mL/h to 180 mL/h (about 28 %). In Figure A2.4 (b), the control strategy was activated for one week from 17th July to 24th July. During this period, except a shortage of substrate on 20th of July, the Q_{feed} increased from 95 mL/h to 202 mL/h (112 % increase). Accordingly, the OLR increased from 3.6 kg/(m³·d) to 8.6 kg/(m³·d). The methane production rate rose from 130 mL/h to 270 mL/h, which was more than doubled.

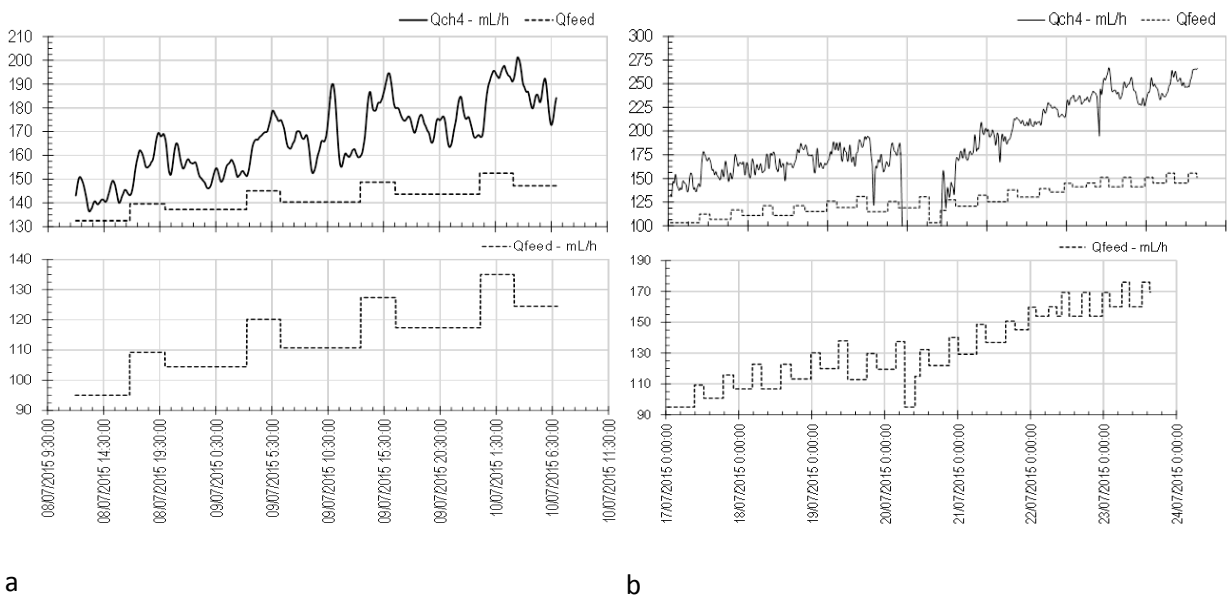


Figure A2.4 Methane flow-rate time response to feeding pulses applied in the UASB reactor (July 2015)

The UASB reactor was operated in the laboratory of TUDelft, while the CEIT control software was managed in Spain. Due to the inconvenience of communication between two locations and two disciplines, the tuning and modification of the strategy was quite challenging. At a current stage, the CEIT control software showed the possibility of developing a control strategy for AD process. Nevertheless, a lot of improvements are still required to achieve a maximum capacity, while avoiding

process imbalances/failures. For example, besides being able to increase the feeding rate, it should also be able to detect the deterioration of the system.

B. pH & Temperature tests

Table B1 Average difference between sensor and GC measurements for demi water matrix (pH test)

pH	Acetic_acid (mg/L)	Butyric_acid (mg/L)	Propionic_acid (mg/L)	Total_VFA (mg/L)
2.63	3398	1893	388	7967
3.94	2699	1254	433	6415
4.97	714	67	550	2346
6.19	110	145	160	595
7.01	63	243	126	623
7.73	13	95	176	403
9.05	158	163	110	585

The lowest difference between the two measurements was observed at a pH of 7.7 in demi water matrix.

Table B2 Average difference between sensor and GC measurements for leachate matrix (pH test)

pH	Acetic_acid (mg/L)	Butyric_acid (mg/L)	Propionic_acid (mg/L)	Total_VFA (mg/L)
3.37	606	1168	1876	920
4.29	570	685	1193	664
5.53	1643	907	1038	2317
6.51	669	330	374	1058
7.65	260	400	362	533
8.29	672	387	342	258
8.97	1795	1284	1336	374

The lowest difference between the two measurements was observed at a pH of 7.7 and 8.3 in leachate matrix.

Table B3 Average difference between sensor and GC measurements for temperature test

Measure Temperature	Acetic_acid (mg/L)	Butyric_acid (mg/L)	Propionic_acid (mg/L)	Total_VFA (mg/L)
°C	(mg/L)	(mg/L)	(mg/L)	(mg/L)
33	570	222	362	521
35	423	418	461	506
36	636	168	533	533
38	599	417	1,009	757
40	769	131	1,065	522
42	778	521	1,541	494
44	745	510	1,598	424

The lowest difference between the two measurements was observed at a temperature of 35 °C. Which means, a background temperature, which is close to the sample temperature, should be selected.

Table B4 VFA dissociation level under different pH

Demi-matrix	Acetate	Propionate	Butyrate
adjusted pH	Dissociation level	Dissociation level	Dissociation level
2,63	10^{-2}	10^{-2}	10^{-2}
3,94	10^{-1}	10^{-1}	10^{-1}
4,97	10^0	10^0	10^0
6,19	10^1	10^1	10^1
7,01	10^2	10^2	10^2
7,73	10^3	10^3	10^3
9,05	10^4	10^4	10^4
Leachate-matrix	Acetate	Propionate	Butyrate
adjusted pH	Dissociation level	Dissociation level	Dissociation level
7,65	10^2	10^2	10^2
3,37	10^{-2}	10^{-2}	10^{-2}
4,29	10^{-1}	10^{-1}	10^{-1}
5,53	10^0	10^0	10^0
6,51	10^1	10^1	10^1
8,29	10^3	10^3	10^3
8,97	10^4	10^4	10^4

C. Re-measure of Oulu calibration samples

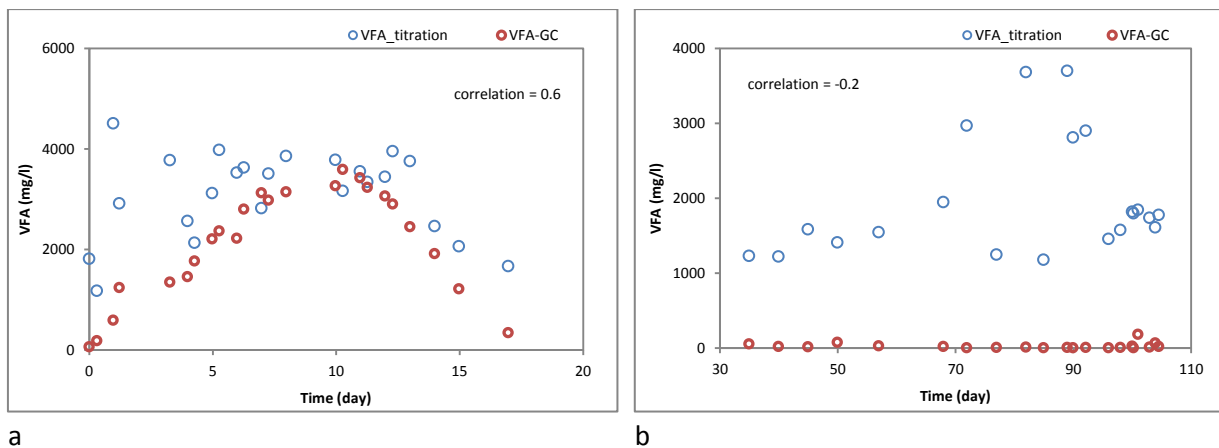
Table C1 GC results of calibration samples

Order	Name	Acetic acid	Propionic acid	IC4	Butyric acid	IC5	C5	IC6	C6	total VFA
1	222	1733	1977	0	1572	0	0	0	0	5283
2	132	66	4147	0	1616	0	0	0	0	5829
3	213	1845	11	0	3003	0	0	0	0	4860
4	121	49	1947	0	0	0	0	0	0	1995
5	233	1879	3938	0	2990	0	0	0	0	8806
6	211	2004	0	0	0	0	0	0	0	2004
7	321	3385	1907	0	0	0	0	0	0	5292
8	222	2016	2058	0	1572	0	0	0	0	5646
9	323	3566	2037	0	3053	0	0	0	0	8657
10	332	4027	4177	0	1572	0	0	0	0	9776
11	112	28	0	0	1583	0	0	0	0	1610
12	312	3924	0	0	1536	0	0	0	0	5460
13	231	2133	4197	0	0	0	0	0	0	6330
14	123	67	2105	0	3126	0	0	0	0	5298
15	222	2122	2101	0	1595	0	0	0	0	5818
16	111	6	0	0	0	0	0	0	0	6
17	333	4255	4297	0	3161	0	0	0	0	11712
18	113	37	0	0	3193	0	0	0	0	3230
19	331	4156	4286	0	0	0	0	0	0	8443
20	122	29	2113	0	1607	0	0	0	0	3749
21	322	4086	2162	0	1649	0	0	0	0	7897
22	131	48	4322	0	0	0	0	0	0	4370
23	313	4231	0	0	3104	0	0	0	0	7335
24	133	45	4258	0	3169	0	0	0	0	7472
25	311	4181	0	0	0	0	0	0	0	4181
26	212	2071	0	0	1631	0	0	0	0	3703
27	232	2020	4200	0	1653	0	0	0	0	7873

Order	Name	Acetic acid	Propionic acid	IC4	Butyric acid	IC5	C5	IC6	C6	total VFA
1	133	2356	3063	94	1015	87	116	0	25	6756
2	222	2386	1076	96	159	88	119	0	25	3949
3	111	3101	2168	93	556	86	114	0	24	6142
4	131	2381	3084	94	159	89	118	0	25	5949
5	313	3986	1087	97	1062	89	119	0	25	6465
6	113	2382	1085	97	1060	89	118	0	26	4856
7	311	3981	1088	96	160	88	124	0	29	5567
8	331	3973	3129	95	159	88	123	0	26	7593
9	333	3948	3226	96	1053	89	123	0	26	8560
10	114	2347	1088	97	4495	87	124	0	26	8264
11	411	6491	1069	94	159	87	129	0	25	8054
12	141	2390	1082	94	159	88	129	0	26	3969

*(): significantly differ from the pipetted concentrations)

D. Titration



a

b

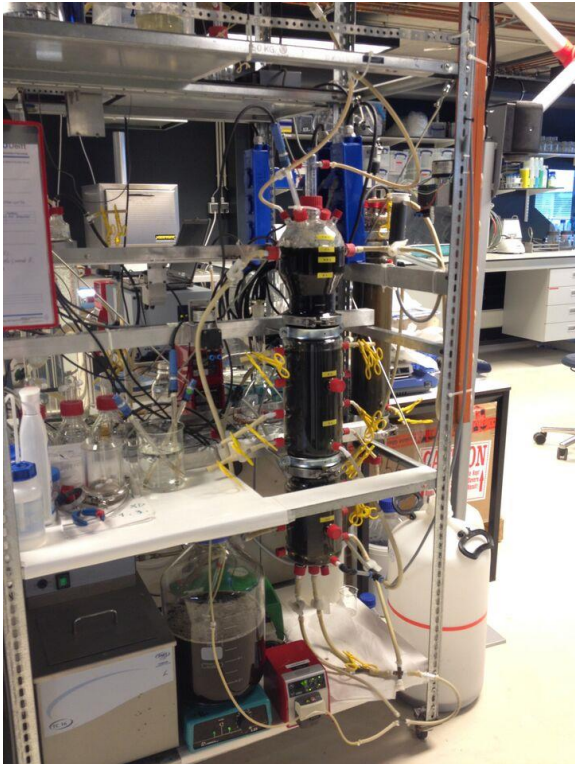
Figure D1 Total VFA measured by titration method and GC

(*a: results of leachate in leaching reactor from Cycle 6; b: results from UASB effluent)

Assuming that acetate consisted most of the total VFA, the difference between TA and PA was calculated into VFA (C2) concentrations. It is shown in Figure C1.

Neither in the leachate nor in the UASB effluent, the titration method could give an accurate measurement of VFA. Which means, this titration method was not able to monitor the VFA concentrations in this two-phase system.

E. Additional experimental details



a
Figure E1 Photo of the lab-scale two-phase AD system
(a: Leaching bed reactor; b: UASB reactor)

b

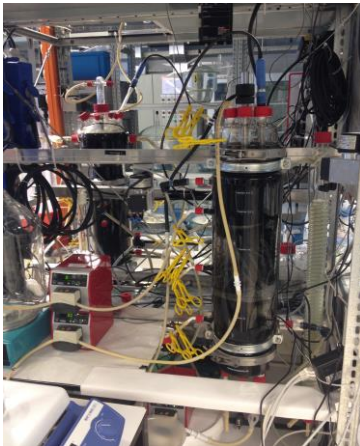
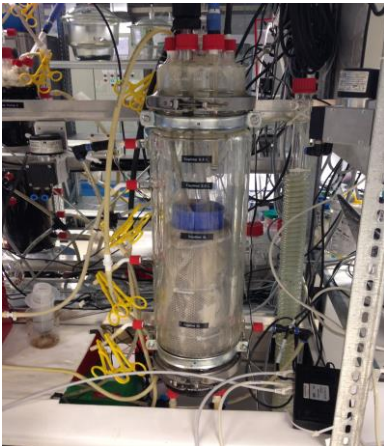
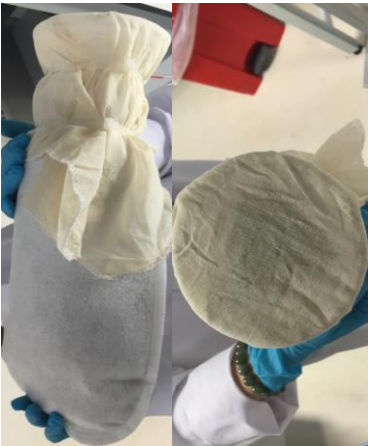


Figure E2 Biowaste package and leaching bed reactor

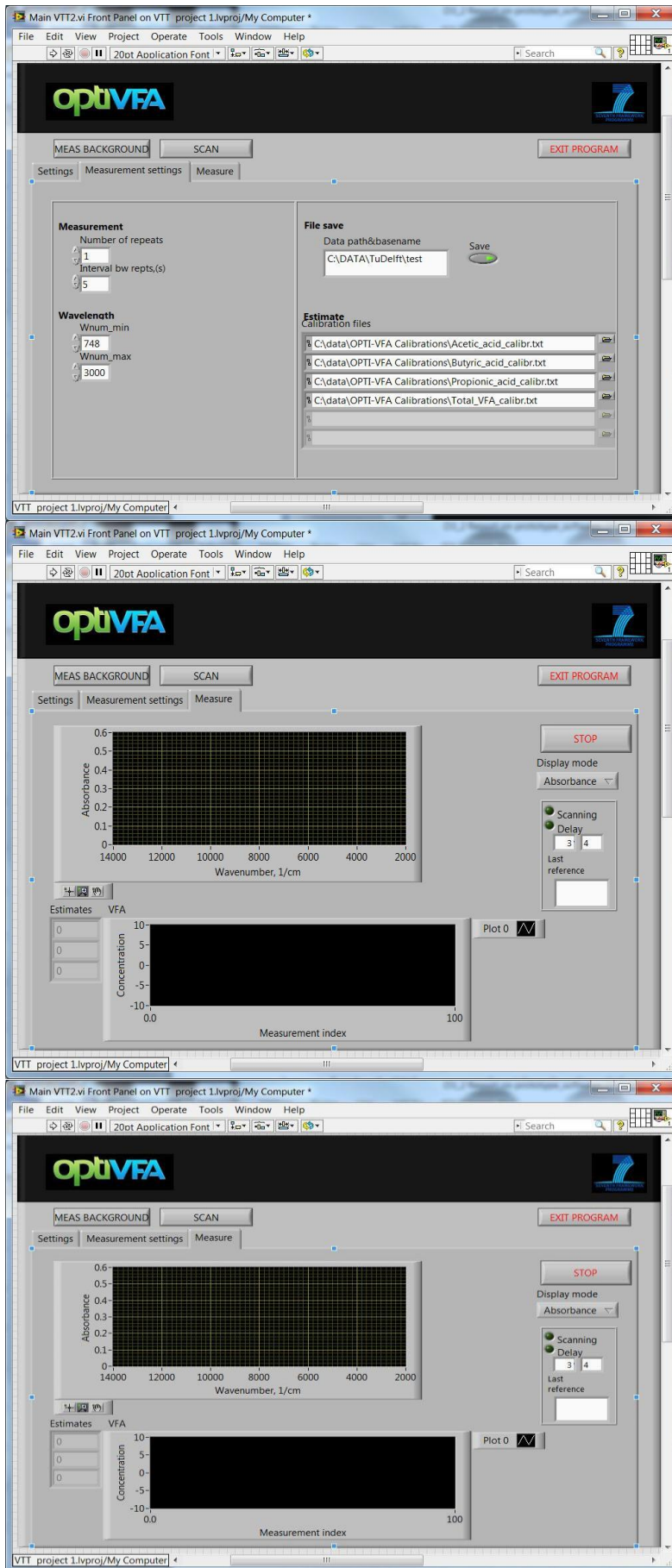


Figure E3 User interface of OPTI-VFA software



Figure E4 PMT TC 16 water bath and IKA® ETS-D6 electronic contact thermometer